

**WASM: Minerals, Energy and Chemical Engineering**

**Beneficiation of Hard Rock Lithium Ore and the Effect of Calcination**

**Muhammad Kashif Nazir**

**This thesis is presented for the Degree of  
Doctor of Philosophy  
of  
Curtin University**

**December 2022**

## **Declaration by Author**

This thesis is composed of my original work, and contains no material previously published or written by another person except where due reference has been made in the text. I have clearly stated the contribution by others to jointly-authored works that I have included in my thesis.

I have clearly stated the contribution of others to my thesis as a whole, including statistical assistance, survey design, data analysis, significant technical procedures, professional editorial advice, and any other original research work used or reported in my thesis. The content of my thesis is the result of work I have carried out since the commencement of my research higher degree candidature and does not include a substantial part of work that has been submitted to qualify for the award of any other degree or diploma in any university or other tertiary institution. I have clearly stated which parts of my thesis, if any, have been submitted to qualify for another award.

## **Published Works by the Author Incorporated into the Thesis**

### Chapter 3:

Nazir MK, Dyer L, Tadesse B, Albijanic B, Kashif N. Effect of calcination on coarse gangue rejection of hard rock lithium ores. *Sci Rep.* 2022 Jul 28;12(1):12963. doi: 10.1038/s41598-022-17277-x. PMID: 35902717; PMCID: PMC9334572.2.

### Chapter 4:

Nazir MK, Dyer L, Tadesse B, Albijanic B, Kashif N. Lithium deportment by size of a calcined spodumene ore. *Sci Rep* 12, 18335 (2022). <https://doi.org/10.1038/s41598-022-22808-7>.

### Chapter 6:

Nazir MK, Dyer L, Tadesse B, Albijanic B, Kashif N. Flotation performance of calcined spodumene, *Advanced Powder Technology*, Volume 33, Issue 11, 2022, 103772, ISSN 0921-8831.

## **Acknowledgements**

I would like to express my appreciation for the following:

- Dr Laurance Dyer, Dr Boris Albijanic and Dr Bogale Tadesse for all the support, guidance and supervision throughout my research work.
- CRC Ore and Curtin university for sponsoring the project.
- Bald hill mine for the provision of the samples.
- Curtin university and Western Australian School of Mines (WASM) for all the technical facilities.
- Dr Tom Payten for providing MLA analysis of the samples
- Last but not least, I would like to dedicate my work to my parents, my spouse Nadia Kashif and my beautiful children.

## Attribution Table

### Attribution table for the papers included in this thesis

1. Nazir MK, Dyer L, Tadesse B, Albijanic B, Kashif N. Effect of calcination on coarse gangue rejection of hard rock lithium ores. Sci Rep. 2022 Jul 28;12(1):12963. doi: 10.1038/s41598-022-17277-x. PMID: 35902717; PMCID: PMC9334572.2.

	Conception and design	Acquisition of data and method	Data conditioning and manipulation	Analysis and statistical method	Interpretation and discussion	Final approval
Mr. Muhammad Kashif Nazir	75	100	75	80	80	50
I acknowledge that these represent my contribution to above research output						
Signed:-						
Dr. Laurance Dyer	10	0	10	10	10	30
I acknowledge that these represent my contribution to above research output						
Signed:-						
Dr. Bogale Tadesse	5	0	5	5	5	10
I acknowledge that these represent my contribution to above research output						
Signed:-						
Dr. Boris Albijanic	5	0	5	5	5	10
I acknowledge that these represent my contribution to above research output						
Signed:-						
Mrs. Nadia Kashif	5	0	5	0	0	0
I acknowledge that these represent my contribution to above research output						
Signed:-						

2. Nazir MK, Dyer L, Tadesse B, Albijanic B, Kashif N. Lithium deportment by size of a calcined spodumene ore. Sci Rep 12, 18335 (2022). <https://doi.org/10.1038/s41598-022-22808-7>.

	Conception and design	Acquisition of data and method	Data conditioning and manipulation	Analysis and statistical method	Interpretation and discussion	Final approval
Mr. Muhammad Kashif Nazir	75	100	75	80	80	50
I acknowledge that these represent my contribution to above research output Signed:-						
Dr. Laurance Dyer	10	0	10	10	10	30
I acknowledge that these represent my contribution to above research output Signed:-						
Dr. Bogale Tadesse	5	0	5	5	5	10
I acknowledge that these represent my contribution to above research output Signed:-						
Dr. Boris Albijanic	5	0	5	5	5	10
I acknowledge that these represent my contribution to above research output Signed:-						
Mrs. Nadia Kashif	5	0	5	0	0	0
I acknowledge that these represent my contribution to above research output Signed:-						

3. Nazir MK, Dyer L, Tadesse B, Albijanic B, Kashif N. Flotation performance of calcined spodumene, *Advanced Powder Technology*, Volume 33, Issue 11, 2022, 103772, ISSN 0921-8831,

	Conception and design	Acquisition of data and method	Data conditioning and manipulation	Analysis and statistical method	Interpretation and discussion	Final approval
Mr. Muhammad Kashif Nazir	75	100	75	80	80	50
I acknowledge that these represent my contribution to above research output Signed:-						
Dr. Laurance Dyer	10	0	10	10	10	30
I acknowledge that these represent my contribution to above research output Signed:-						
Dr. Bogale Tadesse	5	0	5	5	5	10
I acknowledge that these represent my contribution to above research output Signed:-						
Dr. Boris Albijanic	5	0	5	5	5	10
I acknowledge that these represent my contribution to above research output Signed:-						
Mrs. Nadia Kashif	5	0	5	0	0	0
I acknowledge that these represent my contribution to above research output Signed:-						

## Abstract

Calcination is a compulsory pre-treatment during the processing of spodumene ores that transforms  $\alpha$ -phase of spodumene to  $\beta$ -phase that is more reactive. This conversion happens at high temperatures above 900 °C. The resultant  $\beta$ -spodumene has highly altered physical properties with 30% more volume than that of  $\alpha$ -spodumene.  $\beta$ -spodumene is more reactive towards chemical reagents and mechanical treatments due to more open crystal structure.

This PhD project examines the effect of calcination on lithium grade deportment with particle size using different comminution techniques such as crushing, autogenous grinding and semi autogenous grinding. XRD analysis showed a significant amount of  $\beta$ -spodumene in the calcined finest fraction (i.e., the particles less than 0.6 mm). A significant reduction in the bond ball mill work index of the calcined spodumene samples (i.e., 42.3%) was recorded, demonstrating the fracturing and friable appearance of the calcined spodumene following  $\alpha$  to  $\beta$ -spodumene conversion. The deportment of lithium to finer fractions was dramatically higher when the sample was calcined, showing selective breakage of the spodumene. Although the combination of the furnace with the crusher or the mill (autogenous or semi-autogenous grinding) increased the energy consumption of the process, using the furnace increased the lithium grade by the screening of hard rock lithium ores.

This PhD work also examines the energy efficiency of different grinding circuits used for upgrading the lithium content in the finer fraction of the calcined spodumene ore. The results showed that closed-circuit grinding led to 89% lithium recovery of the finest size fractions (-0.6 mm) while open-circuit grinding resulted in 65 % lithium recovery for the same grinding time. Closed-circuit grinding used lower energy than open-circuit grinding. The grade of the finest size fraction in the case of the closed-circuit grinding was 1.7 times less than that in the case of the open-circuit grinding. The results showed the potential of using different grinding modes to optimize energy efficiency and lithium deportment by size.

This PhD project also studies the effect of different calcination temperatures on the lithium grade and recovery in the finest size fraction, i.e., 0.6 mm. The best results for lithium grade and recovery were obtained when the sample was calcined at 1100 °C. The samples calcined at 540 and 950 °C showed very little improvement in the grade and recovery of finest size

fraction (i.e., the particle size is less than 0.6 mm). The samples that were not calcined at all, did not show any significant coarse gangue rejection.

Finally, this PhD project investigates the effect of calcination temperatures on spodumene flotation. It was found that increasing the calcination temperature increased the oleate adsorption due to a fractured spodumene surface and hence increased lithium grade and recovery were observed.

This PhD project showed that calcination could be used as a potential pre-treatment before beneficiation for coarse gangue rejection and may increase lithium grade and recovery in the finer size fractions. Calcination of spodumene ore followed by grinding operations can further increase the lithium grade and recovery. Calcination also made spodumene brittle, fractured the spodumene surface and thus provided better reagent adsorption on spodumene surfaces, which is beneficial for flotation. Most of the energy used in calcination of the ore can be compensated through the decrease in grinding costs due to the reduced hardness of the calcined spodumene ore and thus lithium mining industry may adopt calcination before comminution and beneficiation.



## **Key Words**

Lithium beneficiation, spodumene calcination, coarse gangue rejection, spodumene beneficiation, energy efficiency, spodumene ore, lithium deoprtment, spodumene flotation, calcination temperature, sodium oleate, adsorption, bond ball mill work index, XRD, ICP, mineralogy.

## Statement of Originality

This thesis has not been submitted for a degree in any University, and does not contain material published by another person. The original contributions of this thesis are outlined briefly below:

- A novel approach to coarse gangue rejection in hard rock lithium ores using calcination, comminution methods and screening.
- Comprehensive study to investigate the effect of calcination on the physical properties of spodumene and the effect of these changed physical properties on coarse gangue rejections.
- A study that investigates energy efficiency of different grinding circuits to upgrade the lithium content in the finest size fraction of a calcined spodumene ore.
- An investigation on the effect of different calcination temperatures on coarse gangue rejection in spodumene ore via screening.
- A study on the effect of various calcination temperatures on reagent adsorption and spodumene flotation.

## Table of Contents

<b>Declaration by author</b>	<b>ii</b>
<b>Acknowledgements</b>	<b>iii</b>
<b>Published Works by the Author Incorporated into the Thesis</b>	<b>iv</b>
<b>Abstract</b>	<b>vii</b>
<b>Key Words</b>	<b>ix</b>
<b>Statement of Originality</b>	<b>x</b>
<b>Table of contents</b>	<b>xi</b>
<b>List of figures</b>	<b>xiv</b>
<b>List of tables</b>	<b>xvi</b>
<b>Chapter I: Introduction</b>	<b>1</b>
1. Main hypothesis and sub-hypothesis	2
2. Objective and sub-objectives	3
3. Approach	3
4. Structure of the thesis	4
<b>Chapter II: Review</b>	<b>5</b>
1. Introduction	6
1.1. Lithium occurrence in nature	8
1.1.1. Brines	9
1.1.2. Lithium ores	10
1.2. Worldwide lithium distributions	10
1.3. Lithium extraction	11
2. Ore Mineralogy	12
2.1. Spodumene	12
2.2. Petalite	14
2.3. Lepidolite	14
2.4. Amblygonite	14
2.5. Zinnwaldite	14
2.6. Eucryptite	15
3. Beneficiation of lithium ores	15
3.1. Beneficiation using grade by size department	15
3.1.1. Grade by size department after blasting and primary crushing	16
3.1.2. Grade by size department after differential blasting	17
3.1.3. Grade by size department after using sensor-based bulk and stream sorting	18
3.2. Dense media and gravity separation	19
3.3. Magnetic separation	20
3.4. Flotation	20
3.4.1. Flotation of spodumene	22
3.4.2. Effects of chemical pre-treatment and de-sliming	23
4. Calcination of spodumene	24
5. Hydrometallurgy	26
5.1. Leaching with strong acid	27
5.2. Leaching with base	28
5.3. Sulphate roasting/autoclaving method for $\alpha$ - and $\beta$ -spodumene	29
5.4. Carbonate roasting/autoclaving method for $\alpha$ - and $\beta$ -spodumene	29
5.5. Chlorinating method	30
6. Plant practices	31
6.1. The Greenbushes, Australia	31

6.2.	The Kings Mountain Operations, USA	32
6.3.	Bernic Lake lithium operation, Canada	32
6.4.	The Bikita Operation, Zimbabwe	33
6.5.	Bald Hill lithium and tantalum operations, Australia	33
7.	Conclusions	33
8.	References	34
<b>Chapter III: Effect of calcination on coarse gangue rejection of hard rock lithium ores</b>		<b>44</b>
Abstract		45
1.	Introduction	45
2.	Materials and methods	48
2.1.	Samples	48
2.2.	Calcination	48
2.3.	Comminution	49
2.4.	Bond Ball Mill Work Index	50
2.5.	X-Ray Diffraction	51
3.	Results and discussions	51
3.1.	Effect of calcination and comminution method on mass retention	51
3.2.	Effect of calcination and comminution method on lithium grade and lithium recovery	52
3.3.	Effect of calcination on lithium grade and recovery for very fine sizes	56
3.4.	Effect of calcination on energy consumption during grinding	58
4.	Conclusions	60
5.	References	61
<b>Chapter IV: Lithium deportment by size of a calcined spodumene ore</b>		<b>63</b>
Abstract		64
1.	Introduction	64
2.	Materials and methods	66
2.1.	Ore preparations	66
2.2.	Semi-autogenous grinding and screening	68
2.3.	X-Ray Diffraction (XRD)	69
3.	Results and discussions	70
3.1.	Effect of grinding time on particle size distributions of feed in open and closed-circuit grinding	70
3.2.	Effect of grinding time on lithium deportment in closed-circuit grinding	71
3.3.	XRD analysis of the finest size fractions (-0.6 mm) of open and closed circuit grinding	72
3.4.	Lithium recovery in closed-circuit grinding	74
3.5.	Comparison of the efficiency of the closed and open-circuit grinding	76
4.	Conclusions	79
5.	References	80
<b>Chapter V: Influence of calcination temperatures on lithium deportment by screening hard rock lithium</b>		<b>83</b>
Abstract		84
1.	Introduction	84
2.	Materials and methods	86
2.1.	Ore	86
2.2.	Calcination	87
2.3.	Grinding	89

2.4.	X-Ray Diffraction (XRD)	89
3.	Results and discussions	89
3.1.	Effect of calcination temperature on ore retention	89
3.2.	Effect of calcination temperature on lithium grade and lithium recovery	90
4.	Conclusions	94
5.	References	95
	<b>Chapter VI: Flotation performance of calcined spodumene</b>	<b>98</b>
	Abstract	99
1.	Introduction	99
2.	Materials and methods	100
2.1.	Ore preparation	100
2.2.	Flotation	101
2.3.	Zeta potential	102
2.4.	UV adsorption	102
3.	Results and discussions	103
4.	Conclusions	105
5.	References	106
	<b>Chapter VII: Conclusions and recommendations for future work</b>	<b>108</b>
1.	Conclusions	109
2.	Future research opportunities	110

## List of Figures

### Chapter I

- Figure 1: Approach used in this thesis 4

### Chapter II

- Figure 1. Some facts about lithium (Lithium Resources and Energy Quarterly September 2019 – [www.industry.gov.au/OCE](http://www.industry.gov.au/OCE)) 7
- Figure 2. Global uses of Lithium (Lithium Resources and Energy Quarterly September 2019 – [www.industry.gov.au/OCE](http://www.industry.gov.au/OCE)) 8
- Figure 3. World lithium reserves (US Geological Survey (2018); Department of Industry, Innovation & Science (2019)) 11
- Figure 4. Major Australia Lithium deposits (Lithium Resources and Energy Quarterly September 2019 – [www.industry.gov.au/OCE](http://www.industry.gov.au/OCE)) 11
- Figure 5. Longitudinal and elongated tabular cleavages can be seen in this photograph of a high grade spodumene ore sample from Bald Hill mine site in Western Australia (Bogale et al., 2019) 13
- Figure 6. Stability relationship between  $\alpha$ -spodumene ( $\text{LiAlSi}_2\text{O}_6$ ),  $\beta$ -spodumene ( $\text{LiAlSi}_5\text{O}_{12}$ ),  $\gamma$ -spodumene/ virgilite ( $\text{LiAlSi}_5\text{O}_{12}$ ), eucryptite ( $\text{LiAlSiO}_4$ ) and petalite  $\text{LiAlSi}_4\text{O}_{10}$  in the system  $\text{LiAlSiO}_4\text{-SiO}_2\text{-H}_2\text{O}$  (adapted from the Mineralogical Society of America, American Mineralogist; published by the Mineralogical Society of America, 2019). 25
- Figure 7. Crystal structures of spodumene. (a)  $\alpha$ -spodumene, (b)  $\beta$ -spodumene, (c)  $\gamma$ -spodumene. Red: Oxygen. Yellow: Silicon. Blue: Aluminum. Green: Lithium. Note: The lattices images were obtained with the display module of the Jade2010TM software (Dessemond, Lajoie-Leroux, Soucy, Laroche and Magnan, 2019) 26

### Chapter III

- Figure 1. The experimental flowcharts 50
- Figure 2. Retention of a) TDMS b) PF on different sieves 52
- Figure 3. Influence of calcination and comminution methods on cumulative grade of lithium in the case of a) TDMS and b) PF 53
- Figure 4. Influence of calcination and comminution methods on cumulative lithium recovery in the case of a) TDMS and b) PF 54
- Figure 5. Cumulative grade vs cumulative recovery of lithium in the case of a) TDMS and b) PF 54
- Figure 6. XRD for two calcined finest fractions (-0.6 mm) and two non-calcined coarsest fractions (+3.35 mm) 56
- Figure 7. Influence of calcination on the cumulative grade of lithium in the case of a) feed of the ball mill and b) product of the ball mill 57
- Figure 8. Influence of calcination on cumulative recovery of lithium in the case of a) feed of BBMWI and b) product of BBMWI in the case of PF 57

## Chapter IV

Figure 1.	Estimation of particle properties a) before calcination and b) after calcination (Nazir et al., 2022b)	67
Figure 2.	Development flowchart a) the open-circuit grinding and b) the closed-circuit grinding	69
Figure 3.	Particle size distributions as a function of grinding time (CCG is the closed-circuit grinding and OCG is the open circuit grinding)	71
Figure 4.	Effect of closed-circuit grinding time and screening on lithium grade in the two size fractions.: -0.6 mm and +0.6 mm	72
Figure 5.	XRD results for samples collected after a) the open-circuit grinding and b) the closed-circuit grinding	73
Figure 6.	Effect of grinding time and screening on the lithium recovery in the finest size fractions (-0.6 mm)	75
Figure 7.	Cumulative recovery vs cumulative grade for the finest size fractions during the closed-circuit grinding	76
Figure 8.	The particle size distributions of the products (-0.6 mm); CCG is the closed-circuit grinding and OCG is the open circuit grinding	78

## Chapter V

Figure 1.	XRD for the non-calcined spodumene ore	87
Figure 2.	The images of a) non-calcined ore, b) calcined ore at 540°C, c) calcined ore at 950°C and d) calcined ore at 1100°C	87
Figure 3.	Estimation of particle properties a) before calcination and b) after calcination (Nazir et al., 2022b)	88
Figure 4.	The influence of calcination temperature on ore retention	90
Figure 5.	Effect of calcination temperature on cumulative lithium grade	91
Figure 6.	Mineralogy of a) the fine size fraction (-0.6 mm) and b) the coarse size fraction (+0.6 mm)	92
Figure 7.	Effect of calcination temperature on lithium recovery	94

## Chapter VI

Figure 1.	Estimation of particle properties a) before calcination and b) after calcination	101
Figure 2.	Flotation a) Li recovery and b) Li <sub>2</sub> O grade of non-calcined (25°C) and calcined samples as a function of pulp pH	103
Figure 3.	Zeta potential measurements of non-calcined and calcined samples a) in the distilled water and b) in the presence of sodium oleate	104
Figure 4.	Oleate concentrations in solutions after adsorptions of the non-calcined and calcined sample at different temperatures	105

## List of Tables

### Chapter II

Table 1.	Common lithium minerals of economic values (Bulatovic, 2015; Chelgani et al., 2015; Grosjean et al., 2012)	10
----------	------------------------------------------------------------------------------------------------------------	----

### Chapter III

Table 1.	Mineralogy of the spodumene ore	48
Table 2.	Grinding balls used for BBMWI	50
Table 3.	Energy consumption for different unit operations	59
Table 4.	Energy consumptions and lithium grade for -0.6 mm for different processing operations	60

### Chapter IV

Table 1.	Mineralogy of the spodumene ore	68
Table 2.	Mass balance and energy consumption for both open and closed grinding circuit	78
Table 3.	Comparison of the closed-circuit grinding versus the open-circuit grinding	79



**Chapter I**  
**Introduction**

Lithium metal is alkaline in nature and is soft, very light and has a low density. There are many industrial applications of lithium metal, however in the recent history, it has a very important use in lithium-ion (Li-ion) batteries attributed to its high reactivity, lightness and capability of being recharged. The industry forecast that lithium will have significant demand in the coming years due to evolution of electrical vehicles and increasing demand of renewable energy resources. The increase in lithium demand has led to the importance of beneficiation process, especially for the low-grade ores to achieve high grades and recoveries during lithium metal extraction.

Lithium beneficiation is a process where lithium ore is reduced in size and gangue minerals are significantly reduced from the ore. However, lithium beneficiation is a very challenging and complex process due to the similar properties of lithium and its gangue minerals. Some of the challenges associated with beneficiation of lithium ores are higher energy consumption during crushing and grinding, wastage of fine material during desliming and dusting problems during heat treatment. A closed crystal structure of spodumene does not respond to chemical reagents leading to a higher reagent cost and poor collector adsorption during flotation. Calcination is always done before leaching to convert  $\alpha$ -spodumene to  $\beta$ -spodumene at elevated temperatures above 1000 °C. This is a mandatory step for the lithium metal extraction. The main objective of this thesis was to understand the impact of calcination on beneficiation of hard rock lithium ores.

## **1. Main hypothesis and sub-hypothesis**

The main hypothesis, addressed in this thesis, is that a fully calcined spodumene ores respond more effectively to the beneficiation methods than non-calcined ores.

The sub-hypotheses in this research were:

- A completely calcined spodumene ore is more brittle and thus respond more effectively to comminution methods resulting in coarser gangue rejection and concentrating the lithium minerals in the finer size fraction.
- A spodumene ore sample with incomplete transformation from  $\alpha$ -phase to  $\beta$ -phase resulted in less separation efficiency during beneficiations.

- A completely calcined spodumene ore produced higher grade and recovery of lithium minerals during flotation process.
- A completely calcined spodumene have lower zeta-potential and higher adsorption of collectors (oleate) due to more volume and open crystal structure of  $\beta$ -spodumene.

## 2. Objective and sub-objectives

The main objective of this research was to study the effects of calcination on the efficiency of lithium deportment and flotation and thus maximise lithium recoveries and grades.

The sub-objectives of this research were:

- To study the natural deportment of calcined and non-calcined lithium ores by screening.
- To investigate the most efficient comminution strategy for calcined spodumene ore.
- To study flotation of calcined spodumene ore.
- To study the effects of calcination on energy consumptions during comminution.
- To investigate the influence of different calcination temperature on coarse gangue rejections of spodumene ore by screening.

## 3. Approach

- To use selected comminution techniques to investigate the effect of calcination on beneficiation of calcined spodumene ore.
- To use different calcination temperatures to study lithium deportment by size.
- To use different calcination temperatures to evaluate the flotation efficiency of the spodumene ore.

Figure 1 summarizes the approach used in this thesis.

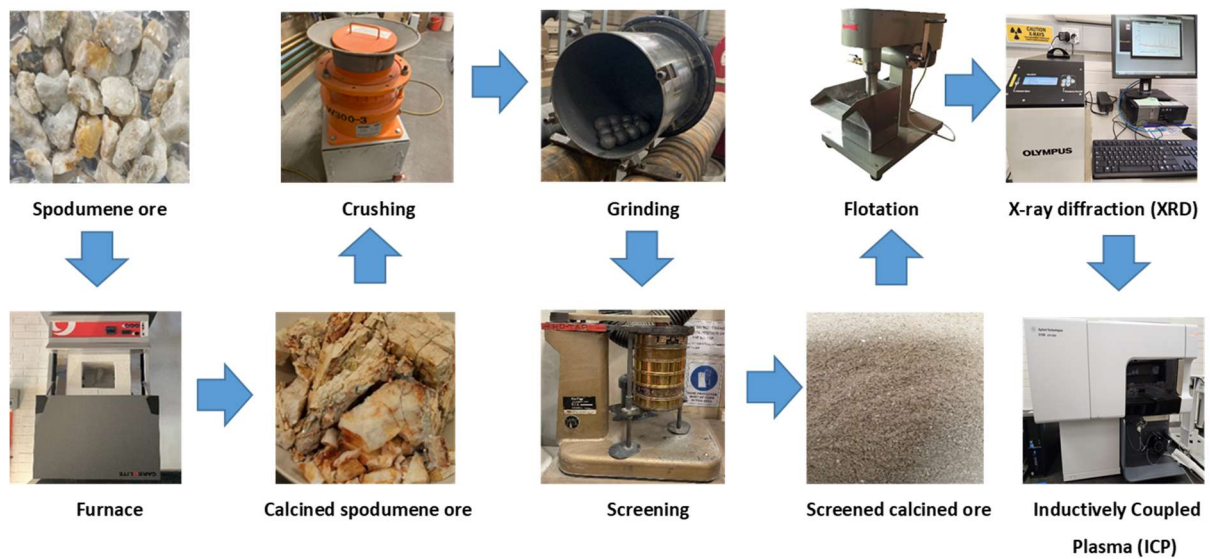


**Figure 1.** Approach used in this thesis.

#### 4. Structure of the thesis

This thesis has been structured in the form of papers and chapters 3-6 are published or submitted papers. **Chapter 1** presents hypotheses, objectives, approach and structure of this thesis. **Chapter 2** is a review of previous literature available on lithium minerals, their applications, and beneficiation methods together with some plant practices used in lithium processing. **Chapter 3** (Nazir MK, Dyer L, Tadesse B, Albijanic B, Kashif N. Effect of calcination on coarse gangue rejection of hard rock lithium ores. *Sci Rep.* 2022 Jul 28;12(1):12963.) investigates coarse gangue rejections for both calcined and non-calcined spodumene ore by screening. **Chapter 4** (Nazir MK, Dyer L, Tadesse B, Albijanic B, Kashif N. Lithium deportment by size of a calcined spodumene ore. *Sci Rep* 12, 18335 (2022)) investigates the energy efficiency of different grinding circuits used for upgrading the lithium content in the finer fraction of the calcined spodumene ore. **Chapter 5** (submitted to a journal) investigates the influence of different calcination temperatures on lithium deportment by screening of hard rock lithium ores. **Chapter 6** (Nazir MK, Dyer L, Tadesse B, Albijanic B, Kashif N. Flotation performance of calcined spodumene, *Advanced Powder Technology*, Volume 33, Issue 11, 2022, 103772, ISSN 0921-8831) investigates flotation performance of calcined spodumene ores. **Chapter 7** discusses conclusions of this thesis and recommendation for future research are provided.

**Chapter II**  
**Review**

## 1. Introduction

The main purpose of this chapter is to review and discuss the work already performed by other researchers. This chapter will share the experiments, observations and conclusions made available by other research students and scientists to study the significance and influence of calcination on beneficiation of hard rock lithium ores. Beginning with the background of lithium applications and its extraction processes, this chapter will illuminate the significance of rising lithium demand in recent and future years. Vital role of calcination during extraction of lithium from hard rock ore as described in other studies shall be reviewed to develop a connection of this research with other studies.

Lithium is a comparatively rare but one of the oldest elements in the universe discovered in 1817 (Kavanagh et al., 2018). It is the lightest metal with very low density (0.534 g/cm<sup>3</sup>) and 6.94 atomic weight making it the least dense metal (Kavanagh et al., 2018). Due to this property lithium can float on the water. It belongs to alkaline metal group and is highly reactive and flammable like all other alkaline metals (British Geological Survey, 2016). It has one of the lowest melting points among all metals (180 °C) (Kavanagh et al., 2018) but at the same time it has the highest melting and boiling points of the alkali metals. Due to its highly reactive nature, lithium never occurs freely in nature, but only in form of (usually ionic) compounds, like pegmatitic minerals. As it is highly soluble as an ion, it is present in oceanic water and is usually extracted from brines. Because of highest mass specific heat capacity of 3.56 kJ/kg-K, lithium metal is often used in coolants for heat transfer applications (Kavanagh et al., 2018). Some other unique properties of lithium like small ionic radius, highest electrochemical potential of all metals combined with good heat and electric conductivity make it a very useful industrial metal. Lithium is a soft, silvery-white alkali metal that shows a metallic luster when cut, but is quickly corroded to dull silvery grey to black tarnish colour by moist air (British Geological Survey, 2016). Some facts about Lithium are presented in Figure 1.

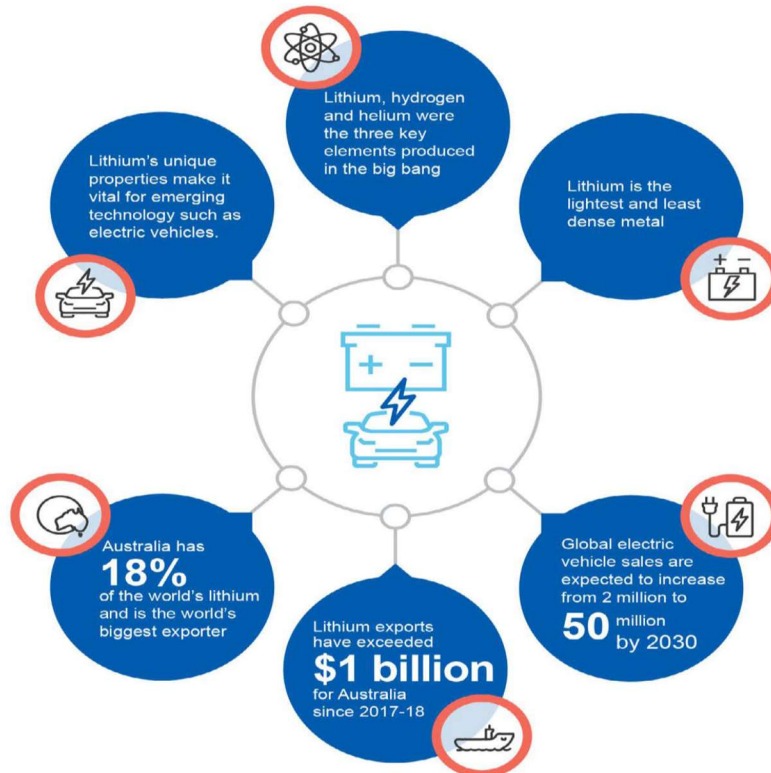


**Figure 1.** Some facts about lithium (Lithium Resources and Energy Quarterly September 2019 – [www.industry.gov.au/OCE](http://www.industry.gov.au/OCE))

Lithium and its compounds are used in the industry of many fields; including heat resistant glass & ceramics, lithium grease lubricants, flux additives for iron, steel and aluminium production, lithium batteries, and lithium-ion batteries. In medical science lithium is used to treat the mood disorders (Garrett, 2004). The most significant application of lithium is in the battery industry. It is a desirable raw material for the fast-growing battery industry. Especially, the requirement for lithium-ion batteries (LIBs) used in vehicles as power sources have experienced an extensive growth, with international market share reached around 39% in 2016 (Jaskula, 2017; Zou et al., 2013). Figure 2 shows the lithium consumption in various industries. It is obvious that major demand is in rechargeable batteries industry which is heavily driven by electric cars industry.

## Global uses of Lithium



**Figure 2.** Global uses of Lithium (Lithium Resources and Energy Quarterly September 2019 – [www.industry.gov.au/OCE](http://www.industry.gov.au/OCE))

Principally battery industry growth has raised the worldwide demand of lithium chemicals in recent years. Latest application of lithium-ion technology in electric automobiles has resulted in an increased demand of lithium minerals (Ebensperger et al., 2005; Peiro et al., 2013). Overall world consumption of lithium is growing fast and is expected to increase at an annual rate of 30% during the outlook period. Sales of electric cars are expected to be the key driver of lithium growth in future, which are expected to increase from 2 million to 50 million by 2030.

### 1.1. Lithium occurrence in nature

Even though lithium is widely disseminated on Earth but due to its high reactivity it does not occur freely in elemental form (Krebs, 2006). Naturally, lithium is found in a number of rocks and brines but in very low concentrations which categorizes it as a rare element. Only few of the known large numbers of lithium mineral and brine deposits have future commercial value (Garrett, 2004).

Lithium content of seawater is very large and is projected as 230 billion tones, with a relatively constant concentration of 0.14 to 0.25 ppm (Institute of Ocean Energy, Saga University Japan,



2009; ENC Labs, 2010) with the presence of higher concentrations up to 7 ppm near hydrothermal vents (ENC Labs, 2010).

Assessments for the Earth's Lithium concentration is 20-70 ppm by mass. Lithium forms a negligible part of igneous rocks, with the largest concentrations in granites. Spodumene and petalite are the most commercially profitable sources that come from granitic pegmatites (Kamienski, et al., 2004).

### **1.1.1. Brines**

Usually, lithium production from brine sources has been proven to be more cost effective than extraction from hard rock ores. Although the lithium market was dominated by hard rock lithium production before 1980 (Kavanagh et al., 2018) but now the lithium carbonate ( $\text{Li}_2\text{CO}_3$ ) is mostly obtained from continental brines in Latin America. This is mainly due to the lower production cost.

Lithium brine deposits are classified as continental, geothermal and oil field (Kavanagh et al, 2018). Continental saline desert basins are the most common brine source. They are also known as salt lakes, salt flats or salars. They contain sand, minerals with brine and saline water with a high concentration of dissolved salts. Their common locations are the areas with geothermal activity. Another type of brine deposit is called playa whose surface is made up of silts and clays and have less salt than a salar. 66% of global lithium resources are in form of brines and are present mostly in the salt flats of Argentina, China, Chile and Tibet.

Most common form of lithium-containing brine is continental. Brine deposits called “Lithium Triangle” are the major contributor towards global lithium production (Ahmad, 2020). It is a region of the Andes mountains that includes parts of Argentina, Chile and Bolivia.

Geothermal lithium brine resources are hot, concentrated saline solution enriched with elements such as lithium, boron and potassium as a result of circulation through rocks in areas of immense high heat flow. New Zealand, Iceland and Chile have some small quantities of this type of lithium brine. Lithium brine deposits in few deep oil reservoirs account for 3% of global lithium resources. The US Gulf Coast Smackover Formation is supposed to have an estimated 1 million metric ton of lithium resources with 0.015% average concentration (Barrera, 2019).

According to geologist Keith Evan’s Oil field brines with concentrations of 700 mg/L are present in North Dakota, Wyoming, Oklahoma, Arkansas and East Texas (Barrera, 2019).

### 1.1.2. Lithium ores

Lithium ores are mostly found as intrusive igneous rocks known as pegmatites. Pegmatites are mainly the deposits of hard rock complex aluminium silicate (Bale and May 1989; Colton, 1957) formed by interlocked mineral grains of feldspar, spodumene, mica, and quartz (Colton, 1957). Spodumene, petalite, lepidolite and amblygonite are the main lithium minerals contained in lithium pegmatite ores (Bulatovic, 2015; Filippov et al., 2022). Some other lithium minerals have been reported in literature as zinnwaldite, triphylite and eucryptite (Colton, 1957; Grosjean et al., 2012). Spodumene is the most abundant and commercially viable pegmatite mineral among all lithium-rich pegmatite minerals. Table 1 shows lithium minerals of economically significant lithium minerals. It can be observed that the exploitable pegmatite deposits can have typical lithium grade in a range of about 1.25–4% Li<sub>2</sub>O (Bale and May, 1989).

Mineral	Formula	Content % Li <sub>2</sub> O		SG	Hardness
		Theoretical	Actual		
Spodumene	LiAl[SiO <sub>3</sub> ] <sub>2</sub>	8.1	4.5-8.0	3.1-3.2	6.5-7
Petalite	LiAlSi <sub>4</sub> O <sub>10</sub>	4.89	2-4	2.4-2.5	6-6.5
Lepidolite	KLiAl <sub>2</sub> Si <sub>3</sub> O <sub>10</sub> (OH,F) <sub>3</sub>	5.9	1.2-5.9	2.8-2.9	2-3
Amblygonite	LiAl[PO <sub>4</sub> ][F,OH]	10.1	4.5-10	3.0-3.2	5.5-6
Zinnwaldite	K[Li,Al,Fe] <sub>3</sub> [Al,Si] <sub>4</sub> O <sub>10</sub> [F,OH] <sub>2</sub>	4.13	3.3-7.7	2.9-3.2	2-3
Eucryptite	LiAlSiO <sub>4</sub>	11.9	11.9	2.67	6.5

**Table 1.** Common lithium minerals of economic values (Bulatovic, 2015; Chelgani et al., 2015; Grosjean et al., 2012) (unit of measurement for specific gravity (SG) is g·cm<sup>-3</sup> and Hardness in on Mohs scale).

## 1.2. Worldwide lithium distributions

Though brines are the key source of lithium with large deposits in countries like Chile and China (see Figure 3) but the lithium global market is rapidly shifting and investing towards the utilization of hard rock lithium ore deposits (Dessemond et al, 2019; Salakjani et al., 2019). Lithium extraction from hard rock ores requires less water consumption than that from brines (i.e SQM and Albemarle).

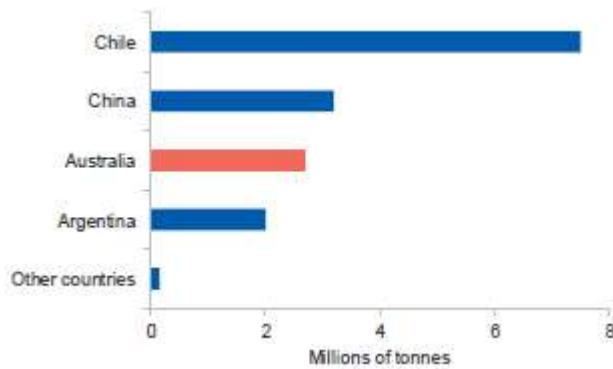


**Figure 3.** World lithium reserves (US Geological Survey (2018); Department of Industry, Innovation & Science (2019)).

Australia produced 58% of the total global mined lithium in 2018 making it the largest producer of mined lithium. Figure 4 shows the Australian lithium resources that mainly are found in Western Australia. Production began at many sites in 2018 including Pilbara Minerals’ Pilgangoora mine, Altura Mining’s, Pilgangoora mine, and Alliance Mineral Assets’ Bald Hill operation with the largest expansion (extra 20,000 tonnes) in Talison Lithium existing Greenbushes mine.

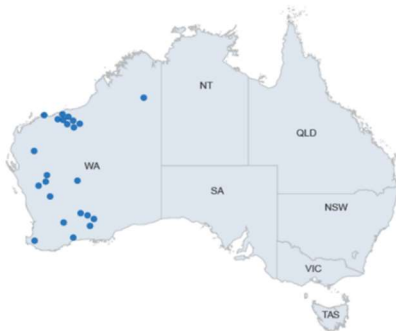


**Figure 4.** Major Australian Lithium deposits (Lithium Resources and Energy Quarterly September 2019 – [www.industry.gov.au/OCE](http://www.industry.gov.au/OCE))

### 1.3. Lithium extraction

Lithium can be extracted from three types of resources: brines, hard rocks (e.g., pegmatite) and soft rocks (e.g., sedimentary rocks) with each resource requiring different extraction techniques. More than 60% of worldwide lithium is sourced from brines (Ebensperger et al., 2005) because of its widespread availability, easy and economical processing as compared with other forms of resources (Swain et al., 2017). Various separation and beneficiation methods

are found in literature for lithium extraction from brines (Luo et al., 2012) depending on the composition of the specific brine reservoir. Decisive factors include pond soil suitability, evaporation possibility, composition of brine, the phase chemistry complexity (Murodjon et al., 2020). Methods for lithium extraction from brines can be by solvent extraction, precipitation, liquid-liquid extraction, selective membrane separation, electrodialysis or ion exchange adsorption, etc. (Grosjean et al., 2012; Hamzaoui et al., 2008; Liu et al., 2011 & 2012; Nie et al., 2017; Stamp et al., 2012).

Although lithium from brines deposits is most cost effective and produces most of the world's lithium, extraction of lithium from pegmatite hard rock ore is becoming more common. The reason is that lithium concentration of pegmatite deposits is higher than that of brines, making their processing economically acceptable. Spodumene is the most economically important lithium rich-mineral among these pegmatite lithium ores. Like most minerals, beneficiation is the first stage in lithium mineral processing followed by downstream extraction operations (Tadesse et al., 2019). The beneficiation techniques include physical separation such as heavy media/ dense media separation, magnetic separation, flotation and optical sorting of lithium ores (Sahoo et al., 2022; Kundu, 2022).

About 8% of known lithium resources of the world are found in sedimentary rocks containing clay deposits (most commonly found as smectite mineral "hectorite" named after its location in Hector, California) and lacustrine evaporites (most commonly found as mineral "jadarite" named after its location in Jadar Valley in Serbia) (Kavanagh et al, 2018; Dessemond et al, 2019).

## **2. Ore Mineralogy**

Ore mineralogy of lithium minerals found in pegmatite ores (i.e., spodumene, petalite, lepidolite, amblygonite (Bulatovic, 2015), zinnwaldite, and eucryptite (Colton, 1957; Grosjean et al., 2012)) has been discussed below:

### **2.1. Spodumene**

The name spodumene is derived from ancient Greek word "spodumenos" that means "burnt to ashes" because of its greyish ash colour when ground. It has an uneven to subconchoidal

fracture (White and McVay, 1958). Spodumene ( $\text{LiAl}(\text{SiO}_3)_2$ ) is a Lithium aluminum silicate (LAS) pegmatite ore that contains 8.03% of  $\text{Li}_2\text{O}$ . Other associated silicate minerals in pegmatite ores bodies are feldspar, micas, and quartz (Zelikman et al.1996, Bulatovic, 2015). For example, the typical composition of pegmatite Li ore found in Kings Mountain, North Carolina, is 20 wt% spodumene, 7% muscovite, 43% feldspar and 30% quartz whereas pure spodumene contains 8.0%  $\text{Li}_2\text{O}$  (Moon and Fuerstenau, 2003). Spodumene can exhibit different colours like grey, white, yellow, purple and green depending on the interlocked impurities in the spodumene structure which can be Fe, Mg, Na, Ti and Mn (Claffy 1953; Gabriel et al. 1942; Salakjani et al. 2016, 2017, 2019; Zelikman et al. 1996). Currently, spodumene is the key lithium containing silicate mineral for lithium extraction, reason being its high Li content and abundant existence (Garrett, 2004). Commonly used concentration techniques for spodumene ore beneficiation are heavy media separation, froth flotation and/or magnetic separation (Garrett, 2004; Gibson et al. 2017 & 2021).

A typical spodumene concentrate suitable for lithium carbonate production contains 6-7%  $\text{Li}_2\text{O}$  (75% - 87% spodumene) as compared with a typical run of mine ore with 1-2%  $\text{Li}_2\text{O}$ . Its prominent longitudinal cleavage can be observed in Figure 5. This Figure is a photograph of spodumene crystals sample that was collected from Bald Hill Mine in Western Australia.



**Figure 5.** Longitudinal and elongated tabular cleavages can be seen in this photograph of a high grade spodumene ore sample from Bald Hill mine site in Western Australia (Tadesse et al., 2019)

## **2.2. Petalite**

Petalite (lithium Aluminum phyllosilicate mineral  $\text{LiAlSi}_4\text{O}_{10}$ ) is usually found with other pegmatites like spodumene, eucryptite and lepidolite, and it is a monoclinic mineral and has a framework silicate structure. Lithium content can vary from 1.4 to 2.2% Li (3.0–4.7%  $\text{Li}_2\text{O}$ ) in some deposits, but theoretically it has 2.27% Li (4.88%  $\text{Li}_2\text{O}$ ). Naturally occurring petalite is transformed to  $\beta$ -spodumene at high temperatures that is more responsive towards leaching (Garrett, 2004).

## **2.3. Lepidolite**

Lepidolite is not a prime source of lithium. It belongs to mica group of minerals with a color resembling to lilac gray (Gem select, 2009). It is present with other lithium bearing minerals like spodumene in pegmatite builds. It is characterized by an uneven fracture type. Most common application of lepidolite is in glasses and ceramics production (Tadesse et al, 2019). Li content varies from 1.39% (3.0%  $\text{Li}_2\text{O}$ ) to 3.58% Li (7.7%  $\text{Li}_2\text{O}$ ). In addition to lithium, presence of significant amounts of rubidium makes lepidolites an important source of Rb (Wietelmann and Bauer, 2003). For enrichment of lepidolite, main gangue minerals are required to be separated that include muscovite, calcite, quartz and feldspar. Flotation is the most commonly used technique for this purpose (Choi et al, 2012). Sulphuric acid digestion is one of the methods used for the extraction of Li from lepidolite that is carried out at temperatures higher than 250 °C.

## **2.4. Amblygonite**

The economical deposits of amblygonite (3.5–4.4% Li) are rare and found in Canada, Brazil, Surinam, Zimbabwe, Rwanda, Mozambique, Namibia, and South Africa (Garrett, 2004). Common methods to separate amblygonite from other lithium minerals and silicate gangue include DMS and flotation (Bulatovic, 2015).

## **2.5. Zinnwaldite**

Zinnwaldite is not an attractive source of lithium because of its high FeO and MnO contents (up to 11.5% and 3.2% respectively) (Paukov et al., 2010). An important reserve of zinnwaldite

is found in the Czech Republic/Cinovec, Erzgebirge at the German/Czech border containing 20 wt% zinnwaldite, (Chelgani et al., 2015; Leißner et al., 2016; Wietelmann and Bauer, 2003). Lithium and rubidium were suggested to be produced from the zinnwaldite wastes of Sn–W ores processing (Jandová et al., 2010). Aeromine series collectors were used to float zinnwaldite from tin-tungsten tailings (Jandová and Vu, 2008; Samkova, 2009). Moreover, the magnetic properties of zinnwaldite due to the high content of iron makes magnetic separation a potential separation method that is followed by water leaching to precipitate  $\text{Li}_2\text{CO}_3$  concentrate of high purity; i.e, >99% (Jandová et al., 2009).

## **2.6. Eucryptite**

Eucryptite ores contain 2.1–3.0% Li (4.5–6.5%  $\text{Li}_2\text{O}$ ) and found their application in glass manufacturing industry. The deposits of The Bikita deposit in Zimbabwe has an average grade of 2.34% Li (5 %  $\text{Li}_2\text{O}$ ). Eucryptite deposits are small in tonnage and not common (Garrett, 2004). Roasting of eucryptite is not required and direct leaching with strong acids is the most possible method for extraction of lithium (Tadesse et al., 2019).

## **3. Beneficiation of lithium ores**

The major lithium beneficiation techniques include gravity and dense media separation (DMS), magnetic separation, and froth flotation while size separation is another potential method that has been recognized in recent years.

### **3.1. Beneficiations using grade by size department**

The ‘Millennium Super Cycle’ from 2003-11 has left the minerals industry with elevated costs, declining ore quality and less efficient functional practices because during this period quantity became the focal point and quality was ignored to achieve high throughput (Walters, 2016). As a result, there is a production and speculation crisis in the mineral industry. Decreasing feed grades have become unavoidable for mining operations due to ore deposit geology and mining technologies. But there are several problems associated with processing of low-grade deposits that have negative effects on the productivity i.e., high cost of energy and capital intensity is involved to process and reject waste materials. An alternative way to mitigate these problems

can be the use of coarse rejection technologies, leading to grinding of middle and high-grade ores and thus reducing of grinding energy.

Five technologies ‘levers’ of Grade Engineering® that are believed to deliver coarse separation outcomes (>10mm) are characterised as Natural preferential grade by size department, differential blasting for grade, sensor based bulk sorting, sensor-based stream sorting and coarse gravity separation. Coarse separation can be applied as individual levers or as sets of levers for specific ores and processes. It is important to understand the comparative response traits through a process of physical testing and imitation. Coarse separation produces two or more streams with different grade or physical properties. In Grade Engineering® relative difference between separated fractions and feed grade is referred to as a Ranking Response (RR) (Carrasco et al, 2015 and 2016). Ranking Response (RR) depends on the type of rock and how it interacts with separation lever technologies. It is a function of mass pull: small mass retained (10-30%) giving a high Ranking Response (RR) while high mass retained results in low values.

Response Rankings range can be between 0 and 200. 200 is the maximum theoretical response and the method can be used for testing and simulation results for all five levers. Higher RR provides higher opportunity to produce two or more separated streams of different grades that can change existing economic destination decisions. One of the main features of Grade Engineering® opportunity evaluation is the ability to place RR’s into an international relative ranking. Experience shows that there is high economic possibility for average deposit scale RR’s greater than 70 for specific levers or set of lever combinations. An average RR’s greater than 100 represent transformational Grade Engineering® opportunity.

### **3.1.1. Grade by size department after blasting and primary crushing**

Preferential breaking and concentration of specific minerals into different size segments during the process of blasting and primary crushing is a well-known fact but has limited applications at industrial scale (Bowman and Bearman, 2014). Some ores exhibit tendency of natural preferential breakage in response to blasting and primary crushing, resulting in concentration of valuable minerals into specific size fractions, this phenomenon is known as Natural Preferential Grade by Size Department (PGS). The valuable minerals can be concentrated mostly in finer size fractions and less likely into coarser fractions depending on the geological



settings (Rutter, 2017; Walters, 2016). No specific relationship has been identified between the blasting magnitude or particle size distributions and the head grade because preferential grade department varies with the rock mass properties, texture, ore paragenesis and mineralogy at a range of scales, especially the texture is considered more important controlling factor than the abundance of a minerals (Rutter, 2017; Walters, 2016).

After blasting and primary crushing, screening is performed for physical separation followed by grade by size testing that is conducted on samples obtained from blasting and crushing material (i.e., materials from +/- primary crushing and crushing drill core). Minimum four size fractions were collected to develop statistically meaningful grade by size response curves (Rutter, 2017; Walters, 2016).

### **3.1.2. Grade by size department after differential blasting**

Differential blasting for grade (DBG) is based on the concept of a controlled blast design to achieve desirable size department. The idea of grade by size department after differential blasting can be employed at bench or stope scale to condition sub-volumes of material through customized blast designs to produce controlled size distributions with higher grade concentrated in finer fractions (Rutter, 2017; Walters, 2016). In the DBG technique, the objective is to apply high blasting energy for the high-grade material to target metal department into finer fraction and low blasting energy for the low-grade material to fracture it lightly to generate low grade coarser size fraction (Rutter, 2017; Walters, 2016). Blasting is followed by screening to separate the two fractions. In DGB design, a number of factors are involved to control the blast energy including powder factor, explosive type, stemming intervals and blast hole spacings/designs. The increase in fine fractions at blasting stage would increase the throughput and at the same time the energy consumption for semi-autogenous mill (SAG) and ball mill would be reduced (Rutter, 2017; Walters, 2016).

Large scale differential blast was successfully carried out at an open pit precious metal operation where narrow reef structures were involved (Walters, 2016). Mill sampling results showed two times higher upgrade factor than the normal average feed grade (Walters, 2016). As a result of the differential blast design with locally higher powder factors involvement, energy intensity increased for blasting but at the same time, energy intensity in the comminution cycle decreased (from 225 to 111 kWhr/oz) (Rutter, 2017; Walters, 2016).

### **3.1.3. Grade by size department after using sensor-based bulk and stream sorting**

Sorting is a method where various material properties such as colour, density or electromagnetism are exploited for separation. It can be manual sorting by using hands or it can be automated sorting by using mechanical assistance (Tadesse et al., 2019). In hand sorting, experienced individuals with the knowledge of mineral properties like density/ weight or color of ores separates the valuable minerals from the gangue by hand (Fenby, 2014), for example hand sorting of spodumene (Munson and Clarke, 1955) and gold ores (Barton and Peverett, 1980) was a practical ore beneficiation method in early days. However, gradual increase of low-grade ore processing involving fine grinding for liberation reduced the popularity of hand sorting (Wills and Finch, 2016). That gave rise to automated ore sorting methods (Ketelhodt, 2009; Wills and Finch, 2016). Automated sorting finds limited application in lithium ore beneficiation. A study by Brandt and Haus (2010) claimed high grade spodumene by exploiting different colour, morphology and grain size of lithium pegmatite ore, quartz and a K-feldspar, but the grade and recovery remained unknown. The similarities between the colors of spodumene and associated gangue minerals could be the possible challenge to use this method.

Sensor based sorting is a vast variety of technologies having a potential to remotely evaluate coarse material for elements and minerals of importance at detection levels and for precise decision making in operations. It can be an advanced technology to examine surface properties in real time or one that can rapidly penetrate into rock mass volumes like shovel buckets, trucks or conveyor belts (Walters, 2016).

On-line sensors and sorting development have a wide use in recycling and food processing industry where the main objective is to remove materials like electronic scrap, plastic bottles, demolition debris and paper. Most of these techniques are not easily applicable into the bulk mining industry (Walters, 2016).

Bulk sensor-based sorting is considered as a main worldwide upcoming technology for base and precious metal industry and significant development and assessment work is being done in this field. But more efforts and research is required for regular site applications in the base and precious metal mining industry (Walters, 2016).

### 3.2. Dense media and gravity separation

The presence of other valuable minerals (i.e., minerals of tin and tantalum) with lithium minerals, makes the beneficiation process of pegmatite ore more complex. Recovering these minerals as by-product results in additional operational stages. For example, spiral circuit is introduced while treating Bernic lake pegmatite to recover tantalum minerals (Ferguson et al., 2000). Similarly, heavy metals (like SnO<sub>2</sub>, Ta<sub>2</sub>O<sub>5</sub> and Fe<sub>2</sub>O<sub>3</sub>) are removed by using spiral and shaking table as gravity separation techniques during processing of Greenbushes' pegmatite ore (Bale and May, 1989).

Dense media separation (DMS) also known as heavy media separation is a pre-concentration method that exploits the difference in specific gravities of the valuable and gangue minerals to reject the gangue minerals before grinding. This technique is very useful in separating spodumene from associated gangue silicates, because spodumene is slightly heavier (with specific gravity 3.1 - 3.2 g/cm<sup>3</sup>) than most of the attached gangue minerals (for example, quartz, albite and muscovite with specific gravities 2.65, 2.60 and 2.8 g/cm<sup>3</sup> respectively). As a result gangue minerals are rejected during DMS in floats while spodumene is recovered as a sink. The first DMS plant is claimed to be established at the Edison mine in the US in 1949 (Munson and Clarke, 1955) where a ferrosilicon and magnetite mixture was utilised as a medium of specific gravity of 2.70 g/cm<sup>3</sup>. The result was a spodumene concentrate of 5.36% Li<sub>2</sub>O and 47.4% recovery (Munson and Clarke, 1955). Redeker (1979) reported 3.5% Li<sub>2</sub>O and 50–60% recovery from a feed with head grade of 1.3% Li<sub>2</sub>O and -10 mm + 212 μm size. In another study (Amarante et al., 1999), feldspar, quartz and muscovite containing ore from Portugal produced 5.17% Li<sub>2</sub>O with 61.1% recovery using bromoform as dense medium. Feed size plays an important role in spodumene recovery and grade (Amarante et al., 1999).

Beneficiation of pegmatite minerals using DMS has been challenging; attributed to a number of factors. First being the small differences in specific gravity (SG) of gangue minerals (e.g., iron bearing silicates such as amphibole) and the target minerals (e.g., spodumene) that makes the separation difficult. Secondly, the SG of spodumene is reduced due to its mineralogical transformation to micaceous and clay minerals as compared with its pure form resulting in further reduced difference between the SG of spodumene and gangue minerals (Munson and Clarke, 1955). Third reason is that the spodumene has a tendency of breaking into acicular particles that can float with gangue minerals affecting the process efficiency (Munson and

Clarke, 1955). The combined effect of these factors results in reduced recoveries of spodumene beneficiation through DMS. Regardless of these limitations, DMS is still used as an effective pre-concentration technique in beneficiation of spodumene ore for coarse particle size (i.e. –850 + 500  $\mu\text{m}$  size fraction). The use of produced coarse grain spodumene concentrate in ceramic and glass manufacturing is one of the few applications (Aghamirian et al., 2012). The undersize of this DMS circuit feeds a flotation circuit (Ferguson et al., 2000). Though, it should be noted that the degree of liberation of spodumene at coarsest grain size is very important for an efficient dense media separation process (Aghamirian et al., 2012).

### **3.3. Magnetic separation**

DMS and/or flotation is not effective when iron bearing minerals, such as amphibole and tourmaline (Bale and May, 1989) are present as gangue in lithium pegmatite ores (Tadesse et al., 2019). Large quantities of iron bearing gangue minerals can be removed by magnetic separation either before flotation or after flotation to make the concentrate acceptable for ceramics and glass manufacturing purpose.

The practice at Greenbushes' pegmatite is a good example of magnetic separation where iron bearing mineral "tourmaline" is removed by wet high intensity magnetic separators before feeding the flotation circuit (McVay and Browning, 1962; Jirestig and Forssberg, 1994). Similarly high iron content of zinnwaldite makes it suitable for magnetic separation from tin-tungsten mining tailings in the Czech Republic (Botula et al., 2005) due to its high magnetic susceptibility of zinnwaldite;  $270 \times 10^{-9} \text{ m}^3/\text{kg}$  (Leißner et al., 2016). The magnetic separation efficiency can be evaluated using automated mineralogy (Leißner et al., 2016). A study showed that the use of relatively broad magnetic induction range ( $3500\text{--}7200 \times 10^{-4}$  Tesla) can recover strongly magnetic zinnwaldite into the magnetic concentrate fraction Botula et al., (2005). Alternatively, a 2.07%  $\text{Li}_2\text{O}$  concentrate at a recovery of 73% was obtained by using wet high intensity magnetic separation on a zinnwaldite flotation concentrate at Trelavour Downs and Rostowrack mine in the UK (Siame and Pascoe, 2011).

### **3.4. Flotation**

The most widely used beneficiation method for lithium minerals (i.e., spodumene) is froth flotation, particularly for complex and low-grade ores (Tadesse et al., 2019). The surface

characteristics of minerals play significant role in froth flotation process when the average particle size or difference in specific gravities between the valuable and gangue are not sufficient for effective separation by gravity. Both reverse and direct flotation methods are used for lithium minerals concentration from pegmatite ores. Cationic collectors are employed in reverse flotation to float gangue minerals while spodumene concentrate is recovered in tailings. On the other hand, anionic collectors are used in direct flotation to recover spodumene in as float and gangue are rejected in tailings (Redeker, 1979). Flotation produces a high-grade lithium concentrate as compared with other separation techniques like DMS (Amarante et al., 1999; Menendez et al., 2004). Due to its higher performance, flotation dominated DMS as a beneficiation method for spodumene in pegmatite ores in the early 1960s (Redeker, 1979). The similar mineralogical properties lithium bearing minerals and the associated gangue minerals make selective flotation of lithium minerals a challenging process (Moon and Fuerstenau, 2003) and (Choi et al., 2012; Vieceli et al., 2016a). The selective flotation of lithium bearing minerals is influenced by a number of factors such as the chemistry of minerals, concentration and type of collector, pH of the suspension, chemical pre-treatment methods and the presence of slimes.

Surface characteristics of aluminosilicate minerals (e.g., the charge, hydrophobicity and free energy) are controlled by the crystal chemistry such as basal planes and cleavage edges) and are reported to influence the flotation (Gupta and Miller, 2010; Yin et al. 2012).

Bonding potential of oxygen in Si-O bond of silicate minerals is not fully utilized because silicon atom in  $(\text{SiO}_4)^{4-}$  tetrahedral framework is shared by four oxygen atoms (Tadesse et al., 2019). Therefore, silicates with different sets of physical and chemical properties are the result of various structural modifications based on the number of oxygen atoms shared in  $(\text{SiO}_4)^{4-}$  tetrahedral structure. As a consequence, comminution of some minerals, for example spodumene, microlite and beryl will result in breaking more Si-O bonds leading to similar points of zero charges between them and similar flotation behaviours (Tadesse et al., 2019). Two unsatisfied coordinates on  $\{1\ 1\ 0\}$  and just one broken Al-O bond on the  $\{0\ 0\ 1\}$  crystal plane result in hydrophobicity variation on the spodumene crystalline planes of  $\{1\ 1\ 0\}$  and  $\{0\ 0\ 1\}$  (Moon and Fuerstenau, 2003) thus making surface chemistry a significant factor in selective flotation of spodumene. Moon and Fuerstenau (2003) suggested  $\{1\ 1\ 0\}$  cleavage plane of spodumene to be the most favourable site for chemisorption of sodium oleate molecules. Zhu et al. (2015) observed that dry grinding exposed more  $\{0\ 1\ 0\}$  crystal plane

while wet grinding exposed more  $\{1\ 1\ 0\}$  planes on the surface of spodumene resulting in higher oleate adsorption density on the surface of wet ground spodumene sample as compared to the dry ground spodumene sample. Consequently, the flotation recovery of wet ground sample was higher than the dry ground sample.

Surface charge is another important factor to determine the flotation behaviour of silicate minerals with similar surface properties (for example spodumene and lepidolite). Surface charge of minerals is assessed in terms of isoelectric point (IEP) using zeta potential measurement at different values of pulp pH. Most lithium bearing minerals have an IEP of less than 3 which is similar to associated silicate gangue minerals like quartz, albite, feldspar and muscovite that have IEP of (2.5), (2.3), (2.15) and (1.0) respectively (Choi et al., 2012; Tian et al., 2017; Fuerstenau and Pradip, 2005). The use of cationic collector for selective flotation of lithium minerals becomes challenging due to the similar IEP values of target and gangue minerals.

#### **3.4.1. Flotation of spodumene**

Oleic acid, sodium oleate, sulphonated and phosphorated fatty acids are widely used anionic collectors in spodumene flotation (Norman and Gieseke, 1940). Using oleic acid can produce up to 90% spodumene recoveries with 6.52%  $\text{Li}_2\text{O}$  concentrate grade (Norman and Gieseke, 1940). For example, Cleveland County (United States) pilot plant studies of spodumene flotation from pegmatite ore showed 76.7% spodumene recovery and 6.4%  $\text{Li}_2\text{O}$  by using oleic acid (McVay and Browning, 1962). On contrary, cationic collectors such as amine acetate are used in reverse flotation to reject quartz, feldspar and mica in froth (Banks et al., 1953). It was observed that increase in oleate ions concentration increases the adsorption density of oleic acid and sodium oleate onto the spodumene surface (Moon and Fuerstenau, 2003; Yu et al., 2015b) with an optimum adsorption at pH 8–9 to give the maximum spodumene flotation at this point (Moon and Fuerstenau, 2003; Yu et al., 2015b; Zhu et al., 2015). Maximum adsorption was also observed at pH where significant change in zeta potential of spodumene-oleate system was observed (Moon and Fuerstenau, 2003). Also, investigation on surface tension of oleic acid solutions indicated that the surface tension was minimal at around pH 8 to 9 which corresponds to maximum flotation of spodumene. The low surface tension of oleic acid at these pHs was ascribed to strong hydrophobicity of the oleic acid collector (Yu et al., 2015b).

The combined use of anionic and cationic collectors improved the selective flotation from the gangue minerals (i.e., feldspar and mica) (Xu et al., 2016a). Cationic collectors when used alone (i.e., dodecylamine) produce high recoveries with low selectivity while anionic collectors produce opposite results (Wang et al., 2018). Xu et al. (2016a, 2016b) showed that using a combination of sodium oleate (NaOL) and dodecyl ammonium chloride (DTAC) in a molar ratio of 9:1, a higher recovery and high selectivity were obtained in the flotation of spodumene from feldspar, partially attributed to the higher density molecular arrangement and increased surface activity in the mixture of NaOL and DTAC than in NaOL or DTAC alone (Tian et al., 2017). Starch and dextrin are used to depress spodumene in the reverse flotation (Redeker, 1979). Flotation of calcium ion-activated spodumene is influenced by using sodium carbonate as a depressant for feldspar when a mixture of anionic and cationic collectors is used (Xu et al., 2016a). Quartz is depressed by using quebracho extract when spodumene is floated with oleate (McVay and Browning, 1962). Limited literature is available on the use of depressants in spodumene flotation.

Studies showed that polyvalent metal cations such calcium and ferric ions can be used as activators during the flotation of spodumene (Yang, 1978; Wang and Yu, 2007; Jie et al., 2014; Yu et al., 2014). However ferric ions were observed to be better activators than calcium ions (Wang and Yu, 2007).

### **3.4.2. Effects of chemical pre-treatment and de-sliming**

The pre-treatment of lithium ores dates back to 1940s and is an important step that is carried out to clean the surface or to alter the surface properties of the minerals (Norman and Gieseke, 1940). NaOH, Na<sub>2</sub>S and NaF are commonly used chemicals for the pre-treatment of lithium pegmatite ores (Moon and Fuerstenau, 2003; Yu et al., 2015a). An improved flotation of spodumene was observed by adding 225 g/t NaOH to the grinding mill (Kings Mountain operations in the US) for cleaning of spodumene before sending it to the flotation circuit (Redeker, 1981). The higher spodumene flotation is attributed to the enhanced interaction between the collector and the exposed aluminum sites on spodumene (Moon and Fuerstenau, 2003; Xu et al., 2016b). By increasing the sodium hydroxide dosage, flotation recovery of spodumene also increased (Yu et al., 2015a).

Detrimental effects of slimes on the flotation circuit leads to the de-sliming before the feed is entered to the flotation circuit. The selective flotation is improved by removing the  $-20\ \mu\text{m}$  size fraction (Bale and May, 1989) using hydro cyclones.

#### 4. Calcination of spodumene

Calcination is a process of converting spodumene from its  $\alpha$ -phase to the  $\beta$ -phase by heating the spodumene at around  $1000\text{--}1100\ \text{°C}$  (Ellestad and Leute 1950, Salakjani et al., 2016 & 2017). The transformation is associated with a volumetric expansion making lithium atoms more moveable to be attacked by extraction reagents. Calcination is also used to promote beneficiation of spodumene as  $\beta$ -spodumene is chalky, soft, and easy to grind structure as compared to gangue minerals like quartz and feldspar. For this reason, grinding the product of calcination followed by size separation has been considered as a process to enrich spodumene (Peltosaari et al. 2016). The suitable heating devices to perform calcination can be muffle furnaces, direct fire furnaces (Ellestad and Leute 1950) or a rotary kiln (Ellestad and Leute 1950; Dwyer and Passaic 1957). Salakjani et al., (2017) and Peltosaari et al., (2015) have investigated hybrid microwave as well as a potential medium of heating source for the calcination of spodumene.

Since 1950, when this process was first patented (Ellestad and Leute; 1950), phase transformation during calcination (also known as decrepitation) is considered the key factor in processing of hard rock lithium ore for lithium extraction. In this conventional process, spodumene ore is crushed and then heated in a furnace at high temperatures (i.e above  $950\ \text{°C}$ ) for more than 30 min to ensure complete phase transformation from  $\alpha$ -spodumene to  $\beta$ -spodumene. It is accompanied by an extensive volume expansion of  $\alpha$ -spodumene up to 27% (Brook, 1991). The calculations show that the lattice volume of  $\gamma$ -spodumene is 8% higher than  $\alpha$ -spodumene and that of  $\beta$ -spodumene is 17% higher than  $\gamma$ -spodumene. As far as the energetics are concerned, transformation from  $\alpha$ -spodumene to  $\beta$ -spodumene and  $\gamma$ -spodumene to  $\beta$ -spodumene transformations are described to be endothermic (Botto et al., 1976) whereas conversion from  $\alpha$ -spodumene to  $\gamma$ -spodumene is reported to be exothermic.

Calcination is a necessary pre-treatment step in lithium extraction to covert  $\alpha$ -spodumene, which is a monoclinic crystal structure with specific gravity  $3.15\ \text{g/cm}^3$  to  $\beta$ -spodumene which is tetragonal crystal structure of lower specific gravity, i.e.  $2.40\ \text{g/cm}^3$ . (Barbosa et al., 2014;



Djingheuzian, 1957). The volumetric expansion is considered to be the main cause of higher reactivity of  $\beta$ -spodumene than  $\alpha$ -spodumene and can be efficiently treated for lithium extraction (Barbosa et al., 2014; Rosales et al., 2014; Ellestad and Leute, 1950) by leaching process.

There are three possible phases of spodumene. Naturally spodumene occurs as  $\alpha$ - phase with the chemical formula  $\text{LiAlSi}_2\text{O}_6$ . It has monoclinic crystal structure and is the densest of all occurring phases of spodumene with a density of  $3.184 \text{ g/cm}^3$ .  $\alpha$ - Spodumene phase is not chemically reactive in the presence of strong acids. Second phase is known as  $\beta$ -spodumene and it has a tetragonal structure (Li and Peacor, 1968; Keat, 1954).  $\beta$ -Spodumene phase is a less densely packed structure with a density of  $2.374 \text{ g/cm}^3$ .  $\alpha$ -Spodumene is heated at elevated temperatures above  $950 \text{ }^\circ\text{C}$  to obtain the  $\beta$ -spodumene phase. A recently discovered third phase is believed to appear during conversion process (Moore et al., 2018, Salakjani et al., 2019, Dessemond et al., 2019). It appears before  $\beta$ -spodumene and is identified by different terms; virgilite,  $\gamma$ -spodumene or spodumene III (Peltosaari et al., 2015). This phase is a hexagonal structure and possess a density of  $2.399 \text{ g/cm}^3$ . The relationship between the three known phases of spodumene and other lithium silicates for example petalite and eucryptite in quartz saturated system is shown in Figure 6.

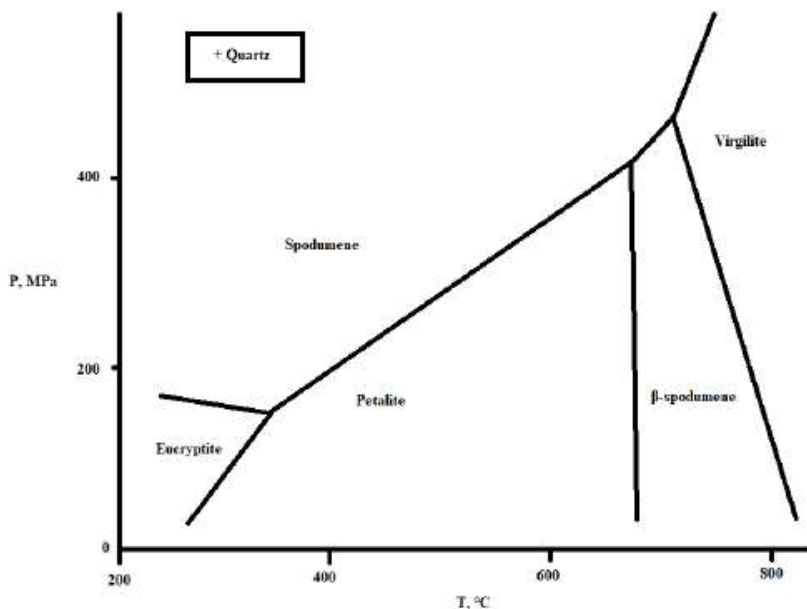


**Figure 6.** Stability relationship between  $\alpha$ -spodumene ( $\text{LiAlSi}_2\text{O}_6$ ),  $\beta$ -spodumene ( $\text{LiAlSi}_5\text{O}_{12}$ ),  $\gamma$ -spodumene/ virgilite ( $\text{LiAlSi}_5\text{O}_{12}$ ), eucryptite ( $\text{LiAlSiO}_4$ ) and petalite ( $\text{LiAlSi}_4\text{O}_{10}$ ) in the system  $\text{LiAlSiO}_4\text{-SiO}_2\text{-H}_2\text{O}$  (Dessemond et al., 2019).

Figure 7 shows the crystal structures of three phases of spodumene. It can be observed from the microscopic view of  $\alpha$ -spodumene (Figure 7 (a)) that it is a compacted dense structure where multiple layers are arranged over each other. On the other hand,  $\beta$ -spodumene (Figure 7 (b)) displays a relatively open structure where the layers are less densely packed with visible cracks on particles (Dessemond et al., 2019). The structure of  $\gamma$ -spodumene (Figure 7 (c)) resembles high quartz. The crystal volume reduction of 67% has been observed during  $\alpha$ -phase to  $\gamma$ -phase conversion accompanied by an expansion of 75% during the following  $\gamma$ -phase to  $\beta$ -phase of spodumene giving a total of about 30% expansion in crystal structure upon completion of  $\alpha$ -spodumene to  $\beta$ -spodumene phase change (Salakjani et al., 2019).

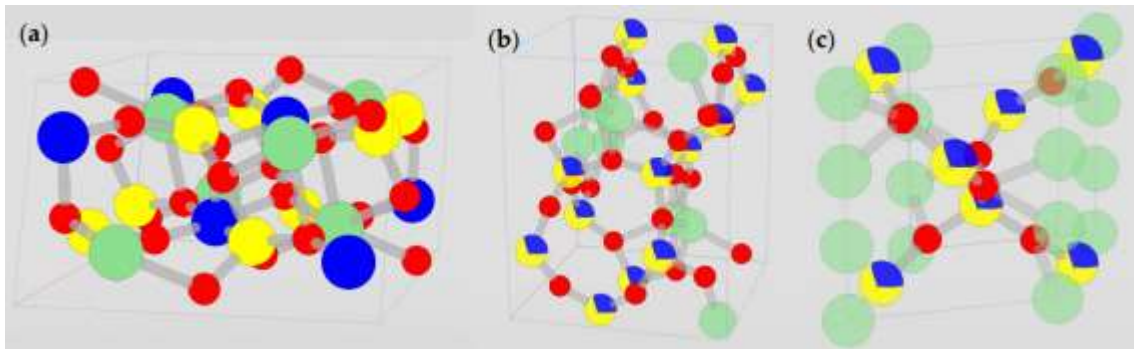


**Figure 7.** Crystal structures of spodumene. (a)  $\alpha$ -spodumene, (b)  $\beta$ -spodumene, (c)  $\gamma$ -spodumene. Red: Oxygen. Yellow: Silicon. Blue: Aluminum. Green: Lithium. Note: The lattices images were obtained with the display module of the Jade2010™ software (Dessemond et al., 2019)

## 5. Hydrometallurgy

The five common hydrometallurgical techniques include acid, alkali, sulphate roasting/autoclaving, carbonate roasting/autoclaving and chlorinating method (Li et al., 2019); some of these are mixed pyro met/ hydro met processes, such as roasting. Acid method uses sulfuric acid ( $H_2SO_4$ ) and can attack  $\beta$ -spodumene only because  $\alpha$ -spodumene does not react with  $H_2SO_4$  (Zeelikman et al., 1966). On the other hand, use of fluorine (in form of hydrofluoric acid (HF) and fluorite ( $CaF_2$ )) has been reported to extract lithium from  $\alpha$ -spodumene directly because HF reacts intensively with silica ( $SiO_2$ )-based materials. Similarly, a strong alkali like sodium hydroxide (NaOH) has the capacity to break Si-O bond (Wilson et al., 1994). It has been reported that lithium can also be extracted from both  $\alpha$ - and  $\beta$ -spodumenes by roasting or autoclaving with carbonates, sulphates and chlorides (Zeelikman et al., 1966).

## 5.1. Leaching with strong acid

Galaxy Resources China was the first to use  $\text{H}_2\text{SO}_4$  method to recover lithium from  $\beta$ -spodumene in 2012 (Meshram et al., 2014) with the final products as lithium and sodium sulfate ( $\text{Na}_2\text{SO}_4$ ). At present, this method dominates the industry for lithium extraction from spodumene (Tadesse et al., 2018; Sardar and Mubashir, 2012). Though, this is still a dominant method but it has some limitations, like increased equipment cost due to the use of concentrated  $\text{H}_2\text{SO}_4$ , acid gas emission (Archambault et al., 1962), Li loss due to the precipitation of voluminous Fe and Al impurities (Dwyer and Passaic 1957)., difficulty to optimize the temperature and energy recovery in case of a rotary kiln (Ellestad and Leute, 1950) and dealing with recovered  $\text{Na}_2\text{SO}_4$  is another issue.

Hydrofluoric acid can be used for  $\alpha$ - and  $\beta$ -spodumene to etch silica ( $\text{SiO}_2$ )-based materials (i.e., glass and stoneware) (Davis, 2000). It also finds its application for digestion of silicate minerals for analytic reasons (Samchuk and Pilipenko, 1987), and to recover diamonds from silicate minerals, such as Venetia diamond mine in South Africa. A 40% concentrated HF was reported to extract Li from  $\alpha$ -spodumene at 127 °C (Kuang et al., 2012). More recently, Rosales et al. (2014) found that Li, Al and Si can be leached from  $\beta$ -spodumene by using HF and can be recovered later from the leached solution. More precisely, leaching for 20 min with 7% HF at 75 °C and 1.82% solid/liquid ratio resulted in extraction of 90% Li from  $\beta$ -spodumene (Rosales et al., 2014). Temperature and time were observed to be significant variables during this process (Rosales et al., 2014). Addition of sodium hydroxide (NaOH) to the leached solution precipitated Al and Si as Sodium aluminum fluoride ( $\text{Na}_3\text{AlF}_6$ ) and sodium hexafluorosilicate ( $\text{Na}_2\text{SiF}_6$ ), respectively. Lithium can be recovered as  $\text{Li}_2\text{CO}_3$  by carbonation. A low leaching temperature and lesser leaching time, makes this process energy and time efficient as compared with sulfuric acid method (Rosales et al., 2014). The drawbacks of this method include the production of voluminous mixed fluoride-salt waste with a problematic disposal.

Guo et al. (2017) investigated the leaching mechanism of combined HF and  $\text{H}_2\text{SO}_4$  effect on  $\alpha$ -spodumene to avoid using high energy for spodumene phase conversion from  $\alpha$  to  $\beta$ . 90% lithium (with 1.5 g/L concentration) was observed to be mobilized into leachate when the conditions were optimum. This method is a significant development as it does not involve a high temperature phase transformation and treats  $\alpha$ -spodumene directly. On the other hand,

intensive use of HF, the recovery of Al and disposal of hexafluorosilicic acid ( $\text{H}_2\text{SiF}_6$ ) are problematic issues associated with this method.

As HF is highly corrosive and toxic, some studies have utilized fluoride instead, to extract lithium from spodumene. Kuang et al. (2012) suggested use of fluorite ( $\text{CaF}_2$ ) and  $\text{H}_2\text{SO}_4$ . The direct use of fluorite is more economical with less safety concerns. This method is reported to be recommended for pilot scale and is considered as a potential application for low grade Li-bearing minerals (Griffin, 2017). However, till date, not much information has been revealed about this method.

## 5.2. Leaching with base

Alkali can react to break Si-O bond to dissolve  $\text{SiO}_2$  in solution, and this effect increases with an increase in alkalinity and temperature of the solution (Leemann et al., 2011; Wilson et al., 1994). This alkaline-silica-reaction was investigated in some studies where lithium was directly extracted from  $\alpha$ -spodumene (a silicate mineral) by using an alkali. For example, Martin (2018) extracted lithium from  $\alpha$ -spodumene in an autoclave by using NaOH, although optimum conditions resulted in 40% extraction efficiency that could be due to the low concentration of NaOH. In another study (Xing et al., 2019), 600 g/L (15 M) NaOH was used at liquid/solid ratio of 5 and at a temperature of 250 °C for 2 hours and as a result 95.8% lithium extraction efficiency was achieved. Lithium was recovered as precipitates of  $\text{Li}_2\text{CO}_3$ . This method avoids calcination by extracting lithium from  $\alpha$ -spodumene at a higher efficiency (Xing et al., 2019). The use of caustic in large amount would require highly anti-corrosive equipment and thus the increased operational safety.

Alkali has the capability to treat  $\beta$ -spodumene as well. McIntosh (1946) reported digestion of  $\beta$ -spodumene in an autoclave by using lime as the main extracting agent. Lithium was leached as lithium hydroxide ( $\text{LiOH}$ ) and the impurities (Fe, Al and Mg) were remained in the residue. The supply of carbon dioxide ( $\text{CO}_2$ ) to the leaching solution results in  $\text{Li}_2\text{CO}_3$  precipitates with 97.8% purity (Choubey et al., 2016; McIntosh, 1946). In another recent patent (Kuang et al., 2014)  $\beta$ -spodumene was digested at 90–250 °C in a CTFR (continuous tubular-flow reactor) at 0.1–1.5 MPa with a  $\beta$ -spodumene/NaOH/lime/water mass ratio of 1/ (0.05–0.35)/(0–0.3)/(1.5–6), and the flow rate in CTFR was kept as 0.08–0.8 m/s. The resultant solution of  $\text{LiOH}$  was later concentrated, purified and crystallized to produce  $\text{LiOH}\cdot\text{H}_2\text{O}$  product. This method uses

less amount of alkali leaving silicone in the residue as compared with the previous method where  $\alpha$ -spodumene was treated with alkali. Moreover, LiOH is the preferred form of lithium salt and has greater value than  $\text{Li}_2\text{CO}_3$  for electrical vehicle batteries (Tadesse et al., 2018).

### **5.3. Sulphate roasting/autoclaving method for $\alpha$ - and $\beta$ -spodumene**

Use of molten alkali sulphate (including  $\text{Na}_2\text{SO}_4$ ) to extract lithium from silicate was patented by Arne and Johan (1941). This method could extract 90% lithium from  $\alpha$ -spodumene grains in only 10 min at 1000 °C. In another work by Zeelikman et al. (1966)  $\alpha$ -spodumene was roasted with potassium sulphate ( $\text{K}_2\text{SO}_4$ ) at 920–1150 °C. Being a reversible reaction, a large amount of  $\text{K}_2\text{SO}_4$  was required for efficient lithium extraction ( $\text{LiSO}_4$ ). Kuang et al. (2018) showed an autoclaving method where lithium could be extracted from  $\beta$ -spodumene by using  $\text{Na}_2\text{SO}_4$  and calcium oxide (CaO) or NaOH (lithium extraction of 93.30% or 90.70% respectively under optimum conditions). The ion exchange between  $\text{Li}^+$  and  $\text{Na}^+$  was found to be the basis of extraction mechanism in X-ray diffraction (XRD) analysis of the residue.

This method could control the dissolution of Al and Fe significantly, simplifying the following steps and also reduces the possible lithium losses. Moreover, the cheap cost and recyclability of  $\text{Na}_2\text{SO}_4$  could make the whole process more economical. The main concern in this method is the expensive grinding costs that would be involved to achieve the fine particle size (39  $\mu\text{m}$ ) (Kuang et al., 2018).

### **5.4. Carbonate roasting/autoclaving method for $\alpha$ - and $\beta$ -spodumene**

The method of lithium extraction with carbonate is based on the ion exchange that takes place between  $\text{Li}^+$  and the metal ion from carbonate (usually  $\text{Na}^+$ ). Roasting at 450–750 °C (Maurice and Olivier, 1968) or autoclaving at 225 °C (Chen et al., 2011) produces  $\text{Li}_2\text{CO}_3$  and analcime.  $\text{Li}_2\text{CO}_3$  may report to residue attributed to its less solubility ( $K_{\text{sp}} = 2.5 \times 10^{-2}$ ), specially at higher temperature (Dean, 1999). Carbonation of  $\text{Li}_2\text{CO}_3$  produces lithium bicarbonate ( $\text{LiHCO}_3$ ) that is separated with residue by filtration. Later,  $\text{LiHCO}_3$  rich filtrate is heated to produce  $\text{Li}_2\text{CO}_3$  of high purity. Tiihonen et al. (2019) used conversion leaching to convert  $\text{Li}_2\text{CO}_3$  into soluble LiOH. Tiihonen et al. (2019) reported 94% lithium extraction and a battery grade purity (i.e., the purity > 56.5% LiOH) in one crystallization stage. Though this method

produces LiOH as a direct product but further treatment is required to remove impurities from the residue like Na, Al, Si and Ca. Moreover, the residue is reduced by around 10%.

Sugyeong (2018) roasted  $\alpha$ -spodumene with  $\text{Na}_2\text{CO}_3$  under certain condition (i.e.,  $\text{Na}_2\text{CO}_3$ /spodumene mass ratio as 1, temperature at 850 °C and duration of 60 min) and then leached with 1.5 M  $\text{H}_2\text{SO}_4$  for 5 h. As a result, 99.98% lithium was found to be extracted from  $\alpha$ -spodumene with 75% of aluminum and silicon (Sugyeong, 2018). This method is energy efficient as no phase change is involved with high lithium extraction efficiency. This method has some drawbacks like high  $\text{Na}_2\text{CO}_3$  consumption and production of unprofitable  $\text{Na}_2\text{SO}_4$  as a by-product in large amounts.

### 5.5. Chlorinating method

This method employs the use of chlorine gas ( $\text{Cl}_2$ ) and chloride as chlorinating agents. Lithium in the spodumene is converted into lithium chloride ( $\text{LiCl}$ ), being water-soluble it is recovered by leaching with water (Barbosa et al., 2013). Barbosa et al. (2014) showed a complete extraction of lithium (as  $\text{LiCl}$ ) from  $\beta$ -spodumene with 100 mL/min pure  $\text{Cl}_2$  supply in a furnace at a temperature of  $\geq 1000$  °C, with reaction completed at 1100 °C after 150 min. The limitations of this methods include the location of the lithium plant to be close to a chlor-alkali industry (for example the Kwinana industrial hub of WA), further treatment of final products (i.e.  $\text{LiCl}$ ,  $\text{FeCl}_3$ ,  $\text{CaCl}_2$ ) to avoid volatilization and contamination with each other (Barbosa et al., 2014), the risks associated with  $\text{Cl}_2$  at high temperature, the requirement of expensive materials of construction and high energy consumption for phase transfer. The possibility of treating  $\alpha$ -spodumene with chlorine can be another option that still needs to be investigated.

Barbosa et al. (2015) extracted lithium from  $\beta$ -spodumene by using calcium chloride ( $\text{CaCl}_2$ ), at a lower temperature of 700 °C. During this method,  $\beta$ -spodumene was converted to  $\text{LiCl}$ . In another study, lithium was extracted from  $\beta$ -spodumene by using a cheap and easily available chemical, sodium chloride (Gabra et al., 1975). The reaction took place under pressure and alkaline environment which was regulated by calcium hydroxide ( $\text{Ca}(\text{OH})_2$ ). This method is observed to be a simple path to produce  $\text{LiCl}$  when high purity is not a requirement. However, the purity of crystalized  $\text{LiCl}$  was reached to 99.9% by solvent extraction with n-butanol and DI water (Gabra et al., 1975).

Another not very common method is using ammonium Chloride ( $\text{NH}_4\text{Cl}$ ) to roast  $\alpha$ -spodumene directly to extract lithium. Around 97% Li was reported to be converted to LiCl by sintering  $\alpha$ -spodumene with  $\text{CaCO}_3$  and  $\text{NH}_4\text{Cl}$  at 750 °C (Medina and El-Naggar, 1984; Zeelikman et al., 1966).

## **6. Plant practices**

Few plants that produce lithium concentrate from ores include Greenbushes, Mt Cattlin, Mt Marion, and Bald Hill in Australia, Mibra in Brazil, Bernic lake in Canada, Sichuan Aba, Maerkang, Jiajika in China, Kings Mountain in United States and Bikita in Zimbabwe (Evans, 2014; Tadesse et al., 2019). The ore mineralogy principally formed the basis of beneficiation and treatment practices at each plant. A brief review of beneficiation methods employed at the selected plants has been included in this section.

### **6.1. The Greenbushes, Australia**

The Greenbushes Lithium Operations is known to be the longest continuous Li operation in Western Australia that has been producing lithium for over 25 years (Bale and May, 1989). The estimated ore reserves at Greenbushes were in excess of 30 million tonnes, with around 7 million tonnes at 4.0%  $\text{Li}_2\text{O}$  (Tadesse et al., 2019). The Greenbushes Lithium Operations consists of two processing plants; producing technical-grade lithium concentrate at one plant and chemical-grade lithium concentrate at the other plant through gravity, heavy media, flotation and magnetic separation techniques. Primary and secondary jaw crushers and tertiary cone crushers are used to reduce the particle size of ROM spodumene to -16mm for ball mill feed. Cyclones is the next stage to receive undersize fraction ( $-250 \mu\text{m}$ ) of the ball mill. The underflow of the cyclones feeds the flotation circuit and the slimes ( $-20 \mu\text{m}$ ) are removed in tailings (Bale and May, 1989). The oversize fraction ( $+250 \mu\text{m}$ ) of the ball mill is screened at  $800 \mu\text{m}$ . The obtained undersize fraction is transported through magnetic separation for glass grade spodumene production while the oversize fraction is returned to the ball mill. Fatty acid collector and soda ash are used for bulk flotation of spodumene and tourmaline in the first stage of flotation circuit. After roughing, cleaning and recleaning stages, spodumene concentrate is produced that contains 7.2%  $\text{Li}_2\text{O}$  and 0.4%  $\text{Fe}_2\text{O}_3$ . Heavy minerals such as cassiterite and tantalite are recovered through gravity separation of flotation concentrate to recover heavy

minerals while tourmaline is removed through magnetic separation. The final concentrate grade has 7.5–7.7% Li<sub>2</sub>O and <0.1% Fe<sub>2</sub>O<sub>3</sub> (Bale and May, 1989).

## **6.2. The Kings Mountain Operations, USA**

Since 1950's, The Kings Mountain was a major producer of glass, ceramic and chemical grade spodumene, but it closed its operations in 1998 when cheaper brine operations were commenced in South America (British Geological Survey, 2016). Mica, feldspar and quartz were the major by-products of The Kings Mountain operations (Tadesse et al., 2019). To achieve a higher degree of liberation, the ore with head grade of 1.64% Li<sub>2</sub>O was reduced to –16mm fraction in a ball mill with addition of about 400 g/t of NaOH for surface cleaning of spodumene. The ball mill was operated in a closed circuit with cyclone. The –15 µm slimes (accounting for 7.4% wt at 1.43% Li<sub>2</sub>O) were removed by re-cycloning the cyclone overflow. After conditioning of +15 µm material at 55% solids at neutral pH 700 g/t of tall oil fatty acid and glycol-type frother, the pulp is floated at 30% solids. Later cleaning and re-cleaning stages produced 6.34% Li<sub>2</sub>O grade concentrate at 93.5% recovery.

## **6.3. Bernic Lake lithium operation, Canada**

Spodumene processing at Bernic Lake lithium operation was started in 1984. Before that it was processing tin (since 1929) and tantalum (since 1969) being a host to more than 100 different minerals (British Geological Survey, 2016). Dense media separation, pre-flotation of amblygonite, magnetic separation and flotation are the major stages involved in the beneficiation process at the Bernic Lake (Tadesse et al., 2019). The dense media separator was fed with –12+0.5mm particle size using a mixture of ferrosilicon and magnetite as media with a density of 2.7. The lighter fraction that is K-feldspar was removed while the denser fraction or sinks were processed further after size reduction to –0.25mm through grinding. Low intensity magnetic separation was used to remove iron and gravity separation was used to remove tantalum bearing fraction. Flotation is the next stage to remove amblygonite by using starch as spodumene depressant and tall oil collector. Reverse flotation is applied to the tailings to remove soda-feldspar and quartz to produce a spodumene concentrate of grade 7.25% Li<sub>2</sub>O (Cerny et al., 1996).



#### **6.4. The Bikita Operation, Zimbabwe**

Major lithium minerals found in Bikita pegmatite deposits include spodumene, petalite, lepidolite, eucryptite and amblygonite (Knorrning and Condliff, 1987; Tadesse et al., 2019). High tonnage of lithium minerals (23,000 Mt lithium) with tantalum, tin, beryl and pollucite (Garrett, 2004; Jaskula, 2015) makes this deposit of high significance. The production of lithium minerals concentrate was reported to be about 44,000 tonnes at an average grade of 4.2% Li<sub>2</sub>O and 0.03% Fe<sub>2</sub>O<sub>3</sub> in 2014 (British Geological Survey, 2016). Hand picking of coarsely crushed run-of-mine was the main beneficiation method in the beginning which was later replaced by DMS. First stage of DMS recovers petalite concentrate in the float fraction while reprocessing of the sinks fraction at a higher media density produces spodumene concentrate.

#### **6.5. Bald Hill lithium and tantalum operations, Australia**

The Bald Hill lithium-tantalum mine started production of spodumene concentrate in early 2018 with an estimated lithium ore reserves of 18.3 Mt at 1.18% Li<sub>2</sub>O (Tadesse et al., 2019). The run-of-mine ore is first subjected to crushing to reduce the particle size to -12 mm particle size. High grade tantalite bearing ore is then separated by spirals and shaking tables. The size fraction of -1 mm is removed by screening for tantalum minerals removal through rougher spirals. Then it is sent for storage. The coarse screening -12+1mm size fraction produces two fractions i.e., a -12+5mm (coarse fraction) and -5+1mm (fines fraction). The coarse fraction is subjected to the primary coarse DMS cyclone after mixing with Ferrosilicon (FeSi) medium. The fines fraction is sent to a reflux classifier for mica removal and the underflow (fine fraction) is pumped to primary fine DMS cyclone. The FeSi is recovered from the underflows and overflows of both the fine and coarse primary DMS cyclones, the overflows are rejected, and the underflow coarse and fine fractions are mixed with a higher specific gravity FeSi and are fed to the respective secondary coarse and fine DMS cyclones. The underflow from the secondary cyclones (coarse and fines), is the main spodumene concentrate product that is obtained after FeSi removal.

### **7. Conclusions**

Different techniques are used in processing of lithium minerals from hard rock pegmatite ores containing petalite, spodumene, amblygonite and lepidolite have been discussed. Flotation and

dense media separation are the major methods used in many plants followed by calcination and leaching with strong acids such as sulfuric acid and strong alkalis. Processing of lithium minerals is very challenging due to similar properties of lithium minerals and their gangues such as specific gravity and solubility. There is not much information available about automated sorting methods in lithium ore beneficiation. However, this method may have great potential in the future because lithium minerals have different colour depending on the presence of impurities and the level of modification of the mineral. Most studies focused on the beneficiation of spodumene considering that this mineral is widely available. Detailed work on zinnwaldite, petalite, and lepidolite is required to maximize separation efficiency of these minerals from pegmatite ores.

## References

- Aghamirian, M., Mohs, C., Grammatikopoulos, T., Imeson, D., Pearse, G., 2012. An overview of spodumene beneficiation. In: 44th Annual Canadian Mineral Processors Operators Conference. pp. 141–153.
- Ahmad, S., 2020. The Lithium Triangle: Where Chile, Argentina, and Bolivia Meet. Harvard International Review.
- Amarante, M. M., Botelho de Sousa, A., Leite, M. M., 1999. Processing a spodumene ore to obtain lithium concentrates for addition to glass and ceramic bodies. *Miner. Eng.* 12 (4), 433–436.
- Archambault, M., Macewan, J.U. and Olivier, C.A., 1962. Method of producing lithium carbonate from spodumene. US Patent 3017243.
- Arne, S.K. and Johan, W.S., 1941. Method of recovering lithium salts from lithium-containing minerals. US Patent 2230167.
- Bale, M.D., May, A.V., 1989. Processing of ores to produce tantalum and lithium. *Miner. Eng.* 2, 299–320.
- Banks, M.K., McDaniel, W.T., Sales, P.N., 1953. A method for concentration of North Carolina spodumene ores. *Trans. AIME* 181–186.
- Barbosa, L.I., González, J.A., Ruiz, M.d.C., 2015. Extraction of lithium from  $\beta$ -spodumene using chlorination roasting with calcium chloride. *Thermochim. Acta* 605, 63–67.
- Barbosa, L.I., Valente, G., Orosco, R.P., González, J.A., 2014. Lithium extraction from  $\beta$ -spodumene through chlorination with chlorine gas. *Miner. Eng.* 56, 29–34.

- Barbosa, L.I., Valente, N.G., Gonzalez, J.A., 2013. Kinetic study on the chlorination of  $\beta$ -spodumene for lithium extraction with Cl<sub>2</sub> gas. *Thermochim. Acta* 557, 61–67.
- Barrera, P., 2019. [www.investingnews.com/daily/resource-investing/battery-metals-investing/lithium-investing/lithium-producing-countries](http://www.investingnews.com/daily/resource-investing/battery-metals-investing/lithium-investing/lithium-producing-countries).
- Barton, P.J., Peverett, N.F., 1980. Automated sorting on a South African gold mine J.SAIMM, 103–111.
- Botto, I. L., Arazi, S.C., Krenkel, T.G., 1976. Aplicación de la teoría de Delmon al estudio del mecanismo de la transformación polimórfica del espodumeno I a espodumeno II. *Boletín De la Sociedad Española De Cerámica Y Vidrio*, 15(1). pp. 5–10.
- Botula, J., Rucky, P., Repka, V., 2005. Extraction of zinnwaldite from mining and processing wastes. *Technical University of Ostrava – geologicka LI (2)*, 9–16.
- Bowman, D. J., Bearman, R. A., 2014. Coarse waste rejection through size based separation. *Minerals Engineering*. 62, 102–110.
- Brandt, F., Haus, R., 2010. New concepts for lithium minerals processing. *Miner. Eng.* 23, 659–661.
- British Geological survey, 2016. Minerals UK, Centre for sustainable mineral development.
- Brook, R.J. 1991. *Concise Encyclopedia of Advanced Ceramic Materials*. Pergamon Press: Oxford, England.
- Bulatovic, S.M., 2015. Beneficiation of lithium ores. *Handbook of Flotation Reagents: Chemistry, Theory and Practice*. pp. 41–56.
- Carrasco, C, Keeney and Napier-Munn, TJ, 2015. Methodology to develop a coarse liberation model based on preferential grade by size responses. *Minerals Engineering* v 86, 149-155.
- Carrasco, C.; Keeney, L.; Walters, S. G., 2016. Development of a novel methodology to characterize preferential grade by size department and its operational significance. *Minerals Engineering*, 91, 100-107.
- Cerny, P., Ercit, T.S., Vanstone, P.T., 1996. Petrology and mineralization of the Tanco rare-element pegmatite, Southeastern Manitoba, Geological Association of Canada/Mineralogical Association of Canada Annual Meeting, Winnipeg, Manitoba, May 27–29.
- Chelgani, S.C., Leißner, T., Rudolph, M., Peuker, U.A., 2015. Study of the relationship between zinnwaldite chemical composition and magnetic susceptibility. *Miner. Eng.* 72, 27–30.

- Chen, Y., Tian, Q., Chen, B., Shi, X., Liao, T., 2011. Preparation of lithium carbonate from spodumene by a sodium carbonate autoclave process. *Hydrometallurgy* 109 (1–2), 43–46
- Choi, J., Kim, W., Chae, W., Kim, S.B., Kim, H., 2012. Electrostatically controlled enrichment of lepidolite via flotation. *Mater. Trans.* 53, 2191–2194.
- Choubey, P.K., Kim, M.-S., Srivastava, R.R., Lee, J.-C., Lee, J.-Y., 2016. Advance review on the exploitation of the prominent energy-storage element: Lithium. Part I: from mineral and brine resources. *Miner. Eng.* 89 (Supplement C), 119–137.
- Claffy, E. W., 1953, Composition, tenebrescence and luminescence of spodumene minerals. *American Mineralogist*, 38(11–12). pp. 919–931.
- Colton, J.W., 1957. Recovery of lithium from complex silicates. *Advances in Chemistry*, vol. 19, American Chemical Society, pp. 3–8.
- Davis, J.R., 2000. *Corrosion: Understanding the Basics*. ASM International.
- Dean, J.A., 1999. *Lange's Handbook of Chemistry (15th Edition)*. McGraw-Hill Inc.
- Dessemond, C.; Lajoie-Leroux, F.; Soucy, G.; Laroche, N.; Magnan, J.-F., 2019. Spodumene: The Lithium Market, Resources and Processes. *Minerals*, 9, 334.
- Djingheuzian, L.E., 1957. Metallurgy developments in recovery of some of less common metals. In: *A Symposium of Extractive Metallurgy of some of the Less Common Metals*, pp. 75–81.
- Dwyer, T. E., and Passaic, N. J., 1957, Recovery of lithium from spodumene ores. U.S Patent No. 2801153.
- Ebensperger, A., Maxwell, P., Moscoso, C., 2005. The lithium industry: its recent evolution and future prospect. *Resour. Policy* 30, 218–231.
- Ellestad, R.B., Leute, K.M., 1950. Method of extracting lithium values from spodumene ores. U.S. Patent No. 2,516,109.
- Evans, R.K., 2014. Lithium. In: Gunn, A.G. (Ed). 2014. *Critical Metals Handbook Chapter 10*. John Wiley and Sons Ltd, Chichester, UK.
- Fenby, P., 2014. Pre-concentration of mineral ores via sensor sorting. *AusIMM Bullet.* 4, 80–82.
- Ferguson, W., Young, S.R., Deveau, C., Hazel, W., Lussier, A., Copeland, R., 2000. Cabot Corp.-Tantalum mining and corporation of Canada Ltd. *Canadian Institute of Mining, Metallurgy and Petroleum*. pp. 225–230.

- Filippov, L. O., Filippova, I. V., Crumiere, G., Sousa, R., Leite, M. M., de Sousa, A. B., Korbel, C., Tripathy, S. S., 2022. Separation of lepidolite from hard-rock pegmatite ore via dry processing and flotation. *Minerals Engineering* 187 107768.
- Fuerstenau, D.W., Pradip, 2005. Zeta potentials in the flotation of oxide and silicate minerals. *Adv. Colloid Interface Sci.* 114, 9–26.
- Gabra, G., Torma, A., Olivier, C., 1975. Pressure leaching of beta-spodumene by sodium chloride. *Can. Metall. Q.* 14 (4), 355–359.
- Gabriel, A., Slavin, M., and Carl, H. F., 1942. Minor constituents in spodumene. *Economic Geology*, 37(2). pp. 116–125. doi:10.2113/gsecongeo.37.2.116.
- Garrett, D.E., 2004. Part 1–Lithium. *Handbook of Lithium and Natural Calcium Chloride*. Elsevier Ltd., London, UK.
- Gem select, 2009. <https://www.gemselect.com/other-info/lilac-lepidolite.php> accessed 13 November 2022
- Gibson, C., Aghamirian, M., and Grammatikopoulos, T. 2017. A review: the beneficiation of lithium minerals from hard rock deposits. *SME Annual Meeting*, Denver, Colorado.
- Gibson, C.E.; Aghamirian, M.; Grammatikopoulos, T.; Smith, D.L.; Bottomer, L., 2021. The Recovery and Concentration of Spodumene Using Dense Media Separation. *Minerals* 11, 649. <https://doi.org/10.3390/min11060649>
- Griffin, A., 2017. Hydrometallurgical Processes for the Recovery of Lithium from Silicates. *Proceeding of ALTA*, Perth, Australia 20–27 May.
- Grosjean, C., Miranda, P.H., Perrin, M., Poggi, P., 2012. Assessment of world lithium resources and consequences of their geographic distribution on the expected development of the electric vehicle industry. *Renew. Sustain. Energy Rev.* 16, 1735–1744.
- Guo, H., Kuang, G., Wang, H., Yu, H., Zhao, X., 2017. Investigation of enhanced leaching of Lithium from  $\alpha$ -Spodumene using hydrofluoric and sulfuric acid. *Minerals* 7 (11), 205.
- Gupta, V., Miller, J.D., 2010. Surface force measurements at the basal planes of ordered kaolinite particles. *J. Colloid Interface Sci.* 344, 362–371.
- Hamzaoui, H. A., Jamoussi, B., M’Nif, A., 2008. Lithium recovery from highly concentrated solutions: Response surface methodology (RSM) process parameters optimization. *Hydrometallurgy*. 90(1):1-7.
- Institute of Ocean Energy, Saga University Japan, 2009; ENC Labs, 2010.
- Jandová, J., Dvořák, P., Vu, H.N., 2010. Processing of zinnwaldite waste to obtain  $\text{Li}_2\text{CO}_3$ . *Hydrometallurgy* 103, 12–18

- Jandová, J., Vu, H.N., 2008. Processing of zinnwaldite wastes to obtain lithium and rubidium compounds. *Miner. Metals Mater. Soc.* 923–929.
- Jandová, J., Vu, H.N., Belková, T., Dvořák, P., Kondás, J., 2009. Obtaining Li<sub>2</sub>CO<sub>3</sub> from Zinnwaldite wastes. *Ceramics – Silikáty* 53, 108–112.
- Jaskula, B.W., 2015. Minerals Yearbook. Lithium. U.S. Geological Survey. U.S. Department of the Interior.
- Jaskula, B.W., 2017. Lithium, Mineral Commodity Summaries USGS. Available at: <https://minerals.usgs.gov/minerals/pubs/commodity/lithium/mcs-2017-lithi.pdf>, Accessed date: 13 November 2022.
- Jie, Z., Weiqing, W., Jing, L., Yang, H., Qiming, F., Hong, Z., 2014. Fe(III) as an activator for the flotation of spodumene, albite, and quartz minerals. *Miner. Eng.* 61, 16–22
- Jirestig, J.A., Forssberg, K.S.E., 1994. Dispersion of flotation concentrates before magnetic separation. *Miner. Eng.* 7, 1505–151
- Kamienski, C.W., McDonald, D.P., Stark, M.W. and Papcun, J.R. (2004). Lithium and Lithium Compounds. In *Kirk-Othmer Encyclopedia of Chemical Technology*, (Ed.). <https://doi.org/10.1002/0471238961.1209200811011309.a01.pub2>
- Kavanagh, L., Keohane, J., Garcia Cabellos, G., Lloyd, A. & Cleary, J., 2018. Global lithium sources—industrial use and future in the electric vehicle industry: A review. *Resources* 7(3), 57.
- Ketelhodt, L. V., 2009. Viability of optical sorting of gold waste rock dumps. *J.SAIMM* 271–278.
- Knorring, O. V., Condliffe, E., 1987. Mineralized pegmatites in Africa. *Geol. J.* 22, 253–270.
- Krebs, R. E., 2006. *The History and Use of Our Earth's Chemical Elements: A Reference Guide*. Greenwood Publishing Group.
- Kuang, G., Chen, Z.B., Guo, H., Li, M.H., 2012. Lithium extraction mechanism from  $\alpha$ -spodumene by fluorine chemical method. *Adv. Mater. Res.* 524-527, 2011–2016.
- Kuang, G., Sun, J., Yang, J. and Jin, R., 2014. A method for the production of lithium hydroxide from spodumene using pipe reactor. CN Patent 104003428 A.
- Kuang, G., Yu Liua, Y., Lia, H., Xinga, S., Lia, F., Guoa, H. 2018. Extraction of lithium from  $\beta$ -spodumene using sodium sulfate solution. *Hydrometallurgy* 177 (2018) 49–56.
- Kundu, T., Rath, S. S., Das, S. K., Parhi, P. K., Angadi, S. I., 2023. Recovery of lithium from spodumene-bearing pegmatites: A comprehensive review on geological reserves, beneficiation, and extraction, *Powder Technology*, Volume 415, 118142, ISSN 0032-5910,

- Leemann, A., Le Saout, G., Winnefeld, F., Rentsch, D., Lothenbach, B., 2011. Alkali–silica reaction: the influence of calcium on silica dissolution and the formation of reaction products. *J. Am. Ceram. Soc.* 94 (4), 1243–1249.
- Leißner, T., Bachmann, K., Gutzmer, J., Peuker, U.A., 2016. MLA-based partition curves for magnetic separation. *Miner. Eng.* 94, 94–103.
- Li, C.T.; Peacor, D.R., 1968. The crystal structure of LiAlSi<sub>2</sub>O<sub>6</sub>-II (β-spodumene). *Zeitschrift für Kristallographie*, 126, 46–65.
- Li, H., Eksteena, J., Ge Kuang, G., 2019. Recovery of lithium from mineral resources: State-of-the-art and perspectives – A review. *Hydrometallurgy* 189 105129.
- Lithium Resources and Energy Quarterly September 2019 – [www.industry.gov.au/OCE](http://www.industry.gov.au/OCE)
- Liu, Q, Ai, H, Li, Z., 2011. Potassium sorbate as an efficient and green catalyst for knoevenagel condensation. *Ultrasonics Sonochemistry*. 18(2):477-479.
- Liu, Q, Ai, H-M., 2012. Sodium benzoate as a green, efficient, and recyclable catalyst for knoevenagel condensation. *Synthetic Communications*. 43(51):3004-3010.
- Luo, Q. P., Guo, P. C., Li, C. Z., Chen, L., 2012. Distribution of lithium resources and research status on lithium extraction technology. *Hydrometallurgy of China*. 31:67-70.
- Martin, A.B., 2018. The Leaching of α-Spodumene. Murdoch University Retrieved from. <https://researchrepository.murdoch.edu.au/id/eprint/44868/1/Albertani2018.pdf>, Accessed date: 13 November 2022.
- Mcintosh, N.C., 1946. Production of lithium compounds. US Patent 2413644.
- McVay, T.L., Browning, J.S., 1962. Flotation of spodumene from pegmatites of Cleveland county, N.C. United States department of the interior bureau of mines report. pp. 1–6.
- Medina, L.F., El-Naggar, M.M.A.A., 1984. An alternative method for the recovery of lithium from spodumene. *Metallurgical Transactions B* 15 (4), 725–726. <https://doi.org/10.1007/BF02657295>.
- Menendez, M., Vidal, A., Torano, J., Gent, M., 2004. Optimisation of spodumene flotation. *Eur. J. Miner. Process. Environ. Protect.* 4, 130–135.
- Meshram, P., Pandey, B.D., Mankhand, T.R., 2014. Extraction of lithium from primary and secondary sources by pre-treatment, leaching and separation: a comprehensive review. *Hydrometallurgy* 150, 192–208.
- Moon, K.S., Fuerstenau, D.W., 2003. Surface crystal chemistry in selective flotation of spodumene (LiAl[SiO<sub>3</sub>]<sub>2</sub>) from other aluminosilicates. *Int. J. Miner. Process.* 72, 11–24.

- Moore, L. R., Mann, J. P., Montoya, A., and Haynes, B. S., 2018, In situ synchrotron XRD analysis of the kinetics of spodumene phase transitions. *Physical Chemistry Chemical Physics*, 55(13). pp. 6426–6434.
- Munson, G.A., Clarke, F.F., 1955. Mining and concentrating spodumene in the black Hills, South Dakota. *Trans. AIME* 202, 1041–1045.
- Murodjon, S., Yu, X., Li, M., Duo, J., Deng, T., 2020. Lithium Recovery from Brines Including Seawater, Salt Lake Brine, Underground Water and Geothermal Water. DOI: 10.5772/intechopen.90371.
- Nie, X-Y., Sun, S-Y., Song, X., Yu, J-G., 2017. Further investigation into lithium recovery from salt lake brines with different feed characteristics by electrodialysis. *Journal of Membrane Science*. 530:185-191.
- Nie, X-Y., Sun, S-Y., Sun, Z., Song, X., Yu, J-G., 2017. Ion-fractionation of lithium ions from magnesium ions by electrodialysis using monovalent selective ion-exchange membranes. *Desalination*. 403:128-135.
- Norman, J., Gieseke, E.W., 1940. Beneficiation of Spodumene Rock by froth flotation. *Trans. Am. Inst. Min. Metall. Eng., Min. Practice* 1, 347–355.
- P.P. Keat, 1954. A new crystalline silica, *Science* 120 (3113) 328–330.
- Paukov, E.I., Kovalevskaya, Y.A., Kiseleva, I.A., Shuriga, T.N., 2010. A low-temperature heat capacity study of natural lithiummicas-heat capacity of zinnwaldite. *J. Therm. Anal. Calorim.* 9, 709–712.
- Peiro, L.T., Mendez, G.V., Ayres, R.U., 2013. Lithium: Sources, production, uses, and recovery outlook. *JOM* 65, 986–996.
- Peltosaari, O., Tanskanen, P., Hautala, S., Heikkinen, E-P., Fabritius, T. 2016. "Mechanical Enrichment of Converted spodumene by selective sieving." *Minerals Engineering* 30-39.
- Peltosaari, O., Tanskanen, P.A., Heikkinen, E.P., Fabritius, T., 2015.  $\alpha \rightarrow \gamma \rightarrow \beta$ -phase transformation of spodumene with hybrid microwave and conventional furnaces. *Miner. Eng.* 82, 54–60.
- Redeker, I. H., 1979. Concentration of spodumene from North Carolina pegmatite Ores. AIME Preprint number 77-H-382. SME fall meeting and exhibit st. Louis, Missouri – October 19-21, 11-13.
- Redeker, I. H., 1981. Flotation of feldspar, spodumene, quartz and mica from pegmatites in North Carolina, USA. In: 13th Canadian Mineral Processors Annual Meeting, Ottawa, Ontario.



- Rosales, G.D., Ruiz, C.M., Rodriguez, M.H., 2014. Novel process for the extraction of lithium from  $\beta$ -spodumene by leaching with HF. *Hydrometallurgy* 147, 1–6.
- Rutter J., 2017. *Grade Engineering and GE View*. CRC ORE White Paper Cooperative Research Centre for Optimising Resource Extraction (CRC ORE). Brisbane Australia.
- Sahoo, S. K., Tripathy, S. K., Nayak, A., Hembrom, K. C., Dey, S., Rath, R. K., & Mohanta, M. K., 2022. Beneficiation of lithium bearing pegmatite rock: a review, *Mineral Processing and Extractive Metallurgy Review*, DOI: 10.1080/08827508.2022.2117172.
- Salakjani, N. K., Singh, P., and Nikoloski, A. N., 2016, Mineralogical transformations of spodumene concentrate from Greenbushes, Western Australia. Part 1: conventional heating. *Minerals Engineering*, 98. pp. 71–79. doi:10.1016/j.mineng.2016.07.018.
- Salakjani, N. K., Singh, P., and Nikoloski, A. N., 2017, Mineralogical transformations of spodumene concentrate from Greenbushes, Western Australia. Part 2: microwave heating. *Minerals Engineering*, 100. pp. 191–199. doi:10.1016/j.mineng.2016.11.004.
- Salakjani, N. K., Singh, P., and Nikoloski, A. N., 2019, Acid roasting of spodumene: microwave vs. conventional heating. *Minerals Engineering*, 138. pp. 161–167. doi:10.1016/j.mineng.2019.05.003.
- Samchuk, A.I., Pilipenko, A.T.E., 1987. *Analytical Chemistry of Minerals*. (VSP).
- Samkova, R., 2009. Recovering lithium mica from the waste after mining tin-tungsten ores through the use of flotation. *GeoSci. Eng. IV* (1), 33–37.
- Sardar, A., Mubashir, S., 2012. Evolution of EV battery: role of materials availability. *Auto Tech Rev.* 1 (5), 20–25.
- Siame, E., Pascoe, R.D., 2011. Extraction of lithium from micaceous waste from china clay production. *Miner. Eng.* 24, 1595–1602.
- Stamp, A., Lang, D. J., Wäger, P. A., 2012. Environmental impacts of a transition toward e-mobility: The present and future role of lithium carbonate production. *Journal of Cleaner Production*. 23(1):104-112.
- Sugyeong, L., 2018. *Extraction of Lithium from Spodumene by Alkali Fusion*. Seoul National University.
- Swain, B., 2017. Recovery and recycling of lithium: A review. *Separation and Purification Technology*. 172. 388-403. 10.1016/j.seppur.2016.08.031.
- Tadesse, B., Makuei, F., Albijanic, B., Dyer, L., 2019. The beneficiation of lithium minerals from hard rock ores: A review, *Minerals Engineering*. 131 (2019) 170–184.

- Tian, J., Xu, L., Deng, W., Jiang, H., Gao, Z., Hu, Y., 2017. Adsorption mechanism of new mixed anionic/cationic collectors in a spodumene-feldspar flotation system. *Chem. Eng. Sci.* 164, 99–107
- Tiihonen, M., Haavanlammi, L., Kinnunen, S., Kolehmainen, E., 2019. Outotec lithium hydroxide process - a novel direct leach process for the production of battery grade lithium hydroxide monohydrate from calcined spodumene. In: *Proceedings of ALTA*. ALTA Metallurgical Services, Perth, Australia
- Vieceli, N., Durão, F.O., Guimarães, C., Nogueira, C.A., Pereira, M.F.C., Margarido, F., 2016a. Kinetic approach to the study of froth flotation applied to a lepidolite ore. *Int. J. Miner. Metall. Mater.* 23, 731–742.
- Walters, S. G. 2016. Driving productivity by increasing feed quality through application of innovative grade engineering technologies.
- Wang, Y., Zhu, G., Yu, F., Lu, D., Wang, L., Zhao, Y., Zheng, H., 2018. Improving spodumene flotation using a mixed cationic and anionic collector. *Physicochem. Prob. Miner. Process.* 54, 567–577.
- Wang, Y.-H., Yu, F.-S., 2007. Effects of metallic ions on the flotation of spodumene and beryl. *J. China Univ. Min. Technol.* 17, 35–39
- White, G. D., and McVay, T. N., 1958. Some aspects of the recovery of lithium from spodumene. *Metallurgy and Ceramics U. S. Atomic Energy Commission, ORNL-2450* 17. pp. 1–17.
- Wietelmann, U., Bauer, R.J., 2003. Lithium and lithium compounds, in *Ullmann's Encyclopedia of Industrial Chemistry 20* WILEY-VCH Verlag GmbH & Co., Weinheim, Germany.
- Wills, B.A., Finch, J.A., 2016. Sensor-based ore sorting. In: *Wills' Mineral processing Technology*, 8th ed., pp. 409–416.
- Wilson, M., Cabrera, J.G., Zou, Y., 1994. The process and mechanism of alkali – silica reaction using fused silica as the reactive aggregate. *Adv. Cem. Res.* 6 (23), 117–125.
- Xing, P., Wang, C., Zeng, L., Ma, B., Wang, L., Chen, Y., Yang, C., 2019. Lithium extraction and hydroxysodalite zeolite synthesis by hydrothermal conversion of  $\alpha$ -spodumene. *ACS Sustain. Chem. Eng.* 7, 9498–9505
- Xu, L., Hu, Y., Tian, J., Wua, H., Yang, Y., Zeng, Z., Wang, J., 2016a. Selective flotation separation of spodumene from feldspar using new mixed anionic/cationic collectors. *Miner. Eng.* 89, 84–92.

- Xu, L., Hu, Y., Wu, H., Tian, J., Liu, J., Gao, Z., Wang, J., 2016b. Surface crystal chemistry of spodumene with different size fractions and implications for flotation. *Sep. Purif. Technol.* 169, 33–42.
- Yang, D.C., 1978. Beneficiation of lithium ore by froth flotation. U.S. patent no. 4098687. pp. 1–10.
- Yin, X., Gupta, V., Du, H., Wang, X., Miller, J.D., 2012. Surface charge and wetting characteristics of layered silicate minerals. *Adv. Colloid Interface Sci.* 179–182, 43–50.
- Yu, F., Wang, Y., Wang, J., Xie, Z., 2014. Investigation on different behaviour and mechanism of Ca(II) and Fe(III) absorption on spodumene surface. *Physiochem. Prob. Miner. Process.* 50, 535–550.
- Yu, F., Wang, Y., Zhang, L., 2015a. Effect of Spodumene leaching with sodium hydroxide on its flotation. *Physiochem. Prob. Miner. Process.* 51, 745–754.
- Yu, F., Wang, Y., Zhang, L., Zhu, G., 2015b. Role of oleic acid-molecular complexes in the flotation of spodumene. *Miner. Eng.* 71, 7–12.
- Zeelikman, A.N., Krein, O.E., Samsonov, G.V., 1966. *Metallurgy of Rare Metals*. Israel Program for Scientific Translations, Jerusalem.
- Zelikman, A. N., Krein, O. E., and Samsonov, G. V., 1996, *Metallurgy of Rare Metals* (translated from Russian), Washington, DC: NASA and National Science Foundation, pp. 458.
- Zhu, G., Wang, Y., Liu, X., Yu, F., Lu, D., 2015. The cleavage and surface properties of wet and dry ground spodumene and their flotation behavior. *Appl. Surf. Sci.* 357, 333–339.
- Zou, H., Gratz, E., Apelian, D., Wang, Y., 2013. A novel method to recycle mixed cathode materials for lithium ion batteries. *Green Chem.* 15 (5), 1183–1191.

### **Chapter III**

#### **Effect of calcination on coarse gangue rejection of hard rock lithium ores**

Muhammad Kashif Nazir, Laurence Dyer, Bogale Tadesse, Boris Albijanic, Nadia Kashif

Published in <https://www.nature.com/articles/s41598-022-17277-x>

## **Abstract**

Processing of spodumene ores requires calcination as a compulsory pre-treatment to convert  $\alpha$ -spodumene to a more reactive  $\beta$ -spodumene phase. This transformation takes place at an elevated temperature of above 900°C and results in a 30 % volumetric expansion of the mineral and the product having highly altered physical properties. This work examines these induced properties and the effect of calcination on lithium grade deportment with particle size. XRD analysis showed a significant amount of  $\beta$ -spodumene in the calcined finest fraction (i.e., the particles less than 0.6 mm). A marked reduction in the bond ball mill work index of the calcined lithium samples (i.e. 42.3%) was recorded supporting the observed fracturing and friable appearance of the sample following  $\alpha$  to  $\beta$ -spodumene conversion. The deportment of lithium to finer fractions was significantly increased when the sample was calcined, indicating selective breakage of the spodumene over gangue minerals.

**Keywords:** Lithium beneficiation; spodumene calcination; coarse gangue rejection

## **1. Introduction**

The application of lithium compounds in the battery industry has increased worldwide lithium demand. Of the two important resources of lithium, extraction from brines is commercially more viable as compared with hard rock mining. However, attention has shifted to an extent towards lithium extraction from more evenly distributed hard rock ores because of two reasons. Firstly, this commodity is monopolised due to its presence in some specific regions. Secondly, the compound annual growth rate of lithium is expected to be 25.5% that is a rise from 47.3 to 117.4 kton of lithium over four years between 2020 to 2024 forcing the expansion of production into other feedstocks (Fawthrop, 2020). This growth is mainly the result of increased sales of

electric vehicles which are projected to rise from 3.4 million vehicles in 2020 to 12.7 million by 2024 (Fawthrop, 2020).

Spodumene ( $\text{LiAlSi}_2\text{O}_6$ ) is the most economically exploitable lithium-bearing mineral and is widely used in lithium extraction (Peltosaari et al., 2015). It is found in pegmatites and may occur with other lithium-bearing compounds such as petalite ( $\text{LiAlSi}_4\text{O}_{10}$ ) and lepidolite ( $\text{K}(\text{Li},\text{Al},\text{Rb})_3(\text{Al},\text{Si})_4\text{O}_{10}(\text{F},\text{OH})_2$ ). The processing of lithium ores starts with beneficiation such as gravity separation/dense media separation, magnetic separation and/or flotation (Tadesse et al., 2019). Beneficiation of lithium from spodumene is not a simple process because of similar properties of lithium-bearing minerals (i.e. spodumene) and their associated gangue minerals i.e. quartz ( $\text{SiO}_2$ ), albite ( $\text{NaAlSi}_3\text{O}_8$ ), microcline ( $\text{KAlSi}_3\text{O}_8$ ) and muscovite ( $\text{KAl}_2(\text{Si}_3\text{Al})\text{O}_{10}(\text{OH},\text{F})_2$ ).

A spodumene concentrate containing more than 6 %  $\text{Li}_2\text{O}$  is considered high-grade (Peltosaari et al., 2016) corresponding to at least 75% spodumene. This concentrate is suitable to feed the next processing stages: heat treatment and lithium extraction (Peltosaari et al., 2015). Heat treatment is required due to the natural existence of spodumene in a less reactive  $\alpha$ -phase (Rosales et al., 2014). Heat treatment at elevated temperatures (above  $950^\circ\text{C}$ ) is an important step in lithium production because this step transforms less reactive  $\alpha$ -spodumene into more reactive  $\beta$ -spodumene (Salakjani et al., 2016). This phenomenon of phase transformation is called calcination or decrepitation which is an endothermic reaction (Dessemond et al., 2019).

$\alpha$ -Spodumene is the most dominant naturally occurring of the three possible phases of spodumene, namely:  $\alpha$ ,  $\beta$ ,  $\gamma$ .  $\alpha$ -Spodumene (monoclinic crystal structure) is a denser and less reactive phase found at ambient temperature. However,  $\beta$ -spodumene (tetragonal crystal

structure) is 30% less densely packed than  $\alpha$ -spodumene. Thus,  $\beta$ -spodumene has lower specific gravity than  $\alpha$ -spodumene (2.4 and 3.15 g/cm<sup>3</sup> respectively). Hexagonal  $\gamma$ -spodumene is recently discovered and is metastable because it is formed during the transition from  $\alpha$  to  $\beta$  phase (Li and Peacor, D.R., 1968).

$\alpha$ -Spodumene presents as a competent rock, while  $\beta$ -spodumene is much more brittle than primary gangue minerals in the ore (e.g., quartz) (Dessemond et al., 2019). A microscopic study reveals  $\alpha$ -spodumene as a compact material composed of multiple layers stacked over each other. Conversely, in  $\beta$ -spodumene samples, many cracks can be observed on particles leading to a more random crystal structure.

Based on the significant and potentially selective change in physical properties of spodumene the objective of this work is to investigate the implications of calcination on behaviour of the samples during comminution and grade deportment by size (coarse gangue rejection). In this work, different comminution techniques were used for calcined spodumene samples: crushing, semi-autogenous grinding, and autogenous grinding. The reason is that different comminution techniques result in varied particle size distributions and hence different grade deportment by size. In other words, crushing produces the coarsest fractions while semi-autogenous grinding generates the finest fractions. It should be noted that although it is understood that calcination of the whole ore would involve a marked increase in energy usage, the potential for separation and upgrading for challenging ores or mineralized waste streams is of interest.

## 2. Materials and methods

### 2.1. Samples

Spodumene ores were provided from a mine in the Eastern Goldfields, Western Australia. The received ores had particle size -7 mm i.e., the particles less than 7 mm. The ore sample was collected by belt cut from the final crusher product and is designated as the plant feed (PF). The other sample was collected by strafing a bucket through the tailings stream of the secondary (cleaner) dense media separation (TDMS). Table 1 shows the mineralogy of PF and TDMS samples. The lithium contents in the TDMS and PF samples were 0.36 % and 0.30%, respectively. The lithium content was determined by forming a borate glass fusion bead, digestion in 10 % citric acid, and subsequent ICP-OES (Agilent Technologies, Inc., US), analysis. The solution was transported by a peristaltic pump in the nebulizer to convert the solution into a fine aerosol spray. Finer droplets enter the hot plasma, leading to evaporation of the sample. As a result, atoms and ions are excited causing the characteristic wavelengths emission which is quantified by the ICP-OES system; the wavelength used for ICP-OES analysis for lithium (Bach et al., 2016) was 610.4 nm.

**Table 1.** Mineralogy of the spodumene ore

<b>Mineral</b>	<b>% mass</b>	
	<b>TDMS</b>	<b>PF</b>
Spodumene	10.6	8.3
Feldspar	70.2	71.5
Quartz	13.4	13.9
Mica	5.5	5.9
Others	0.3	0.4

### 2.2. Calcination

The ore samples were calcined for 1 h at 1100°C in a muffle furnace (Cupellation furnace, Carbolite Sheffield England). The holding time of one hour allowed complete conversion of



spodumene from  $\alpha$ -phase to  $\beta$ -phase for accurate results. The calcined and non-calcined samples were used to understand the influence of calcination on comminution operations (crushing, autogenous milling or semi-autogenous milling). The mill had a low-ball loading (10 %) in contrast to standard ball milling (50 %) and thus the mill was used to simulate a semi-autogenous grinding mill.

### 2.3. Comminution

Figure 1 shows the flowcharts used in this work. As seen in Figure 1, underwent a range of comminution processes to provide information under a range of breakage processes (semi-autogenous or autogenous mill), screened in six different size fractions (+3.35 mm, -3.35 +2.36 mm, -2.36 +1.7 mm, -1.7+ 1.18 mm, -1.18 + 0.6 mm, -0.6 mm) and then the lithium grades were determined using ICP-OES (Agilent Technologies, US) in each size fraction; the standard deviation for three repeats of the lithium grade did not exceed 3%. The lithium recoveries (R) were determined using Equation (1):

$$R = \frac{m_p \times g_p}{m_f \times g_f} \quad (1)$$

Where  $m_p$  and  $m_f$  are the mass of the product and the feed, respectively;  $g_p$  and  $g_f$  are the lithium grade in the product and the feed.

Crushing was performed using a cone crusher (Wescone, Australia) with a motor power of 9.2 kW; the closed side setting of the crusher is 3 mm. Semiautogenous and autogenous grinding were performed using a mill (the motor power of 1 kW) for 20 min. Semiautogenous grinding was conducted using 12 grinding balls (each grinding ball had 27.3 mm in diameter) that had a total mass of 1060 g; the rotational speed of the mill was 70 rpm. The calcined ores were investigated using crushing, semi-autogenous or autogenous mill.

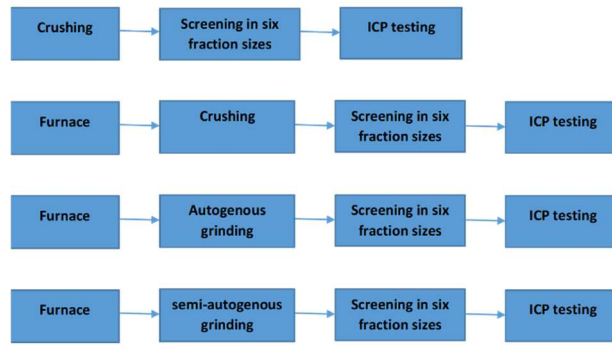


Figure 1. The experimental flowcharts.

#### 2.4. Bond Ball Mill Work Index

The Bond Ball Mill Work Index (BBMWI) is defined as the resistance offered by a material to the grinding during ball milling (Lynch et al., 2015). The purpose is to find out the grinding power required for a certain throughput of material under ball mill grinding circumstances. Different steel balls were used for grinding in each test as seen in Table 2. BBMWI was determined for both non-calcined and calcined samples. The standard bond ball mill procedure was followed (Lynch et al., 2015).

**Table 2.** Grinding balls used for BBMWI.

Ball diameter (mm)	Number of balls
38.10	43
31.75	67
25.40	10
19.05	71
15.87	94
Mass of balls	20.125 kg

The power required for grinding,  $W_i$ , was determined using Eq (2) (Lynch et al., 2015).

$$W_i = \frac{44.5 \times 1.102}{S^{0.23} \times G^{0.82} \left( \frac{10}{\sqrt{P_{80}}} - \frac{10}{\sqrt{F_{80}}} \right)} \quad (2)$$

Where the screen size required for 80% of a product or a feed to pass through the screen are  $P_{80}$  and  $F_{80}$ , respectively;  $F_{80}$  and  $P_{80}$  were 1700  $\mu\text{m}$  and 53  $\mu\text{m}$ , respectively.  $G$  is the ore grindability and  $S$  is the sieve size through which ore passes.

## 2.5 X-Ray Diffraction

Mineralogical analyses of the lithium ore samples were conducted using an Olympus BTX™ II Benchtop (Co-K $\alpha$ ) X-ray diffractometer (XRD). The XRD experiments were performed using two calcined finest fractions (-0.6 mm) and two non-calcined coarsest fractions (+3.35 mm) considering that these samples had the maximum lithium content. This is very important to identify changes in the crystalline structure of spodumene before and after calcination.

## 3 Results and discussions

### 3.1. Effect of calcination and comminution method on mass retention

Figure 2 shows the influence of calcination and comminution method on mass retention on different sieve sizes for the TDMS and the PF sample. As seen in Figure 2a., in the case of the TDMS sample, the highest percentage of ore was found on the largest size fraction when the ore was treated using the crushing only. It means that ore particles have high hardness considering that spodumene in the ore is in  $\alpha$ -phase at 25°C and has a compact crystal structure (Peltosaari et al., 2015; Dessemond et al., 2019). However, when calcination was performed before any comminution methods, the mass retention of the largest size fraction decreased significantly inducing fracturing before crushing. The difference between the non-calcined and calcined material is greater with more comminution.

Figure 2 also shows that the lowest mass retention for the largest size fraction was when the ore was calcined followed by cone crushing. Similar trends were also obtained in the case of

the PF sample. However, in the case of the PF (Figure 2b), calcination followed by semi-autogenous grinding had more mass retention of the largest size fraction than calcination followed by autogenous grinding. The smallest mass in the largest size fraction was obtained after calcination and cone crushing; the reason could be that the calcined ore was more brittle and thus more easily crushed than treated by autogenous grinding or semi-autogenous grinding.

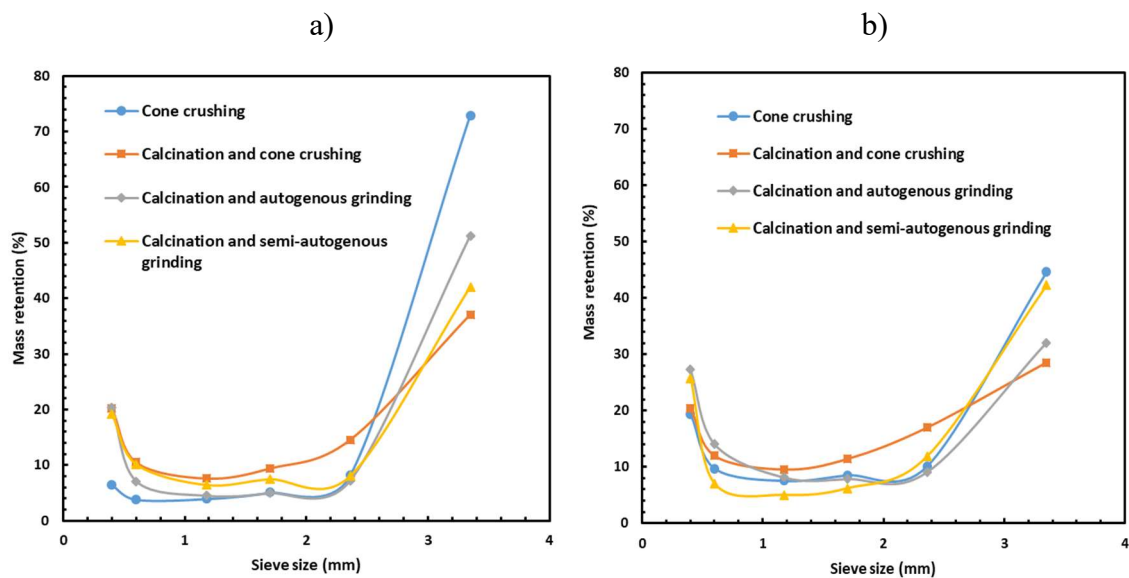


**Figure 2.** Retention of a) TDMS b) PF on different sieves.

### 3.2. Effect of calcination and comminution method on lithium grade and lithium recovery

Figure 3 shows the influence of the calcination and comminution method on the lithium grade for various size fractions for the TDMS and the PF sample. In the case of the TDMS sample (Figure 3a), the cone crushing method without calcination resulted in the maximum lithium grade of the largest size fraction while the lithium grade was lowest for the smallest size fraction. However, the opposite trend was observed when calcination was used before comminution. This is particularly true when autogenous grinding or semi-autogenous grinding was conducted after calcination i.e. the lithium grade for the finest size fraction was the highest, displaying the highest potential gangue rejection.

The calcination impact on coarse gangue rejection in the case of the PF sample (Figure 3b) was similar to that in the case of the TDMS (Figure 3a). However, the lithium grade in the finest fraction was significantly higher when semi-autogenous grinding was conducted after calcination than that when cone crushing and autogenous grinding were performed after calcination.

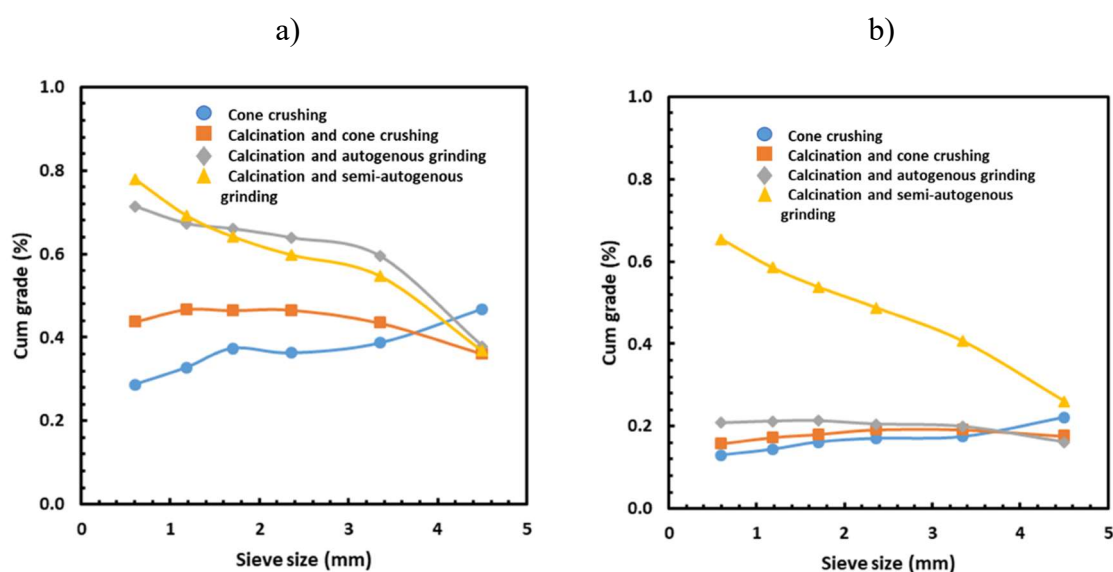


**Figure 3.** Influence of calcination and comminution methods on cumulative grade of lithium in the case of a) TDMS and b) PF.

The influence of calcination on lithium recovery can be seen in Figure 4. As seen in Figure 4, the lithium recovery after cone crushing and without calcination was the lowest at the finest screen size. However, when calcination was performed before crushing or grinding operations, the lithium recovery improved in the finest size fractions, leading to coarse gangue rejection. The highest lithium recovery was achieved when calcination was performed before semi-autogenous grinding.

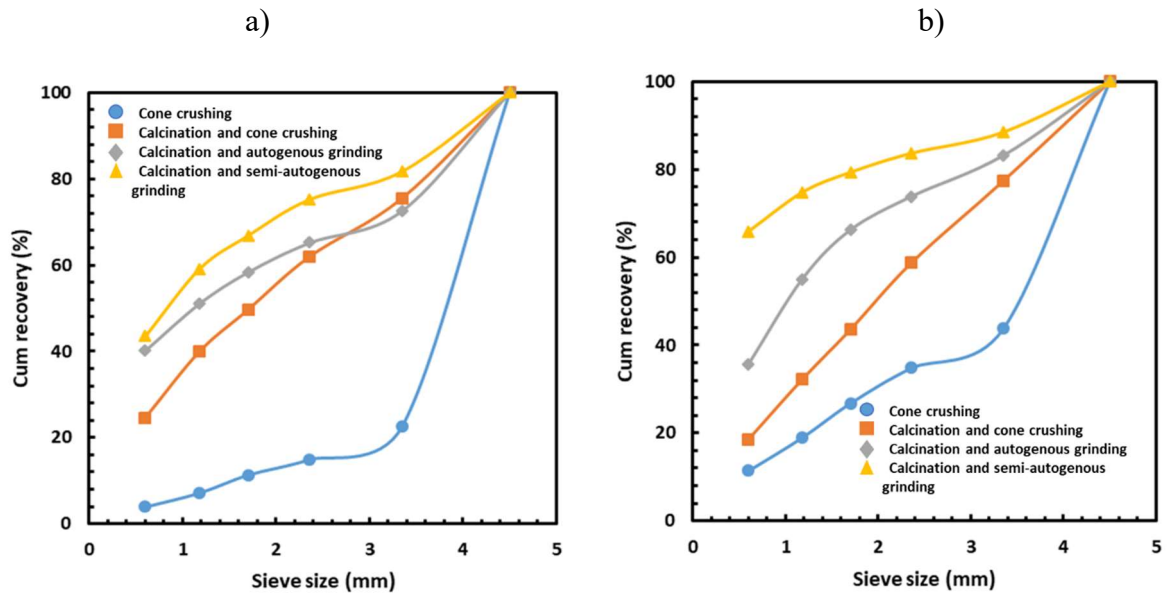


**Figure 4.** Influence of calcination and comminution methods on cumulative lithium recovery in the case of a) TDMS and b) PF.

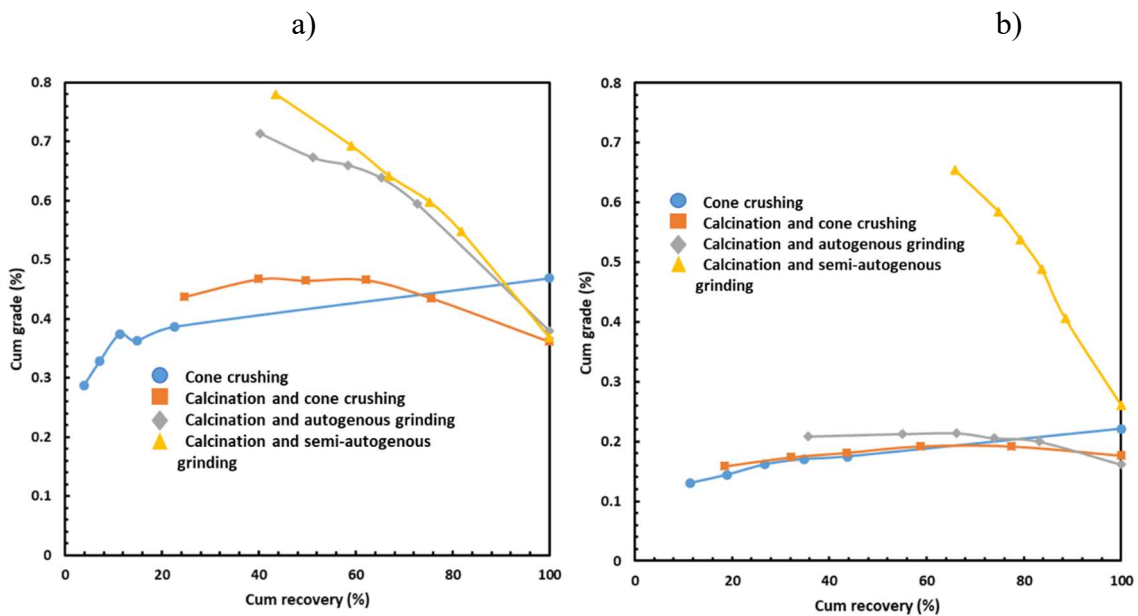


**Figure 5.** Cumulative grade vs cumulative recovery of lithium in the case of a) TDMS and b) PF.

Figure 5 shows the relationships between the cumulative grade and the cumulative recovery. The higher the lithium recovery the lower the lithium grade, which is true when calcination was used for both the TDMS (Figure 5a) and the PF sample (Figure 5b). It means that

calcination may be effective in the rejection of coarse gangue. The effect of calcination was more pronounced when the samples were ground after calcination. However, in the case of the non-calcined sample, there was a preferential department of lithium to the largest size fraction because spodumene was present as a competent  $\alpha$  phase.

In the case of the TDMS sample, there are similarities between the grade recovery curves when calcination was performed before autogenous or semi-autogenous grinding; it may suggest that the TDMS sample was more amenable to autogenous grinding than the PF sample. In the case of the PF sample, the similarity between these curves was observed for the samples treated by cone crushing only, calcination and cone crushing, and calcination and autogenous grinding. The differences between the TDMS and the PF sample were probably due to their differences in gangue mineralogy (see Figure 6). Even though the lithium content was low in both TDMS and PF, significant coarse gangue rejections were achieved only when calcination was performed before semi-autogenous grinding (i.e., the most efficient comminution method).

X-ray diffraction was used to investigate the impact on the mineral components of the samples through the various treatment schemes; Figure 6 shows the diffraction patterns of the size fraction with the highest Li content from 4 sample sets. As anticipated  $\beta$ -spodumene replaces  $\alpha$ -spodumene with calcination and is more prominent for both TDMS and PF samples as it is concentrated in the finer fraction (Ellestad and Leute, 1950; Abdullah et al., 2019). For both TDMS and PF samples, the amount of albite also increased in the finest fraction of the calcined sample due to the albite transformation from the triclinic to monoclinic crystal structure (Shaocheng and Mainprice, 1987) and thus degradation in strength. Figure 6 also shows that the amount of quartz was higher in the non-calcined TDSM sample than that in the calcined

TDMS sample showing that quartz was retained in the highest sieve size as it remained competent through calcination.

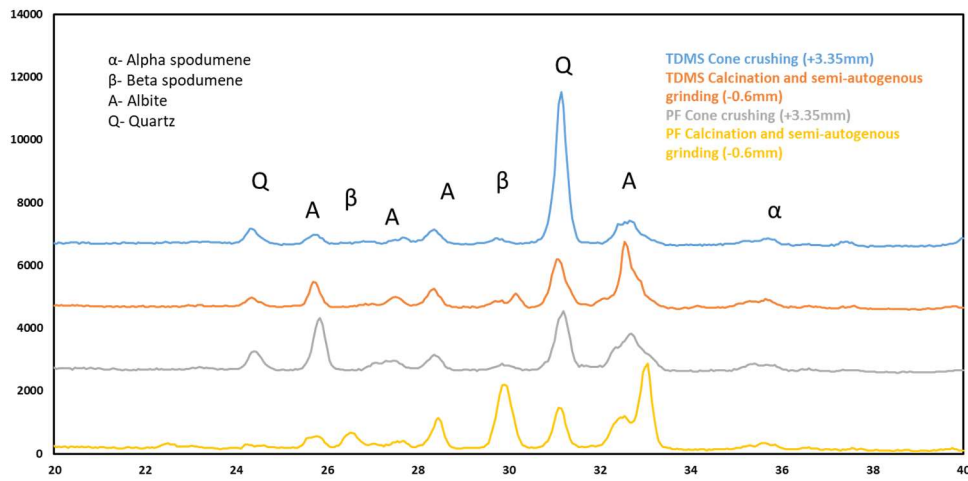


**Figure 6.** XRD for two calcined finest fractions (-0.6 mm) and two non-calcined coarsest fractions (+3.35 mm).

### 3.3. Effect of calcination on lithium grade and recovery for very fine sizes

The influence of calcination on lithium deportment to very fine sizes was investigated using the sieves in the range of 150 and 53  $\mu\text{m}$ . Both feed and products from the ball mill were analysed to address this matter as seen in Figures 7 and 8; the ball mill product was collected after conducting the BBMWI test. It was found that the calcination was also very beneficial for lithium grade by sieve size even at very fine sizes (150 and 53  $\mu\text{m}$ ). The increase in sieve size reduced the amount of lithium grade for the sample retained on the sieve but increased the cumulative lithium recovery. These trends were also observed in the case of the largest sieve sizes (see Figures 3 to 5). However, Figures 7 and 8 showed that the cumulative recovery increased more dramatically with increasing in sieve size in the case of the ball mill product than that of the feed.



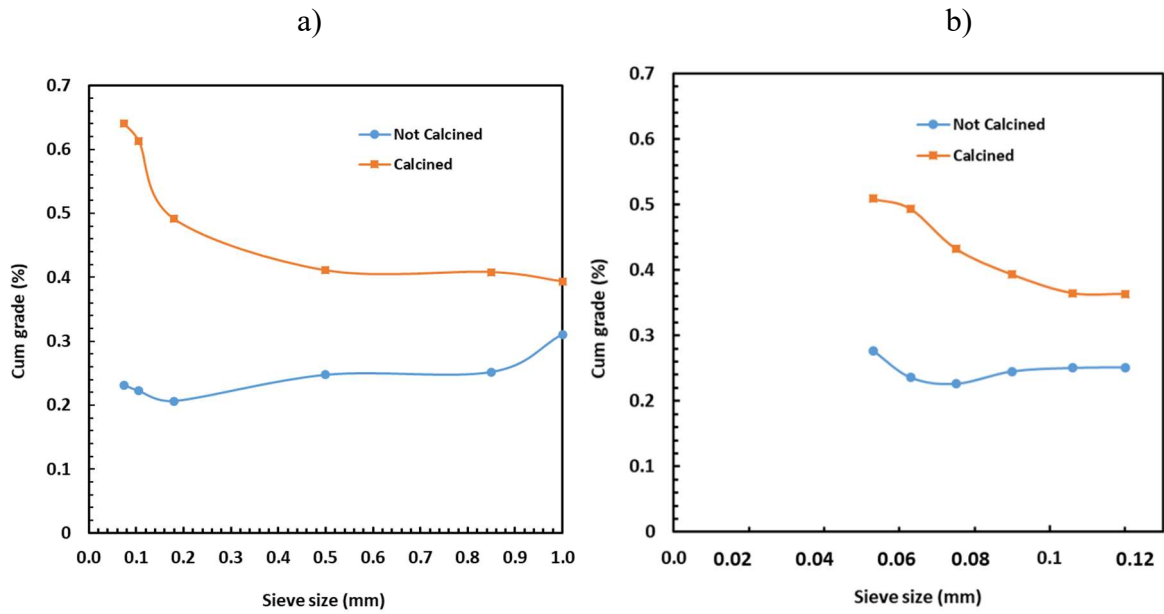


**Figure 7.** Influence of calcination on the cumulative grade of lithium in the case of a) feed of the ball mill and b) product of the ball mill.

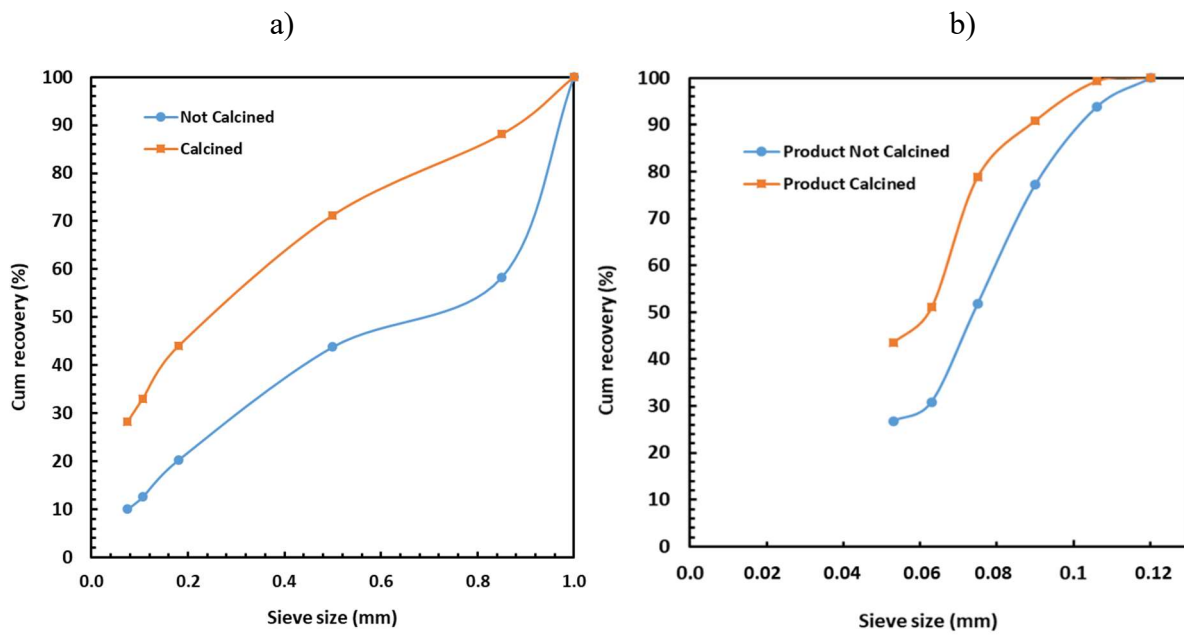


**Figure 8.** Influence of calcination on cumulative recovery of lithium in the case of a) feed of BMWI and b) product of BMWI in the case of PF.

### 3.4. Effect of calcination on energy consumption during grinding

The results showed that the non-calcined ore required 1.73 times more energy for grinding than the calcined ore i.e.,  $W_i$  (i.e., BBMWI) for the non-calcined ore was 44.9 kWh/t and for the calcined ore was 25.9 kWh/t. It should be noted that the non-calcined ore had significantly higher BBMWI than  $\alpha$ -spodumene (Perry and Chilton, 1985) i.e., 13.70 kWh/t; the reason is due to the presence of different gangue minerals such as mica, quartz, albite and other silicates; the BBMWI for mica (Perry and Chilton, 1985) is 134.5 kWh/t, quartz (Perry and Chilton, 1985) is 32.2 kWh/t and albite (Perry and Chilton, 1985) is 34.9 kWh/t.

The energy consumed,  $Q$ , during calcinations of spodumene is obtained using the energy balance i.e., Equation (3):

$$Q = \frac{m}{M} \int_{298}^{1373} C_p(T) dT + Q_{\alpha\beta} \quad (3)$$

Where  $C_p(T) = 354.7 - 3375.7 T^{-0.5} \text{ J mol}^{-1} \text{ K}^{-1}$  as reported by Desmond and colleagues (2019)<sup>7</sup>;  $T$  is the temperature;  $m$  is the mass of the sample;  $M$  is the molecular mass of spodumene (186 g/mol). It should be noted that the energy transformation from  $\alpha$  to  $\beta$  spodumene,  $Q_{\alpha\beta}$ , was 116.1 kJ/kg as reported by Desmond and colleagues (Desmond et al., 2019). The energy consumed during calcination was 582 kWh/t or 2096 kJ/kg. Therefore, calcination before grinding resulted in increased overall energy consumption.

The summary of energy consumption for all unit operations is given in Table 3. The energy for crushing, autogenous grinding and semi-autogenous grinding were determined by considering the duration of each operation, motor power and sample mass. As seen in Table 3, the furnace consumes vastly more energy than the comminution circuit.

**Table 3.** Energy consumption for different unit operations.

Unit operation	Energy consumption (kJ/kg)
Furnace	2096
Crusher	69
Autogenous grinding	75
Semiautogenous grinding	237

Table 4 compares energy consumption and lithium grade for the finest size fractions (-0.6 mm) for four different processing options used in this work. As seen in Table 4, although the combination of the furnace with the crusher or the mill (autogenous grinding or semi-autogenous grinding) increased the energy consumption of the process, using the furnace increased the lithium grade by the screening of hard rock lithium ores. It is also very important to highlight that if calcination is not used before grinding, calcination is used always after grinding and before leaching since leaching of spodumene is not possible without calcination. When ore calcination is conducted before leaching or after flotation, the amount of energy consumed for calcination is approximately 1257.6 kJ/kg considering that flotation concentrates have typically 60% of spodumene (Tadesse et al., 2019) (i.e.,  $2096 \times 60/100 = 1257.6$  kJ/kg; 2096 kJ/kg is the energy consumption of calcination for pure spodumene as seen in Table 3). It is important to highlight that the main objective of this paper is not to develop a new flowsheet but to investigate the implications of calcination on behaviour of the samples during comminution and grade department by size (coarse gangue rejection).

**Table 4.** Energy consumptions and lithium grade for -0.6 mm for different processing operations.

Processing options	Energy consumption (kJ/kg)	Li grade % (TDSM) (-0.6 mm)	Li grade % (PF) (-0.6 mm)
Crusher	69	0.28	0.12
Furnace+crusher	2165	0.44	0.16
Furnace+mill (autogenous grinding)	2171	0.72	0.2
Furnace+mill (semiautogenous grinding)	2333	0.76	0.64

#### 4. Conclusions

This paper studies the influence of calcination of spodumene ore and comminution circuits on coarse gangue rejections by screening. The results showed that the calcination made spodumene brittle, having a positive effect on coarse gangue rejection by increasing lithium grade and recovery in the finest fraction. This effect was observed when the sieve size was in the range between 0.6 and 5 mm as well as 0.063 and 1 mm. The results of this work display the significantly altered properties of calcined material that promote preferential breakage of the spodumene over other components. Semi-autogenous grinding after calcination generated significantly more fines than autogenous grinding or crushing after calcination in the case of the PF sample. The energy consumed during the bond ball mill work test of the calcined ores was 42% less than that of the non-calcined ores. It must be noted that the reduction in comminution energy does not account for the additional energy consumption in calcining feed streams rather than concentrates.

#### Acknowledgements

The collaboration between the authors would not have been possible without the financial support from CRC ORE. CRC ORE is part of the Australian Government's CRC Program,

which is made possible through the investment and ongoing support of the Australian Government. The CRC Program supports industry-led collaborations between industry, researchers and the community.

The Bald Hill Mine (Alliance Mineral Assets Limited, Western Australia) is acknowledged for the provision of samples for all the experiments. Financial support from Curtin University for this research work is appreciated.

### **Declaration of Competing Interest**

The authors declare that they have no conflict of interest.

### **5. References**

- Abdullah, A. A.; Oskierskia, H. C.; Altarawneh, M. N.; Senanayake, G.; Lumpkin, G.; Dlugogorski, B. Z., 2019. Phase transformation mechanism of spodumene during its calcination. *Miner. Eng.* 140, 105883.
- Bach, T. C.; Schuster, S. F.; Fleder, E.; Muller, J.; Brand, M.J.; Lormann, H.; Jossen, A.; Sextl., G., 2016. Nonlinear aging of cylindrical lithium-ion cells linked to heterogeneous compression. *J. Energy Storage.* 5, 212–223.
- Dessemond, C.; Lajoie-Leroux, F.; Soucy, G.; Laroche, N.; Magnan, J-F., 2019. Spodumene: The Lithium Market, Resources and Processes, *Minerals.* (accessed 12 March 2021).
- Ellestad, R.B.; Leute, K.M., 1950. Method of extracting lithium values from spodumene ores. U.S. Patent 2, 516,109.
- Fawthrop, A., 2020. Global lithium demand to more than double by 2024, say analysts, Available online: <https://www.nenergybusiness.com/news/industry-news/global-lithium-demand-2024/> (accessed 16 December 2021).
- Li, C.T.; Peacor, D.R., 1968. The crystal structure of LiAlSi<sub>2</sub>O<sub>6</sub>-II ( $\beta$ -spodumene). *Z. Kristallogr.* 126 (1–3), 46–65.
- Lynch, A.; Mainza, A.; Morell, S., 2015. Ore comminution measurements techniques, in: Lynch A.J., (Ed.), *The AusIMM Comminution Handbook* Carlton: AusIMM, pp. 43-60.
- Peltosaari, O.; Tanskanen, P.A.; Heikkinen, E.P.; Fabritius, T., 2015.  $\alpha \rightarrow \gamma \rightarrow \beta$ -phase transformation of spodumene with hybrid microwave and conventional furnaces. *Miner. Eng.* 82, 54–60.
- Peltosaari, O.; Tanskanen, P.A.; Heikkinen, E.P.; Fabritius, T., 2016. Mechanical enrichment of converted spodumene by selective sieving. *Miner. Eng.* 98, 30-39.

- Perry, R. O.; Chilton, C. H., 1985. Int Student's ed, McGraw Hill, p 8-11, and SME Mineral Processing Handbook, Weiss (ed), p 3A-27.
- Rosales, G.D.; Ruiz, M.D.C.; Rodriguez, M.H., 2014. Novel process for the extraction of lithium from b-spodumene by leaching with HF. *Hydrometallurgy*. 147–148, 1–6.
- Salakjani, N.K.; Singh, P.; Nikoloski, A.N., 2016. Mineralogical transformations of spodumene concentrate from Greenbushes, Western Australia. Part 1: Conventional heating. *Miner. Eng.* 98, 71–79.
- Shaocheng J. S.; Mainprice, D., 1987. Experimental deformation of sintered albite above and below the order-disorder transition, *Geodinamica Acta*, 1:2, 113-124.
- Tadesse, B.; Makuei, F.; Albijanic, B.; Dyer, L., 2019 The beneficiation of lithium minerals from hard rock ores: A review. *Miner. Eng.* 131, 170–184.

## **Chapter IV**

### **Lithium deportment by size of a calcined spodumene ore**

Muhammad Kashif Nazir, Laurence Dyer, Bogale Tadesse, Boris Albijanic, Nadia Kashif

Published in <https://www.nature.com/articles/s41598-022-22808-7>

## Abstract

Calcination of spodumene is used to convert  $\alpha$ -spodumene to more reactive  $\beta$ -spodumene, has been shown to greatly impact the physical characteristics of some of the components in the ore. This work investigates the energy efficiency of different grinding circuits used for upgrading the lithium content in the finer fraction of the calcined spodumene ore. The results showed that closed-circuit grinding resulted in 89% lithium recovery of the finest size fractions (-0.6 mm) while open-circuit grinding led to 65 % lithium recovery for the same grinding time. Closed-circuit grinding consumed lower energy than open-circuit grinding. The grade of the finest size fraction in the case of the open-circuit grinding was 1.7 times more than that in the case of the closed-circuit grinding. This work shows the potential of using different grinding modes to maximize energy efficiency and lithium department by size. However, it is suggested that open circuit grinding should be used for beneficiations of spodumene ores.

**Keywords:** Calcination; spodumene beneficiation; energy efficiency

## 1. Introduction

Lithium has gained great interest since its discovery in the early 1800s due to its application in glass, ceramic, rubber, grease manufacturing, air conditioning, aluminium industry (Yaksic and Tilton, 2009; Dessemond et al., 2019). The recent application of lithium in lithium-ion batteries has resulted in drastic increases in demand (Ebensperger et al., 2005; Peiró et al., 2013; Reichel et al., 2017; Swain, 2017).

Brine deposits have been the dominant source for lithium extraction in the 1990s being generally more economically favourable. However, lithium content in hard rock lithium ores is higher than that in brine deposits, making the mining of lithium ores a substantial contributor to meet the growing lithium demand (Bell, 2020).



While there are 145 lithium-bearing minerals, only a few (such as spodumene, petalite, and lepidolite) are commonly used in the production of lithium (Meshram et al., 2014; Kavanagh et al., 2018). Spodumene is the most important of all these minerals with a high theoretical  $\text{Li}_2\text{O}$  content of 8 % (Dessemond et al., 2019). Spodumene is a member of the pyroxene group and naturally occurs in  $\alpha$ -phase monoclinic form with associated gangue minerals like quartz, albite, microcline and micas in pegmatite deposits (Aylmore et al., 2018; Tadesse et al., 2019).

The natural occurring  $\alpha$ -phase of spodumene is highly refractory and thus calcination (i.e., thermal treatment at the temperature over  $900^\circ\text{C}$ ) is used to convert  $\alpha$ -phase to  $\beta$ -phase (Ellestad and Leute, 1950). The process of calcination makes spodumene more brittle and reactive for acid roasting. The reason is that  $\alpha$ -spodumene crystals have a 30% lower volume than  $\beta$ -spodumene crystals. At higher temperatures, the  $\alpha$ -phase expands, leading to an increased volume of  $\beta$ -spodumene crystals (Salakjani et al., 2016). Therefore,  $\beta$ -spodumene is less dense than  $\alpha$ -spodumene. Previous work (Nazir et al., 2022a) has shown that this expansion induces fracturing between and within spodumene crystals, weakening the particles and facilitating further breakage. This was displayed by a reduction in Bond ball mill work index (BBMWI) of the ore from 44.9 to 25.9 kWh/t after calcination.

Gangue mineral rejections by screening is a very simple method for upgrading a mineral stream based on the propensity of the grade to report to specific size fractions (also known as preferential breakage) (Carrasco et al., 2016; Walters et al., 2016). When treating raw materials, the behaviour in this regard is driven by the mineralogical association of the valuable element(s), the gangue minerals present and the style of mineralisation (geology). For effective gangue mineral rejections, the gangue minerals must be liberated during breakage. The separability comes from differences in produced particle size of the various minerals during breakage.

Other key component minerals in these samples also undergo phase transitions within the temperature range relevant to calcination. Quartz is well known to undergo a reversible transition from  $\alpha$ - to  $\beta$ -quartz at approximately  $575^\circ\text{C}$  (Ohno et al., 2006). The crystal lattice parameters in mica increase at a temperature in the range of  $650^\circ\text{C}$ , which is related to a

decrease in the strength of the material (Neißer-Deiters et al., 2019). Plagioclase is shown to have reversible changes at approximately 400 °C and irreversible changes at 800 – 900 °C (Kono et al., 2008). Therefore, the properties and response to breakage, handling, and screening will be complex as many components of the ore will be impacted during calcination and grinding. To better understand the physical behaviour of the calcined minerals (ore and gangue) as well as look at other modes of breakage, this work investigates the behaviour of calcined spodumene under both open and closed-circuit grinding.

It should be noted that understanding closed grinding circuits is important for most mineral processing operations for the design and optimizations of grinding circuits. Simulations and scale-up of grinding circuits can be done based on the specific energy to reduce the particle size of the product i.e., the Bond method which could be beneficial for coarse gangue rejection in hard rock lithium ores (Bond et al., 1952; Bond, 1960; Bond, 1961); however, the Bond method may overpredict a mill capacity (Austin and Brame, 1983). The accuracy of grinding circuit simulations can be improved by considering breakage kinetics of valuable minerals, material transport through a mill, and size classification performances (Herbst and Fuerstenau, 1980). Advances in computational fluid dynamics - discrete element method (CFD-DEM) simulations of grinding circuits may be also used for the design and optimizations of grinding circuits (Jayasundara et al., 2012). Although simulations of grinding circuits are very important in mineral processing industries, this is beyond the scope of this work.

## **2. Materials and methods**

### **2.1. Ore preparations**

Spodumene ore samples (-15 mm) were obtained from the Bald Hill Mine Eastern Goldfields, Western Australia. Table 1 shows the mineralogy of the sample determined using XRD. As seen in Table 1, the ore contains spodumene as a valuable mineral with the presence of feldspar, quartz and mica as associated gangue minerals. The ores samples were collected from a low-grade plant feed parcel that has approximately 0.32 % Li. The ore (i.e., 3000 g plant feed) was calcined in a muffle furnace (Cupellation furnace, Carbolite Sheffield England) at 1100°C and held at that temperature for 1 h to ensure complete conversion of  $\alpha$  to  $\beta$ -spodumene. After that, the sample was air-cooled slowly to room temperature; the cooling process took 15 h. Other

researchers (Fosu et al., 2021; Peltosaari et al., 2016) also used the same conditions (i.e., 1100°C and 1 h calcination time) as used in this study. The muffle furnace temperature was calibrated using the thermocouples with the measurement errors of less than 1.1%. The changes in ore properties after calcination at 1100 °C were characterized by MLA (mineral liberation analyser) and shown in Figure 1; the MLA software was developed at the University of Queensland in Australia (Gu and Napier-Munn, 1997). As seen in Figure 1, after calcination, spodumene became more porous and hence more brittle.

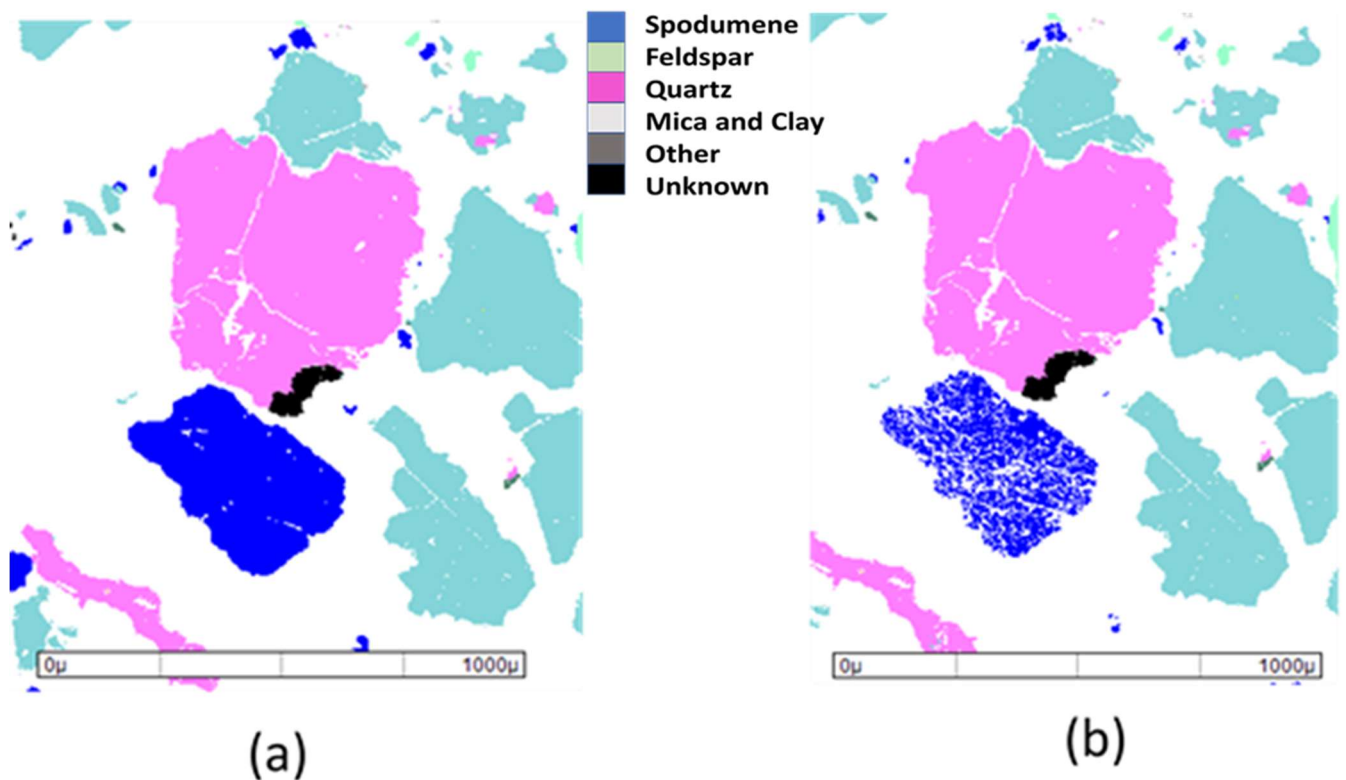


**Figure 1.** Estimation of particle properties a) before calcination and b) after calcination

(Nazir et al., 2022b).

The calcined sample was split into two samples to study the influence of different modes of grinding (closed and open-circuit) on coarse gangue rejection and energy consumption of both grinding modes.

**Table 1.** Mineralogy of the spodumene ore

<b>Mineral</b>	<b>% mass</b>
Spodumene	10.6
Feldspar	70.2
Quartz	13.4
Mica	5.5
Others	0.3

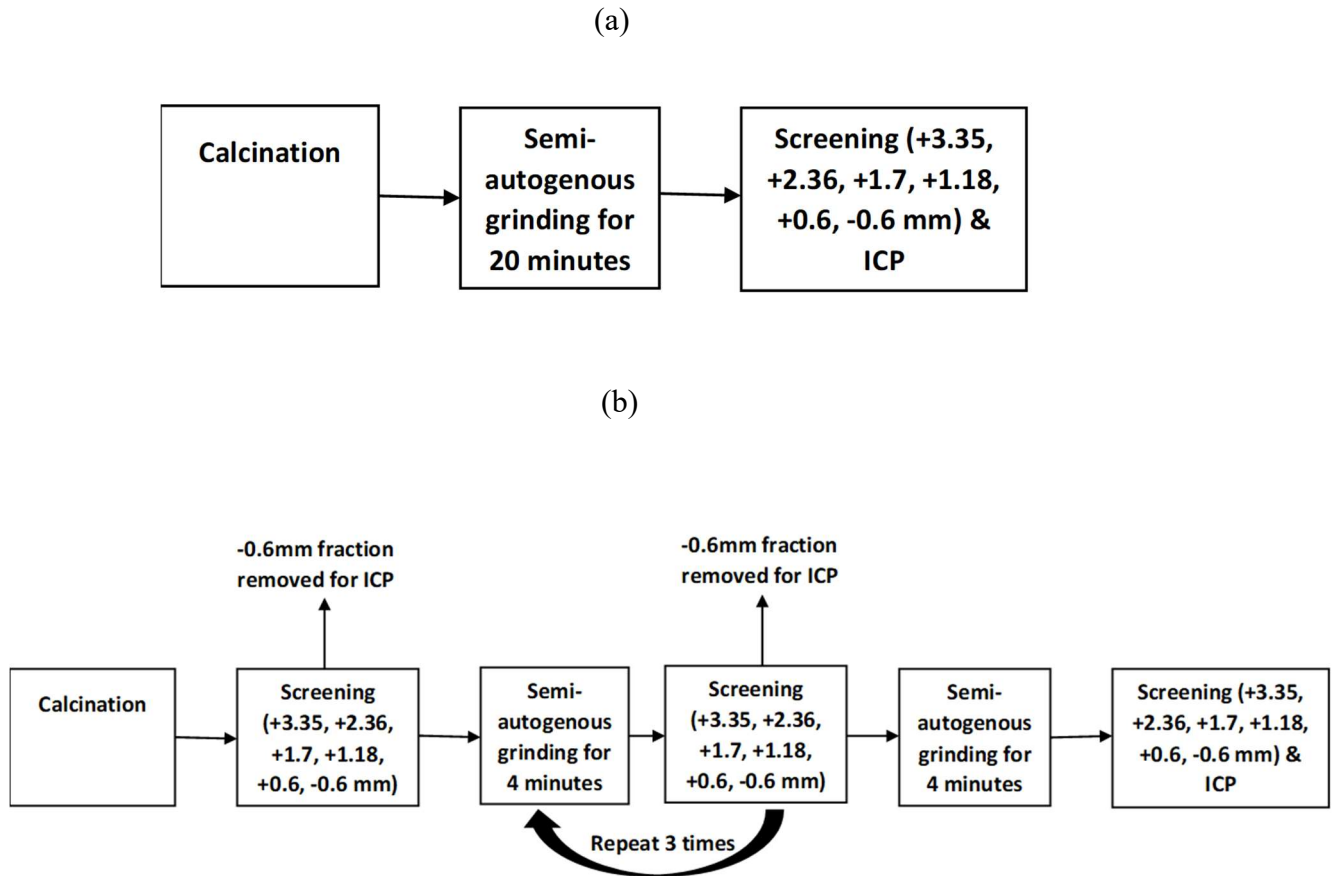
## 2.2. Semi-autogenous grinding and screening

Figure 2 shows two flowsheets used in this work. As seen in Figure 2 both closed and open-circuit grinding was conducted using the calcined spodumene samples. Figure 2a shows that the calcined sample was subject to the open-circuit grinding for 20 min in a ball mill. The ball mill had 12 grinding balls (each grinding ball had 27.3 mm in diameter) with a total mass of 1060 g; the rotational speed of the mill was 70 rpm. The grinding product was screened into six different size fractions (+3.35 mm, -3.35 +2.36 mm, -2.36 +1.7 mm, -1.7+ 1.18 mm, -1.18 + 0.6 mm, -0.6 mm) to study the particle size distribution (PSD) and the lithium grade in the finest fraction (-0.6 mm). Considering that the ball mill had a low-ball mill loading (10 %) in contrast to standard ball milling (50 %), the ball mill was used to simulate a semi-autogenous grinding mill.

The calcined sample (Figure 2b) was also screened into six different size fractions (+3.35 mm, -3.35 +2.36 mm, -2.36 +1.7 mm, -1.7+ 1.18 mm, -1.18 + 0.6 mm, -0.6 mm) to determine the particle size distributions of the feed. This sample was ground using the closed-circuit grinding in the same ball mill used for the open-circuit grinding to compare this mode of grinding with the open-circuit grinding.

As seen in Figure 2b, there are 5 grinding stages, and each grinding stage was 4 min i.e. the overall time for grinding was 20 min. After each grinding stage, the calcined sample was screened into two different size fractions: -0.6 mm (the fine fraction) and +0.6 mm (the coarse fraction). The fine fraction was not ground again to prevent overgrinding of the feed and thus

reduce energy during grinding. The coarse fraction was ground after each grinding stage. The coarse fraction was screened into five different size fractions (+3.35 mm, -3.35 +2.36 mm, -2.36 +1.7 mm, -1.7+ 1.18 mm, -1.18 + 0.6 mm) to study the PSD (particle size distribution) after each grinding stage. The chemical analysis was conducted through digestion of the solids, and ICP-OES (Agilent Technologies 5100) was used to determine the lithium content in the fine size fraction (-0.6 mm). The standard deviation for three repeats of the lithium grade did not exceed 3%.



**Figure 2.** Development flowchart a) the open-circuit grinding and b) the closed-circuit grinding.

### 2.3. X-Ray Diffraction (XRD)

Mineralogical analyses of the lithium ore samples were conducted using an Olympus BTX™ III Benchtop (Co-K $\alpha$ ) XRD with radiation Co-K $\alpha$  in the range between 5 and 55° (2 $\theta$ ). X Powder from Olympus was used for analysing the diffractogram. The XRD experiments were

performed using six calcined finest size fractions collected after each grinding stage to identify the changes in the mineralogy of spodumene after grinding. These experiments were also conducted for the finest size fraction collected after the open-circuit grinding. The XRD trends were detected via visible inspection of the peak intensity and shape and there is a notable change in relative intensities which correlates well with the assays.

### 3. Results and Discussions

#### 3.1. Effect of grinding time on particle size distributions of feed in open and closed-circuit grinding

Figure 3 shows the influence of grinding time on particle size distributions. As would be expected the overall PSD (i.e., particle size distribution) after each additional stage of grinding is shifting to finer fractions. However, it must be noted that after each grinding stage the -0.6 mm fraction is removed from the system, therefore in each subsequent stage, a greater proportion of fines is generated with the same energy input. Again, this is expected as with each subsequent stage there is less sample mass in the mill.

Figure 3 also compares the particle size distribution for the open-circuit grinding and that for the closed-circuit grinding. As seen in Figure 3, the open-circuit grinding produced significantly more coarse particles (-3.35+2.36 mm) than the closed-circuit grinding. The reason is that during the closed-circuit grinding, the fine particles (-0.6 mm) were removed from the mill every 4 min of grinding while during the open-circuit grinding the ore remained in the mill for 20 min. Therefore, the closed-circuit grinding after 20 min produced 8.3 times more fine particles (-0.6 mm) than the open-circuit grinding. The removal of fine particles during closed-circuit grinding makes it possible for new materials to have direct contact with the grinding media which enhances the grinding, hence generating more fine particles. Removing fine and softer material allows breakage for harder minerals. Nevertheless, the open-circuit grinding produced 27% of ore particles less than 0.6 mm while the closed-circuit grinding after the fifth stage produced 17% of the same size fraction.

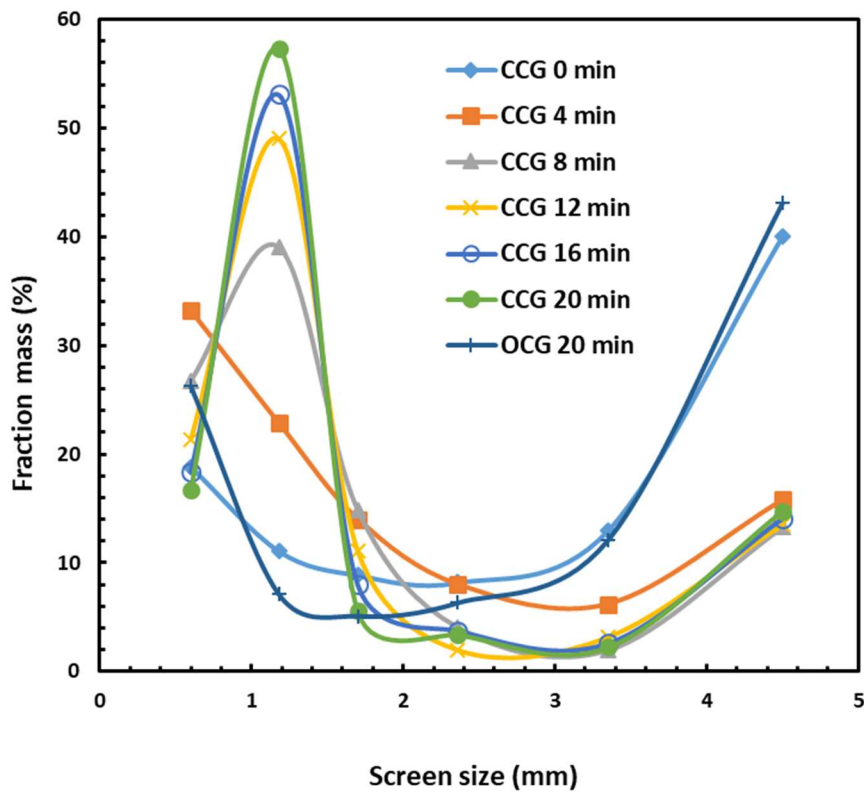


**Figure 3.** Particle size distributions as a function of grinding time (CCG is the closed-circuit grinding and OCG is the open circuit grinding).

### 3.2. Effect of grinding time on lithium deportment in closed-circuit grinding

Figure 4 shows the changes of Li grade for the -0.6 mm fraction during closed-circuit grinding. As seen in Figure 4, the Li grade changed significantly after each 4 min grinding interval resulting in two maxima and two minima. The first maximum occurred after 4 min due to preferential grinding of the brittle  $\beta$ -spodumene. In the second stage of grinding (i.e. the first minimum), after removal of the -0.6 mm fraction, the lithium grade decreased because the  $\beta$ -spodumene was not completely deported in the finest size fractions, and the removal of fines induced breakage of coarser minerals; it means that spodumene was occluded in the gangue. In the third stage (i.e., the second maximum), Li grade in the finest size fraction increased due to  $\beta$ -spodumene liberation from gangue minerals. In the fourth stage, the same trend was also observed as in stage two. Finally, in the last stage, the Li grade increased, which is similar to stage three; however, the Li grade in the last stage was 69 % less than the highest Li grade achieved (i.e., the first stage of grinding); the Li grade after the fifth stage was 0.38%. It should be noted that the Li grade (-0.6 mm) after the open-circuit grinding was 0.65%. These results

showed that the closed-circuit grinding resulted in oscillating of Li grade with different grinding times. The progressive depletion of Li in the residual coarse fraction (+0.6 mm) is also shown in Figure 4.

It should be noted that (Fosu et al., 2021) found that calcined spodumene is highly liberated when  $P_{80}$  was between 50 and 80  $\mu\text{m}$ . In our work,  $P_{80}$  was between 600 and 800  $\mu\text{m}$  (see Figure 8), indicating that spodumene was less liberated. However, Figure 1 shows that the sample of spodumene is fully liberated, and Figure 1 did not show unliberated spodumene. However, based on the results obtained in Figure 4, spodumene was occluded. Further research is required to investigate the liberation degree of calcined spodumene as a function of grinding time.

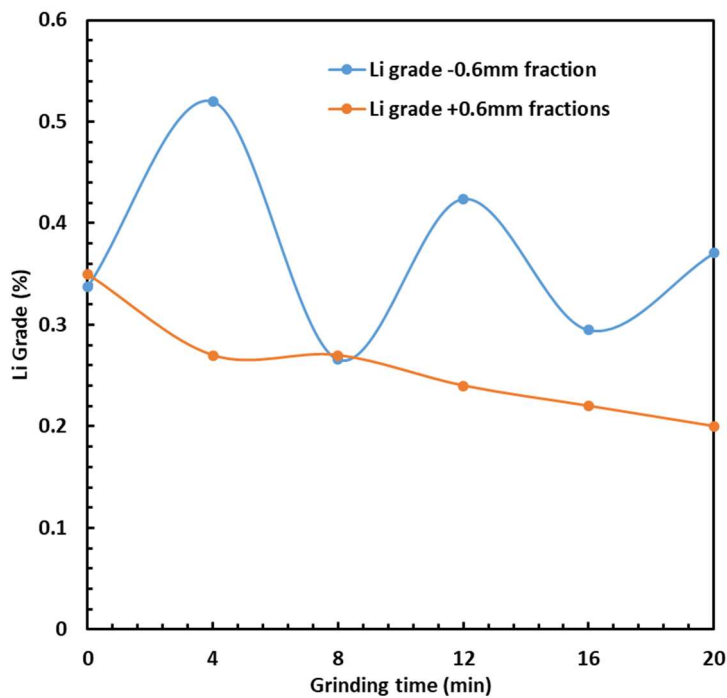


**Figure 4.** Effect of closed-circuit grinding time and screening on lithium grade in the two size fractions.: -0.6 mm and +0.6 mm.

### 3.3. XRD analysis of the finest size fractions (-0.6 mm) of open and closed circuit grinding

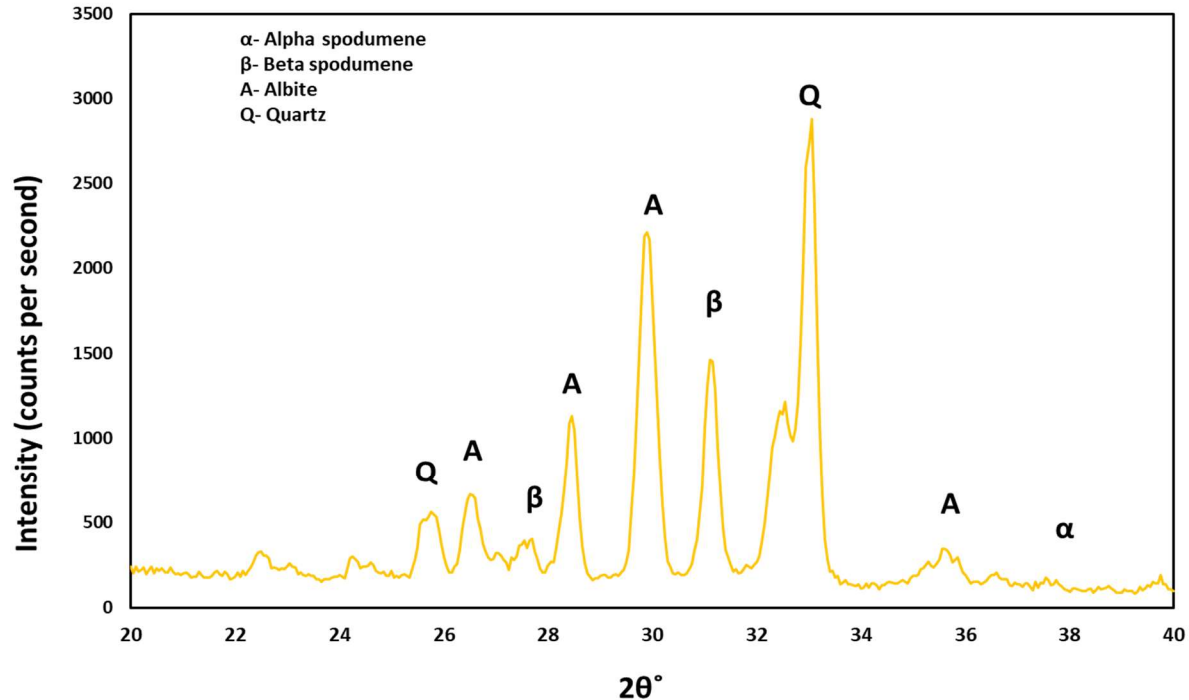
The mineralogy of the grinding products for the finest size fractions (-0.6 mm) obtained after the closed-circuit and open-circuit grinding is shown in Figure 5. The XRD analysis for the open circuit grinding (see Figure 5a) shows that a significant amount of  $\beta$ -spodumene was



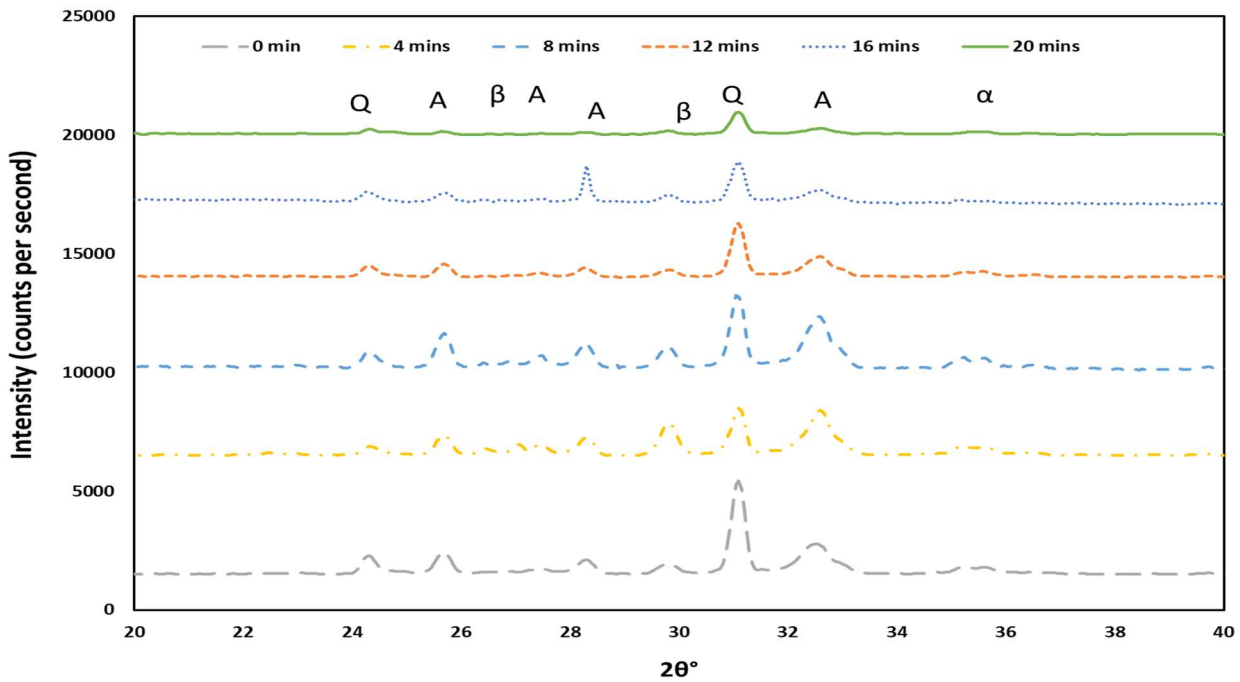
deported to the finest size fraction, leading to the lithium grade of 0.65% which is higher than that achieved after the fifth stage of the closed-circuit grinding (i.e., 0.38%).

Figure 5b shows the XRD analysis conducted to investigate the changes in the mineralogy of the products after each stage of the closed-circuit grinding. The amount of quartz was the highest before grinding. However, the amount of  $\beta$ -spodumene was the highest after the first stage of grinding which agrees well with the maximum lithium grade shown in Figure 4. The amount of albite and quartz was large after the second and fourth stages of grinding, leading to a lower lithium grade (see Figure 4). The reason is that albite has irreversible changes at 800 – 900 °C (Kono et al., 2008), resulting in a higher crystal lattice angle. The amount of albite after the third and fifth stages of grinding was lower than that after the second and fourth stages of grinding, resulting in a higher lithium grade after the third and fifth stages of grinding. These results showed that the XRD analysis is a useful method for understanding the changes in ore mineralogy after the closed-circuit grinding of calcined spodumene samples.

a)



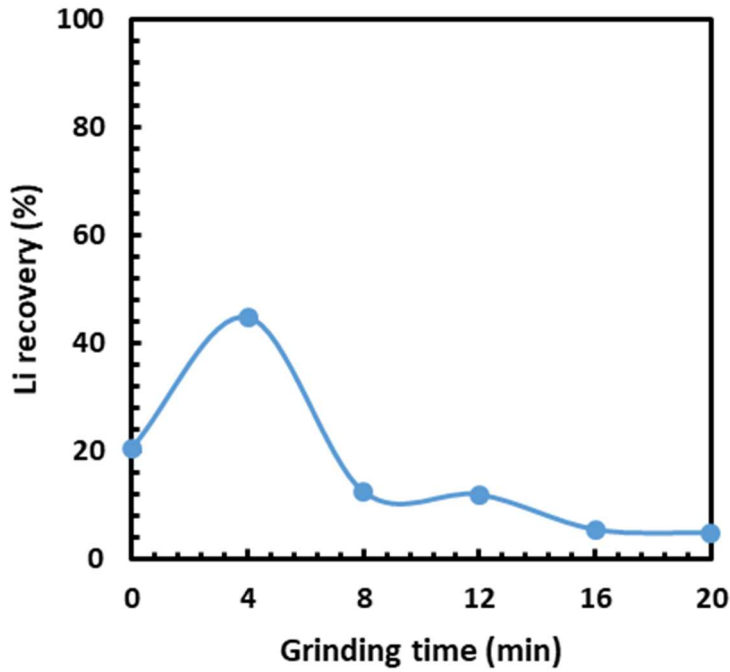
b)



**Figure 5.** XRD results for samples collected after a) the open-circuit grinding and b) the closed-circuit grinding.

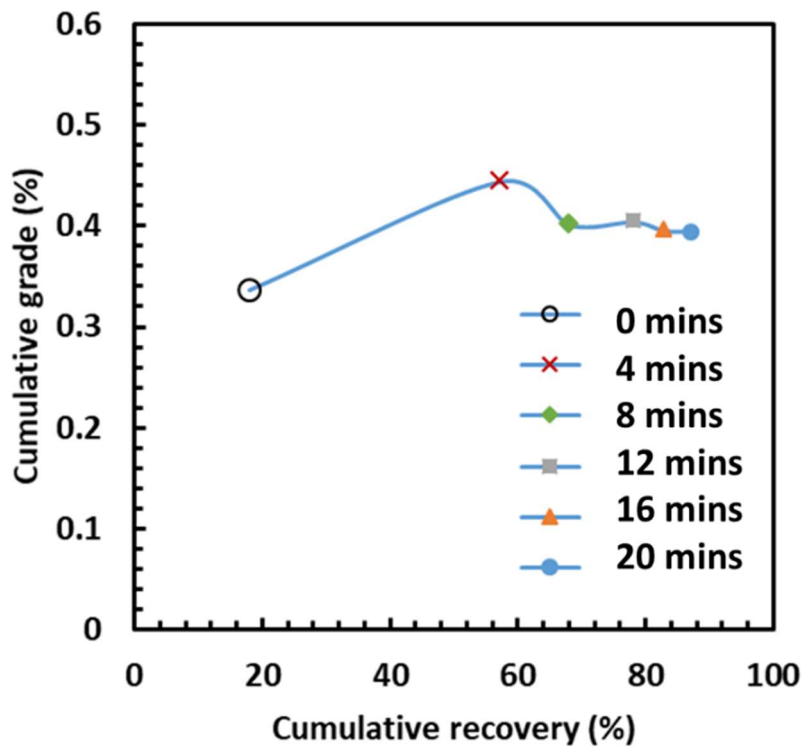
### 3.4. Lithium recovery in closed-circuit grinding

Figure 6 shows the changes in Li recovery for the finest size fraction during closed-circuit grinding. As seen in Figure 6, the maximum Li recovery was achieved after the first stage of grinding (i.e after 4 min) because the maximum amount of  $\beta$ -spodumene (i.e., very brittle mineral) was deported to the finest size fraction. However, in the second stage of grinding, the Li recovery dropped considerably, indicating that the amount of  $\beta$ -spodumene was significantly reduced. This trend was also observed after the third, fourth and fifth stages of grinding due to the decreasing remaining mass of the ore in the mill.



**Figure 6.** Effect of grinding time and screening on the lithium recovery in the finest size fractions (-0.6 mm).

Figure 7 shows the relationships between the cumulative Li grade and the cumulative Li recovery at different grinding stages. As seen in Figure 7, the maximum Li grade and Li recovery were obtained after the first stage of grinding (i.e., after 4 min) because  $\beta$ -spodumene was deported in the finest size fraction. In the subsequent grinding stages (the second, third, fourth, and fifth stage), the oscillating relationship between the cumulative Li grade and the cumulative Li recovery was observed, indicating that the department of Li in the finest size fraction changes with every grinding stage.



**Figure 7.** Cumulative recovery vs cumulative grade for the finest size fractions during the closed-circuit grinding.

### 3.5. Comparison of the efficiency of the closed and open-circuit grinding

Table 2 compares the efficiency of the closed and open-circuit grinding. The results showed that in the case of the finest size fraction (-0.6 mm), the mass recovery for the closed-circuit grinding was 77% while that for the open-circuit grinding was 26% (i.e., the closed-circuit grinding generated 1159 g of the finest fraction whereas the open-circuit grinding generated 389 g; the total mass was 1482 g). The reason is that after each increment of closed-circuit grinding, the finest size fraction was removed from the system, leading to enforced grinding of the coarse material. In the open-circuit grinding, the softest components are preferentially ground and then overground generating an overall finer PSD (Figure 8) and leaving the harder components in the coarse fraction. The closed-circuit grinding also led to a 24% higher lithium recovery than that of the open-circuit grinding. It means that the closed-circuit grinding generated 3 times finer fractions than open-circuit grinding. This work showed that the closed-circuit grinding is more energy efficient than the open-circuit grinding due to the generation of more finer fractions during the closed-circuit grinding, using 3 times less energy per unit mass of fines produced.

However, in the finest size fraction, the Li grade of the products in the case of the closed-circuit grinding was 56% less than that of the open-circuit grinding. The reason is that the particle size in the -0.6 mm size fraction produced by the open-circuit grinding was lower than that produced by the closed-circuit grinding as seen in Figure 8. Thus, finer particles were deported in the finest size fraction (-0.6 mm) during the open-circuit grinding than during the closed-circuit grinding, leading to a higher lithium grade during the open-circuit grinding. Similar observations were obtained by (Peltosaari et al., 2016) using autogenous grinding of the calcined spodumene.

Table 2 shows the mass and energy balance for both open and closed grinding circuit. Table 3 compares the total performance of both open and closed grinding circuit. As seen in Table 3, the closed-circuit grinding led to 89% lithium recovery while the open-circuit grinding resulted in 65 % lithium recovery. The energy consumption during the open-circuit grinding was 3 times higher than that during the closed-circuit grinding. It should be noted that the energy consumption was determined using the motor power of 1 kW, the grinding time of 0.33 h, and the mass of the sample produced in the finest size fraction (-0.6 mm) (i.e. the overall mass of the finest size fractions in the closed-circuit grinding was 1159 g and that in the open-circuit grinding was 389 g). The energy consumed (E) during grinding is determined using Eq. (1):

$$E^* = \frac{E}{m} t \quad (1)$$

$E^*$  is the consumed energy in kWh/t, E is the energy in kW, m is the mass of the product in the fine size fractions (-0.6 mm); t is the time (h).

This work demonstrated that the closed-circuit grinding should be used for maximizing Li recovery and minimizing energy consumption while the open-circuit grinding should be used for maximizing Li grade. These results demonstrated the benefits of the closed-circuit grinding for a significant energy reduction per ton of product due to the elimination of overground fines,

which agrees well with the literature (Kaya and McIvor, 1992; Wills and Napier-Munn, 2006). This grinding mode also increased the Li recovery.

**Table 2.** Mass balance and energy consumption for both open and closed grinding circuit.

Closed-circuit grinding				
Cycle number	Cycle duration (min)	Mass (feed) g	Mass (product -0.6 mm) g	Energy consumption per ton of product (kWh/t)
1	0	1482	279	
2	4	1199	398	130
3	8	799	214	70
4	12	585	125	41
5	16	458	84	27
6	20	355	59	19
Open-circuit grinding				
1	20	1492	389	857

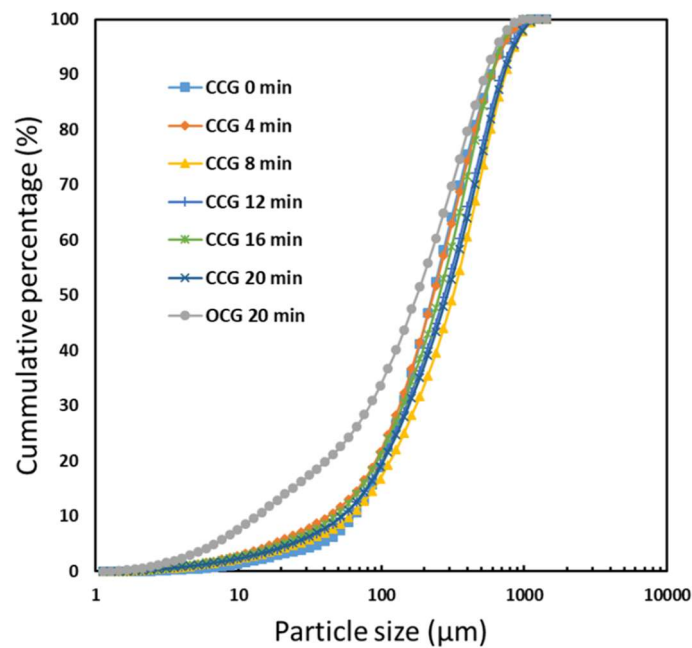


**Figure 8.** The particle size distributions of the products (-0.6 mm); CCG is the closed-circuit grinding and OCG is the open circuit grinding.

**Table 3.** Comparison of the closed-circuit grinding versus the open-circuit grinding.

<b>Grinding type</b>	<b>Product particle size (<math>\mu\text{m}</math>)</b>	<b>Li grade (%)</b>	<b>Mass recovery (%)</b>	<b>Li recovery (%)</b>	<b>Energy consumption (kWh/t)</b>
Open-circuit	-0.6	0.65	26%	65%	857
Closed-circuit	-0.6	0.38	77%	89%	287

#### 4. Conclusions

This work investigates the behaviour of calcined spodumene ore using different modes of grinding. The results showed that the maximum amount of  $\beta$ -spodumene (i.e., very brittle mineral) was deported to the finest size fraction (-0.6 mm) after the first stage of grinding (i.e., after 4 min), resulting in the maximum Li grade and recovery at this grinding stage. Although the lithium recovery was almost constant in the next four grinding stages, the lithium grade oscillated after each grinding stage. The results showed that there was greater preferential deportment of Li to the fines in open-circuit grinding, the recovery was lower due to the much lower fine generation. As would be expected, closed-circuit grinding is far more efficient in generating fine material but is far less discriminatory between phases as the softer material is ground faster and removed leading to the harder components of the ore being ground over time. Whereas, open-circuit grinding continues to preferentially grind the softer material generating much finer particles at the lower end of the size distribution. The XRD analysis of the samples shows that the hardness of other materials such as albite may also be impacted by calcination. This work shows the potential for selection of milling process and conditions to optimise Li deportment to the fines in calcined material.

#### Availability of Data and Materials

All data generated or analysed during this study are included in this published article.

## Acknowledgements

This research was funded by the Co-operative Research Centre for Optimising Resource Extraction (CRC ORE), a member of the Commonwealth Government of Australia's CRC program. Technical support of staff at Western Australian School of Mines, Curtin University is appreciated. The authors would like to thank Mr Thomas Bede Payten for providing information about the mineralogy.

## 5. References

- Austin, L.G.; Brame, K., 1983. A comparison of the Bond method for sizing wet tumbling mills with a size mass balance simulation method. *Powder Technology*, 34, 261-274.
- Aylmore, M. G.; Merigot, K.; Rickard, D.A. W.; Evans, J. N.; McDonald, J. B.; Catovic, E.; Spitalny, P., 2018. Assessment of a spodumene ore by advanced analytical and mass spectrometry techniques to determine its amenability to processing for the extraction of lithium. *Minerals Engineering*. 119, 137-148.
- Bell, T., 2020. "An Overview of Commercial Lithium Production." ThoughtCo. <https://www.thoughtco.com/lithium-production-2340123> (accessed July 11, 2022).
- Bond, F.C., 1952. The Third Theory of Comminution. *Trans.AIME* 193 (1), 484-494.
- Bond, F.C., 1960. New Equation for Calculating the Work Index from A-C Closed Circuit Ball Mill Grindability Tests. Allis Chalmers Publication.
- Bond, F.C., 1961. Crushing and grinding calculations. *British Chemical Engineering Part I* 6 (6), 378–385 (Part II 6(8), 543–548).
- Carrasco, C.; Keeney, L.; Walters, S. G., 2016. Development of a novel methodology to characterize preferential grade by size department and its operational significance. *Minerals Engineering*, 91, 100-107.
- Dessemond, C.; Lajoie-Leroux F.; Soucy, G.; Laroche, N.; Magnan, J-F., 2019. Spodumene: The Lithium Market, Resources and Processes, *Minerals*.
- Ebensperger, A.; Maxwell, P.; Moscoso, C., 2005. The lithium industry: its recent evolution and future prospect. *Resour. Policy* 30, 218–231.
- Ellestad, R.B.; Leute, K.M. 1950. Method of extracting lithium values from spodumene ores. U.S. Patent 2,516,109.
- Fosu, A.Y.; Kanari, N.; Hodge, H.; Vaughan, J.; Chagnes, A., 2021. Physico-Chemical Characteristics of Spodumene Concentrate and Its Thermal Transformations. 1–19.



- Gu, Y.; Napier-Munn, T., 1997. JK/Philips mineral liberation analyzer – an introduction. Minerals Processing '97 Conf. Cape Town, SA, p. 2.
- Herbst, J.A.; Fuerstenau, D.W., 1980. Scale-up procedure for continuous grinding mill design using population balance models. *International Journal of Mineral Processing*, 7(1), 1-31.
- Jayasundara, C.T.; Yang, R.; Yu, A., 2012. Effect of the size of media on grinding performance in stirred mills. *Minerals Engineering*, 33, 66-71. <https://doi.org/10.1016/j.mineng.2011.10.012>.
- Kavanagh, L.; Keohane, J.; Cabellos, G. G.; Lloyd, A.; Cleary, J., 2018. Global Lithium Sources—Industrial Use and Future in the Electric Vehicle Industry: A Review. *resources MDPI*.
- Kaya, M.; McIvor, R., 1992. A Comminution Study for Reduction of Grinding Energy Cost. Conference: 4th International Mineral Processing Symposium (IMPS-1992) At: Antalya, Turkey.
- Kono, Y.; Akira, M.; Masahiro, I.; Makoto, A., 2008. Temperature derivatives of elastic wave velocities in plagioclase (An<sub>51±1</sub>) above and below the order-disorder transition temperature. *The American Mineralogist*, 93(4), 558-564.
- Meshram, P.; Pandey, B.D.; Mankhand, T.R., 2014. Extraction of lithium from primary and secondary sources by pre-treatment, leaching and separation: A comprehensive review. *Hydrometallurgy*. 150, 192–208.
- Nazir, K. M.; Dyer, L.; Tadesse, B.; Albijanic, B.; Kashif, N., 2022a. Effect of calcination on coarse gangue rejection of hard rock lithium ores. *Scientific Reports*. 12963.
- Nazir, M.K., Dyer, L., Tadesse, B., Albijanic, B., Kashif, N., 2022b. Flotation performance of calcined spodumene. *Advanced Powder Technology* 33(11), 103772.
- Neißer-Deiters, A.; Scherb, S.; Beutner, N.; Thienel, K-C., 2019. Influence of the calcination temperature properties of a mica mineral as a suitability study for the use as SCM. *Applied Clay Science*, 179, 105168.
- Ohno, I.; Harada, K.; Yoshitomi, C., 2006. Temperature variation of elastic constants of quartz across the  $\alpha$  -  $\beta$  transition, *Physics and Chemistry of Minerals*, 33, 1-9.
- Peiró, L.T.; Méndez, G.V.; Ayres, R.U., 2013. Lithium: Sources, production, uses, and recovery outlook. *J. Miner. Met. Mater. Soc. TMS*, 65, 986–996.
- Peltosaari, O.; Tanskanen, P.A.; Heikkinen, E.P.; Fabritius, T., 2016. Mechanical enrichment of converted spodumene by selective sieving. *Miner. Eng.* 98, 30-39.
- Reichel, S.; Aubel, T.; Patzig, A.; Janneck, E.; Martin, M., 2017. Lithium recovery from lithium-containing micas using sulfur oxidizing microorganisms. *Miner. Eng.* 106, 18–21.
- Salakjani, N.K.; Singh, P.; Nikoloski, A.N., 2016. Mineralogical transformations of spodumene concentrate from Greenbushes, Western Australia. Part 1: Conventional heating. *Miner. Eng.* 98, 71–79.

- Swain, B., 2017. Recovery and recycling of lithium: a review. *Sep. Purif. Technol.* 172, 388–403.
- Tadesse, B.; Makuei, F.; Albijanic, B.; Dyer, L., 2019. The beneficiation of lithium minerals from hard rock ores: A review. *Miner. Eng.* 131, 170–184.
- Walters, S. G., 2016. Driving productivity by increasing feed quality through application of innovative grade engineering technologies. Cooperative Research Centre for Optimising Resource Extraction (CRC ORE). Brisbane, Australia.
- Wills, B.A.; Napier-Munn, T., 2006. *Mineral Processing Technology Books*. Elsevier Sci.Technol.
- Yaksic, A.; Tilton, J.E., 2009. Using the cumulative availability curve to assess the threat of mineral depletion: The case of lithium. *Resour. Policy*, 34, 185–194.

## **Chapter V**

### **Influence of calcination temperatures on lithium deoprtment by screening hard rock lithium**

Muhammad Kashif Nazir, Laurence Dyer, Bogale Tadesse, Boris Albijanic, Nadia Kashif

Accepted in a journal

## Abstract

Calcination of spodumene is a pre-treatment stage in preparation for sulfation roasting and leaching in lithium recovery. During calcination,  $\alpha$ -spodumene (less reactive, monoclinic crystal structure) is converted to  $\beta$ -spodumene (more reactive, tetragonal crystal structure). A third, metastable  $\gamma$ -phase has been identified at lower temperatures than full conversion to the  $\beta$ -phase. It has been previously observed that calcination greatly alters the physical properties of the various minerals in pegmatite ores, impacting comminution energy and liberation. Thus, the objective of this work is to investigate the relationships between calcination temperatures and the physical behaviour of hard rock lithium ores. The results showed that the increase in calcination temperature resulted in a higher lithium deportment in the finest size fraction ( $-0.6$  mm) and thus a higher lithium grade and recovery. The samples calcined at  $540^{\circ}\text{C}$  and  $950^{\circ}\text{C}$  did not show a significant increase in lithium grades in the finest size fraction. This work shows the incremental change in the physical properties of various minerals in the ore with increasing calcination temperature.

**Keywords:** Spodumene ore; calcination; lithium deportment; coarse gangue rejection.

## 1. Introduction

Spodumene ( $\text{LiAlSi}_2\text{O}_6$ ) is a lithium aluminosilicate that acquired its name from the Greek word “spodumene” (burnt to ashes) due to its post-grinding ash-like grey colour. Spodumene is the most important lithium mineral to produce lithium compounds from hard rock lithium ores because of its significant  $\text{Li}_2\text{O}$  content (Choubey et al., 2017; Garrett, 2004; Habashi, 1997). This mineral is found in association with other minerals like quartz, albite, and beryl traces (Anthony et al., 2015).

There are three known phases of spodumene:  $\alpha$ ,  $\beta$ ,  $\gamma$ . Naturally occurring  $\alpha$ -spodumene has the highest density ( $3.27 \text{ g/cm}^3$ ) due to its monoclinic crystal structure (Dessemond et al., 2020).  $\beta$ -Spodumene has an open tetragonal structure (Li et al., 1967; Keat, 1954) while  $\gamma$ -Spodumene (Peltosaari et al., 2015; Li, 1967) has a hexagonal structure; however, both  $\beta$ -Spodumene and  $\gamma$ -Spodumene have the same density ( $2.45 \text{ g/cm}^3$ ). It should be noted that  $\gamma$ -spodumene is

recently discovered as a meta-stable phase (Peltosaari et al., 2015, Salakjani et al., 2016 & 2017; Abdullah et al., 2019).

$\alpha$ -Spodumene is weakly reactive in the presence of strong acids and thus a common practice is to convert  $\alpha$  to  $\beta$ -spodumene through a thermal treatment (Rosalesa et al., 2019). The extraction process of lithium from spodumene was patented in 1950 (Ellestad and Leute, 1950) using the heat treatment to transform  $\alpha$ -spodumene to  $\beta$ -spodumene which is a less dense tetragonal allotrope of spodumene. The phenomenon of thermally activated phase transition is known as calcination or decrepitation (Ellestad and Leute, 1950). During calcination, crushed spodumene concentrate is heated in a furnace at temperatures above 950 °C for more than 30 min. This thermal treatment allows  $\alpha$ -spodumene to convert completely to  $\beta$ -spodumene, leading to a crystal lattice expansion of  $\beta$ -spodumene. The lattice volume of  $\gamma$ -spodumene is 8% more than that of  $\alpha$ -spodumene while that of  $\beta$ -spodumene is 17% more than  $\gamma$ -spodumene (Dessemond et al., 2020). It means that the lattice volume of  $\beta$ -spodumene is the highest while the lattice volume of  $\alpha$ -spodumene is the lowest. For energetics,  $\alpha$ -spodumene to  $\beta$ -spodumene and  $\gamma$ -spodumene to  $\beta$ -spodumene transition are reported to be endothermic (Botto, et. al, 1976, Gasalla and Pereira, 1990, Salakjani et. al, 2016 & 2017, while the transition from  $\alpha$ -spodumene to  $\gamma$ -spodumene is exothermic (Brook, 1991).

Numerous authors have investigated the phase transformations that takes place during calcination of spodumene (Dessemond et al., 2020; Salakjani et al., 2016, 2017, 2019; Changes and Fosu, 2020; Abdullah et al., 2019). A study by Salakjani et al. (2017) showed that the dislocation of  $Al^{+3}$  during calcination is responsible for the volumetric expansion of spodumene crystal structure making lithia species mobile and reactive with strong acids (Changes and Fosu, 2020). Comminution was observed to be improved as a result of this phase transformation attributed to a flaky and softer structure of  $\beta$ -spodumene (Salakjani et al, 2020; Peltosaari et al., 2015; Abdullah et al., 2019). With the recent discovery of a third meta-stable  $\gamma$ -phase, the sequence of the phase transformation during calcination is now described as  $\alpha \rightarrow \gamma \rightarrow \beta$  (Salakjani et al., 2016; Peltosaari et al., 2015; Dessemond et al., 2020). The interlocking gangue associated with spodumene can play a detrimental role in downstream beneficiation process, but some studies have shown that the presence of these impurities can expedite the heat conduction and thus effective phase transition of spodumene (Salakjani et al., 2020; White and McVay, 1958).

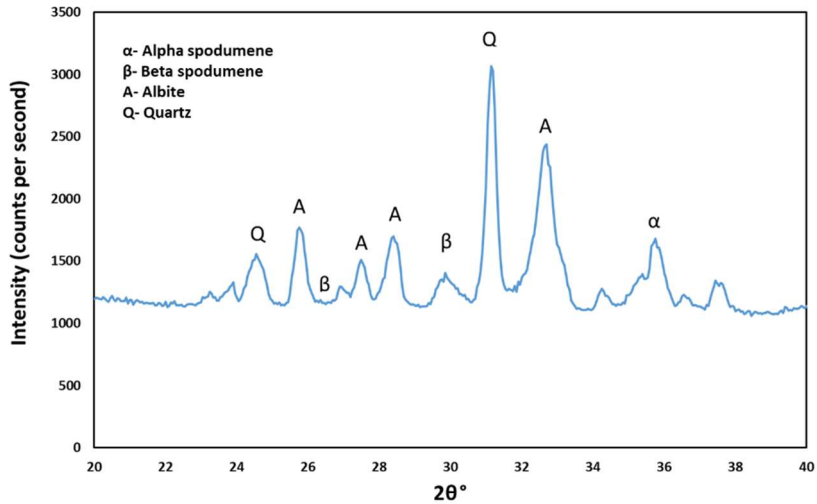
Moore et al. (2018) observed that the mass fraction of transformed phases during calcination was unaffected by the heating temperature and the heating method, however, Salakjani et al. (2017) showed that the temperature and residence time are the major factors to define the phase transformation during calcination of spodumene. Various studies (Salakjani et al., 2016; Peltosaari et al., 2015; Abdullah et al., 2019; Moore et al., 2018) have shown that a number of factors can influence the phase transformation during the calcination of spodumene at elevated temperature, that include the heating technique, the morphology of the spodumene sample after initial comminution, and the quantity of gangue materials present in the sample.

Most research work and studies have focused on two stable phases of spodumene that are  $\alpha$  and  $\beta$ . These two phases got more attention due to their known reactions with strong inorganic acids. Our previous work showed that calcination altered the physical properties of spodumene, reducing comminution energy requirements and thus improving lithium grade and recovery (Nazir et al., 2022a). However, it has not been quantified the effect of different calcination temperatures on the deportment of lithium to the finest size fraction by screening. Therefore, this study aims to examine the effect of calcination temperatures on lithium grade and recovery by screening hard rock lithium ores.

## **2. Materials and methods**

### **2.1. Ore**

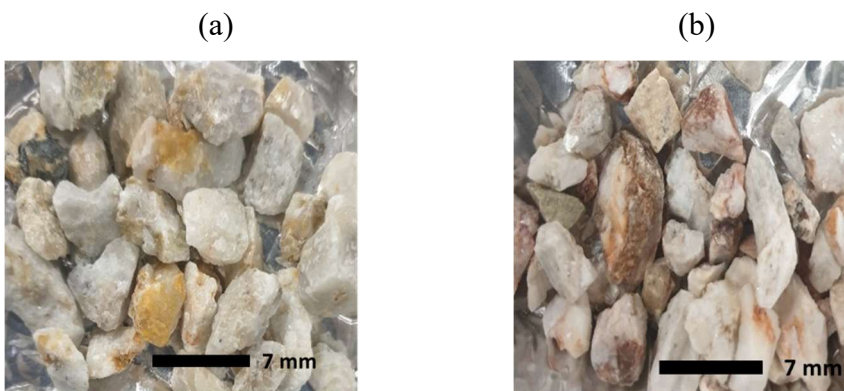
A spodumene ore (Bald Hill Mine Eastern Goldfields, Western Australia) was used in this work. The ore had quartz and albite as main gangue minerals with spodumene as a valuable mineral as found using XRD (X-ray diffraction). The ore grade was 0.3 % lithium (i.e., 8.5% of spodumene), and the particle size was -15 mm.



**Figure 1.** XRD for the non-calcined spodumene ore.

## 2.2. Calcination

The ore was split into four samples, and the mass of each sample was 1500 g. All these samples were calcined at 540, 950, or 1100°C in a muffle furnace (Cupellation furnace, Carbolite Sheffield England) for 1 h, which was sufficient for complete phase transformation at the given temperature; the air atmosphere was used for calcination. After calcination, the mass of the sample was reduced by 0.6% (at 540°C), 1% (at 950°C), and 1.4% (1100°C). It should be noted that one sample was not calcined. Figure 2 shows the photos of both non-calcined and calcined samples. The increase in temperature affected the physical appearance of the samples. For example, the fracturing of the sample calcined at 1100 °C was evident due to the conversion of  $\alpha$  to  $\beta$ -spodumene, which agrees well with the literature (Peltosaari et al., 2016, Salakjani et. al, 2019).



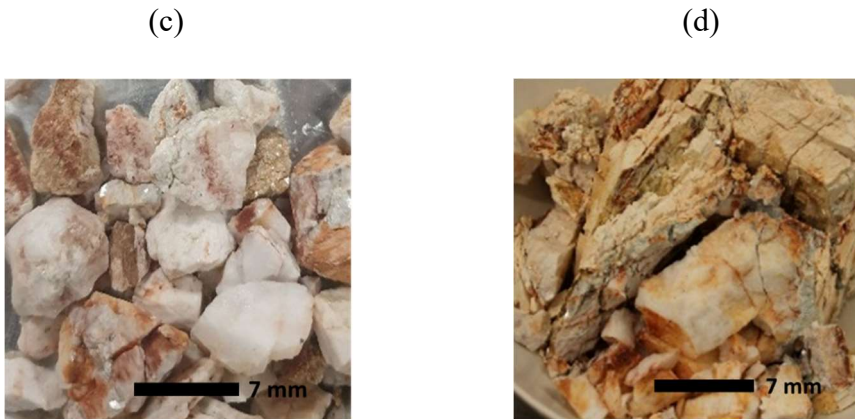


**Figure 2.** The images of a) non-calcined ore, b) calcined ore at 540°C, c) calcined ore at 950°C and d) calcined ore at 1100°C.

The variations in ore properties after calcination at 1100°C were characterized by MLA (mineral liberation analysis) and represented in Figure 3. The MLA contains a FEI Quanta 600F field emission SEM (US, Oregon), two Bruker Quantax X-Flash 5010 EDX detectors (US, Massachusetts), and FEI’s MLA software 3.1.3 for data acquisition and processing. Figure 3 shows that spodumene was more fractured after calcination due to the complete conversion of  $\alpha$  to  $\beta$  spodumene (Peltosaari, et. al, 2016; Salakjani, et. al, 2016.).

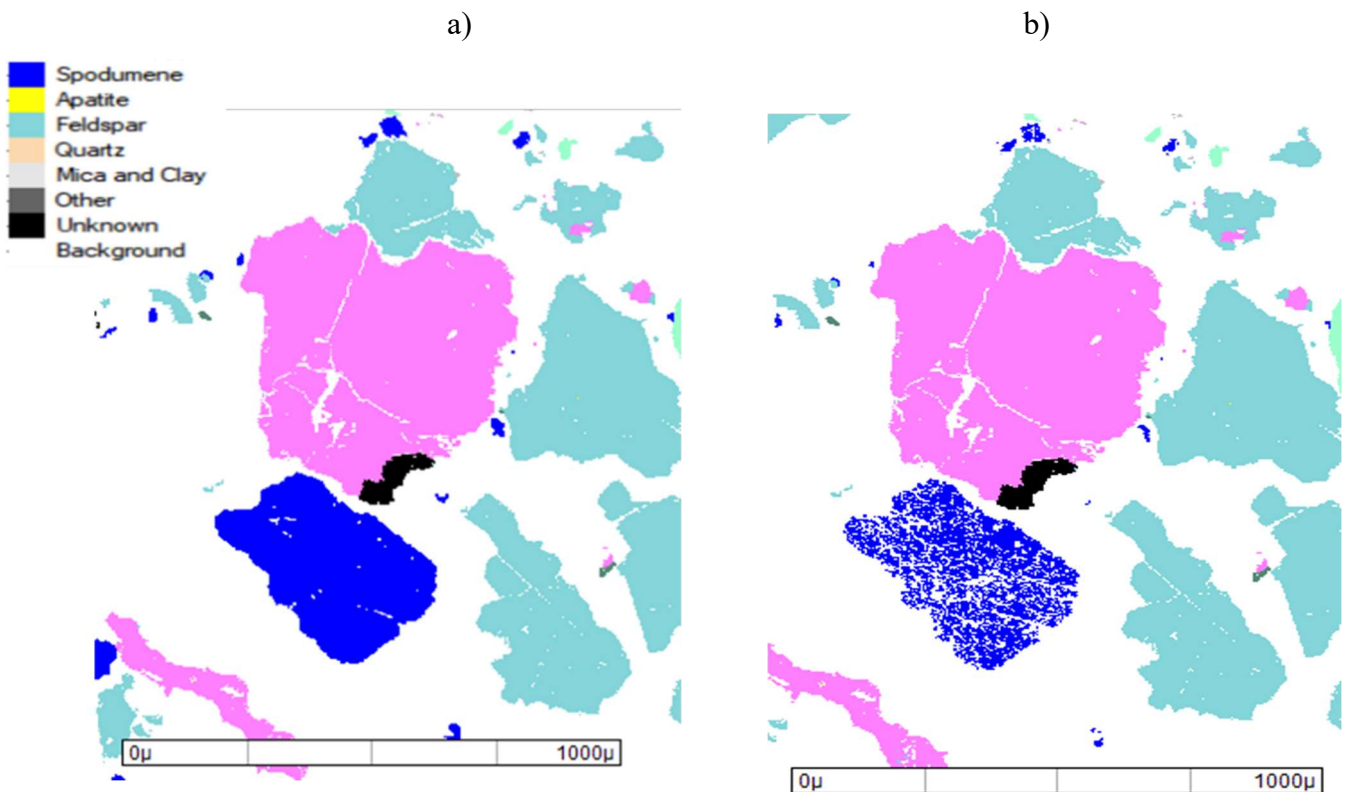


**Figure 3.** Estimation of particle properties a) before calcination and b) after calcination (Kashif et al., 2022b).



### 2.3. Grinding

Both non-calcined and calcined samples (1500 g of the ores) were ground in a laboratory mill. The ball mill had 12 forged balls and a sample mass of 1060 g (the ratio of the forged balls to the ore was 0.7); each grinding ball had 27.3 mm in diameter. The rotational speed of the mill was 70 rpm. Each sample was ground for 20 min and subsequently screened in six different size fractions (+3.35 mm, -3.35 +2.36 mm, -2.36 +1.7 mm, -1.7+ 1.18 mm, -1.18 + 0.6 mm, - 0.6 mm). The lithium content of each size fraction was determined by preparing a fusion glass bead, digesting in 10 % citric acid, and using ICP-OES (Agilent Technologies, US).

### 2.4. X- Ray Diffraction (XRD)

Mineralogical analyses of the lithium ore samples were performed using an Olympus BTX™ III Benchtop (Co-K $\alpha$ ) X-ray diffractometer (XRD) to study the phase transformation of spodumene in the range between 20 and 40° (2 $\theta$ ) as a function of different calcination temperatures; this instrument is a transmission XRD and it does not have steps. The AMCSD database cards for the phases are:  $\alpha$ -spodumene – Set 1 (file 408),  $\beta$ -spodumene Set 2 (file 2119), quartz – Set 2 (file 1936), albite – Set 1 (file 2289).

The XRD experiments were conducted on fine fractions (-0.6 mm) and coarse fractions (+0.6 mm) of all four products obtained after calcination and grinding. It should be noted that the maximum lithium content was found in the finer size fraction after calcination. The finest fraction is generally the most relevant for coarse gangue rejection since lithium tends to deport to the finest fractions.

## 3. Results and discussions

### 3.1. Effect of calcination temperature on ore retention

Figure 4 shows the influence of different calcination temperatures on particle size distribution. The vast majority of the non-calcined material was oversized, reporting to the +3.35 mm fraction. However, the minimum ore retention was obtained for the grinding product calcined at the highest temperature (i.e., 1100°C); the ore retention represents the amount of the ore retained on each screen after sieving. Figure 4 also shows that calcination shifted the particle size distributions toward the finer fraction and to a greater extent with higher temperatures.

The reason is that the increase in calcination temperature made spodumene and albite more brittle, resulting in more efficient grinding and thus more department of the grinding products to the finest screen size.

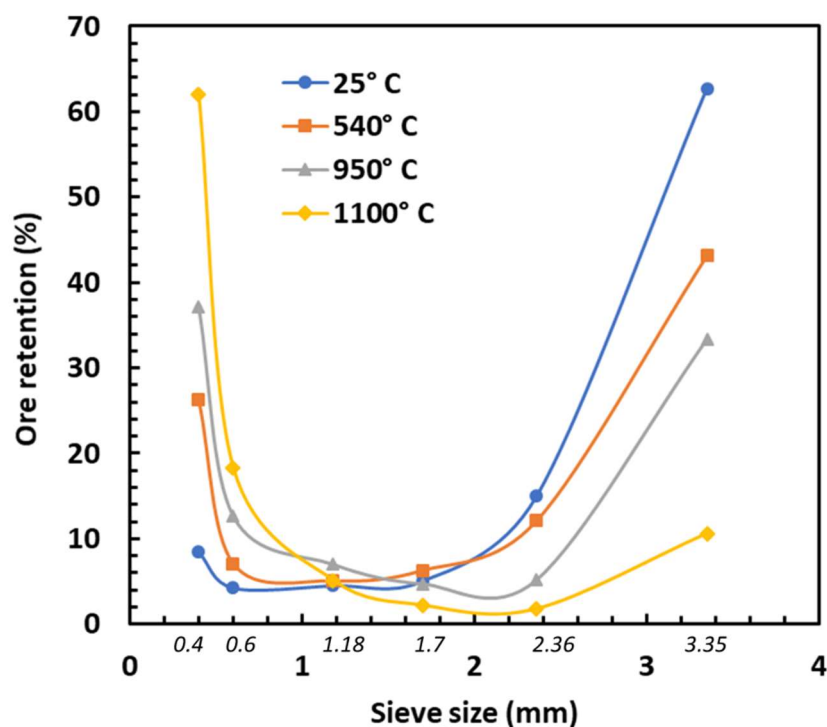


**Figure 4.** The influence of calcination temperature on ore retention.

### 3.2. Effect of calcination temperature on lithium grade and lithium recovery

Figure 5 shows the influence of calcination temperature on cumulative lithium grade; the cumulative lithium grade represents the accumulation of lithium in the finest size fraction (-0.6 mm). As seen in Figure 5, for the non-calcined sample (i.e., 25 °C), the higher the lithium grade, the largest the screen size. It means that the lithium department to the finest screen did not happen after the grinding of the non-calcined sample. However, in the case of the sample calcined at 1100 °C, the opposite trend was observed, indicating an improvement in coarse gangue rejection. In other words, the maximum lithium grade was obtained in the smallest screen size (0.6 mm) while the minimum lithium grade was achieved in the coarsest screen size (3.35 mm). The reason is that when the sample was calcined to 1100 °C,  $\alpha$ -spodumene was

completely transformed to  $\beta$ -spodumene, making the sample very brittle and thus leading to coarse gangue rejections after grinding and screening operation.

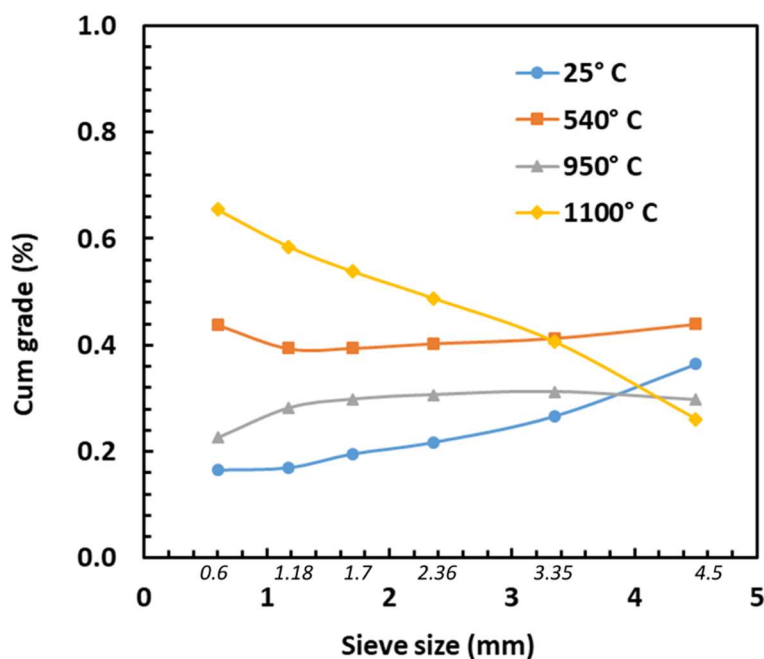


**Figure 5.** Effect of calcination temperature on cumulative lithium grade.

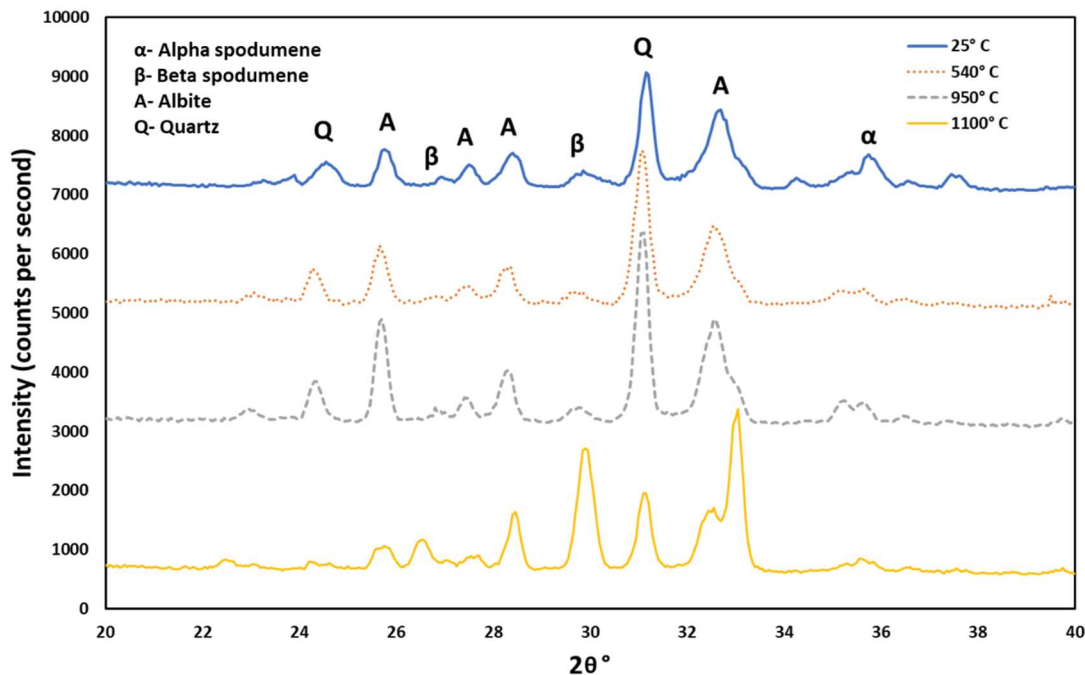
However, when the sample is calcined to 540 or 950 °C, the lithium content was similar across the screen sizes, demonstrating some shift from the non-calcined sample behavior was achieved but not to the extent of the sample treated at 1100°C. This observation could be due to the incomplete transformation from  $\alpha$  to  $\beta$ -spodumene and dilution in the fines due to greater grinding of other phases. It is worth mentioning that the lithium grade in the case of the sample calcined to 950 °C was lower than that in the case of the sample calcined to 540 °C. The reason is that at 950 °C albite deported to the fine fraction, leading to a lower lithium grade of the sample in all the screen sizes (see Figure 6).

Figure 6 shows the mineralogy of the fine size (-0.6 mm) and coarse size (+0.6 mm) fractions which are required to understand the lithium deportment as a function of temperature. As seen in Figure 6a, the maximum amount of  $\beta$ -spodumene was found when the calcination temperature was 1100 °C. The amount of  $\beta$ -spodumene in the non-calcined sample was almost the same as that in the samples calcined at 540 °C and 950 °C because  $\alpha$ -spodumene did not

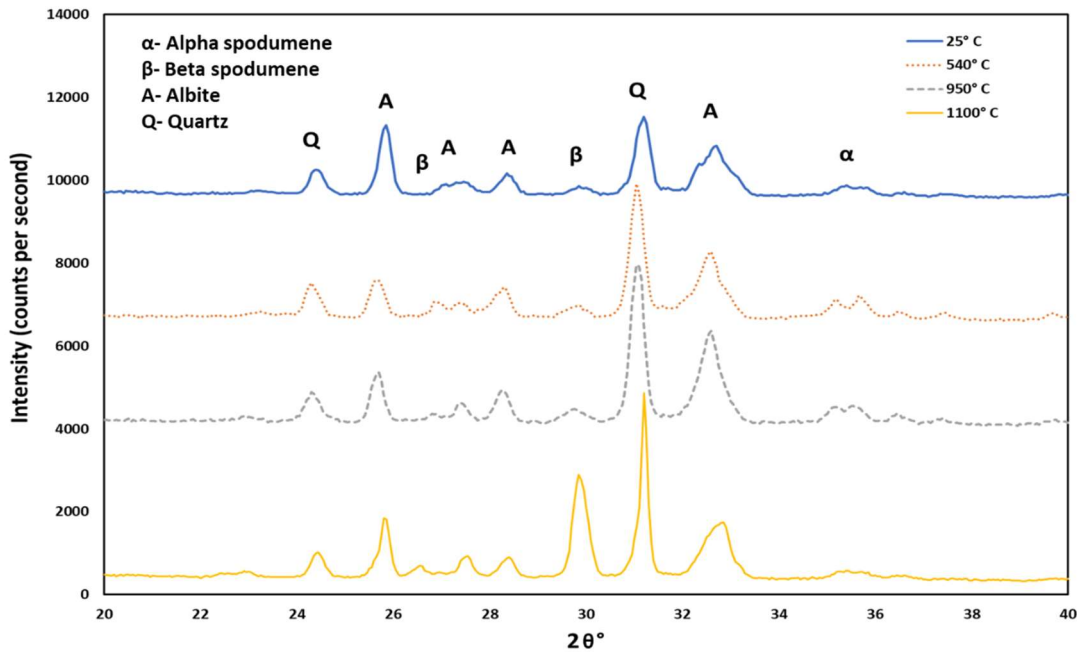
transform to  $\beta$ -spodumene at these temperatures. Figure 6a also shows that the higher the calcination temperature, the higher the amount of albite in the fine size fraction. As a result, the lithium grade in the fine size fraction for the sample calcined at 540 °C was higher than that for the sample calcined at 950 °C. However, due to a complete phase transformation from  $\alpha$  to  $\beta$ -spodumene at 1100 °C, most of  $\beta$ -spodumene departed to the fine size fraction, leading to the highest lithium grade in the fine size fraction.

Figure 6b shows that the amount of  $\beta$ -spodumene in the coarse size fractions followed the same pattern as that in the case of fine size fractions. However, the amount of albite for the coarse size fraction was the highest at 950°C. Therefore, due to a significant amount of albite present in the finest size fraction at 950°C, the lithium grade for the sample calcined at this temperature was lower than that at 540°C.

(a)



(b)



**Figure 6.** Mineralogy of a) the fine size fraction (-0.6 mm) and b) the coarse size fraction (+0.6 mm).

Figure 7 shows the influence of calcination temperature on cumulative lithium recovery with size fraction; the cumulative lithium recovery is the sum of the recovered lithium (i.e., the sum of the mass of lithium on each screen divided by the mass of lithium in feed) for each size fraction. As seen in Figure 7, in the finest size fraction (-0.6 mm), the increase in calcination temperature led to a higher lithium recovery due to the department of lithium to the finest size fraction. A similar trend was also observed for particle sizes higher than 0.6 mm. However, when the screen size was higher than 0.6 mm, the recovery for the sample calcined at 950 °C was slightly higher than the sample calcined at 1100°C. The reason is that the transformation from  $\alpha$  to  $\beta$  spodumene at 950 °C was not complete.

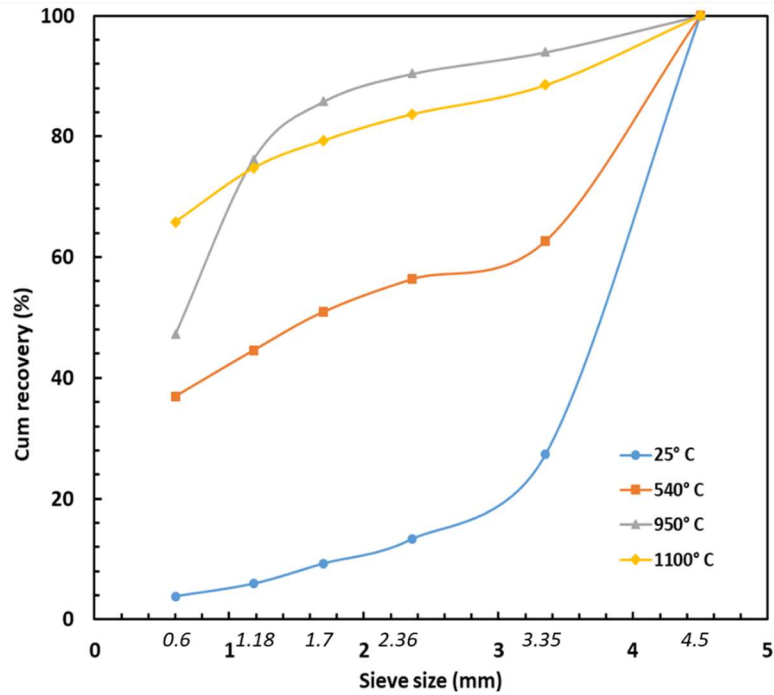


**Figure 7.** Effect of calcination temperature on lithium recovery.

This work shows the correlations between calcination temperature, coarse gangue rejections and physical properties of the spodumene ore. A similar correlation may exist for other minerals in which there are phase transformations during the calcination process, leading to the change in the physical properties of these minerals.

#### 4. Conclusions

This work investigates the influence of calcination temperature on lithium grade and recovery by screening a spodumene ore. It was found that the lithium grade in the finest size fraction (-0.6 mm) was the lowest when the sample was not calcined. A strong lithium department to fines was observed at 1100°C but not after calcination conducted at temperatures lower than 950°C. The reason is due to incomplete transformation from  $\alpha$  to  $\beta$  spodumene at temperatures below 950°C, leading to a higher amount of non-brittle spodumene phase (i.e.,  $\alpha$ -spodumene). The lithium grade in the finest size fraction when the sample was calcined at 540°C was slightly higher than that when the sample was calcined at 950°C. The reason is that at 950°C albite deported to the finest size fraction, reducing the lithium grade. The highest lithium grade in the finest size fraction was obtained when the sample was calcined at 1100°C due to the complete transformation from  $\alpha$  to  $\beta$  spodumene. The highest lithium recovery was also achieved at the

same temperature in the case of the finest size fraction. Further work is required to investigate calcination as a potential treatment for increasing grade and recovery by screening hard rock ores in which phase transformations of some minerals occur as a function of calcination temperature.

### **Acknowledgements**

The collaboration between the authors would not have been possible without the financial support from CRC ORE. CRC ORE is part of the Australian Government's CRC Program, which is made possible through the investment and ongoing support of the Australian Government. The CRC Program supports industry-led collaborations between industry, researchers and the community.

The Bald Hill Mine (Alliance Mineral Assets Limited, Western Australia) is acknowledged for the provision of samples for all the experiments. Financial support from Curtin University for this research work is appreciated.

### **References**

- Abdullah, A.A.; Oskierski, H.C.; Altarawneh, M.; Senanayake, G.; Lumpkin, G.; Dlugogorski, B.Z., 2019. Phase transformation mechanism of spodumene during its calcination. *Miner. Eng.* 140, 105883, doi:10.1016/j.mineng.2019.105883.
- Anthony, J.W.; Bideaux, R.A.; Bladh, K.W.; Nichols, M.C., 2015. *Handbook of Mineralogy; Mineralogical Society of America: Chantilly, VA, USA*, Available online: <http://www.handbookofmineralogy.org/> (accessed on 12 March 2019).
- Botto, I.L.; Arazi, S.C.; Krenkel, T.G., 1976. Aplicación de la teoría de Delmon al estudio del mecanismo de la transformación polimórfica de espodumeno I en espodumeno II. *Boletín Sociedad Española Cerámica Vidrio.* 15, 5–10.
- Brook, R.J., 1991. *Concise Encyclopedia of Advanced Ceramic Materials*; Pergamon Press: Oxford, England.
- Changes, A., Fosu, A. Y., 2020. Retrieved from <https://encyclopedia.pub/3834>
- Choubey, P.K., Chung, K.-S., Kim, M., Lee, J., Srivastava, R.R., 2017. Advance review on the exploitation of the prominent energy-storage element lithium. Part II: from sea water and spent lithium ion batteries (LIBs). *Miner. Eng.* 110, 104–121, <http://dx.doi.org/10.1016/j.mineng.2017.04.008>.
- Dessemond, C., Soucy, G., Jean-Philippe Harvey, J-P., Ouzilleau, P., 2020. Phase Transitions in the  $\alpha$ - $\gamma$ - $\beta$  Spodumene Thermodynamic System and Impact of  $\gamma$ -Spodumene on the Efficiency of Lithium Extraction by Acid Leaching, *Minerals*.

- Ellestad, R.B.; Leute, K.M., 1950. Method of Extracting Lithium Values from Spodumene Ores. U.S. Patent Application 2,516,109.
- Garrett, D.E., 2004. Handbook of Lithium and Natural Calcium Chloride. Elsevier, <http://dx.doi.org/10.1016/B978-0-12-276152-2.X5035-X>.
- Gasalla, H.; Pereira, E., 1990. Activation-deactivation mechanisms in spodumene samples. *Solid State Ion.* 42, 1–6.
- Habashi, F., 1997. Handbook of Extractive Metallurgy, vol. IV. Wiley, Weinheim.
- Keat, P.P., 1954. A new crystalline silica *Science*. 120, 328–330.
- Li, C.T., 1967. The crystal structure of LiAlSi<sub>2</sub>O<sub>6</sub> III (high-quartz solid solution). *Zeitschrift für Kristallographie*, 127, 327–334.
- Li, C.T.; Peacor, D.R., 1968. The crystal structure of LiAlSi<sub>2</sub>O<sub>6</sub>-II (B-spodumene). *Zeitschrift für Kristallographie*, 126, 46–65.
- Nazir, M.K., Dyer, L., Tadesse, B., Albijanic, B., Kashif, N., 2022a. Effect of calcination on coarse gangue rejection of hard rock lithium ores. *Scientific Reports* 12, 12963.
- Nazir, M.K., Dyer, L., Tadesse, B., Albijanic, B., Kashif, N., 2022b. Flotation performance of calcined spodumene. *Advanced Powder Technology* 33(11), 103772.
- Moore, R.L.; Mann, J.P.; Montoya, A.; Haynes, B.S., 2018. In situ synchrotron XRD analysis of the kinetics of spodumene phase transitions. *Phys. Chem. Chem. Phys.* 20, 10753–10761, doi:10.1039/C7CP07754H.
- Peltosaari, O.; Tanskanen, Hautala, S.; P.A.; Heikkinen, E.P.; Fabritius, T., 2016. Mechanical enrichment of converted spodumene by selective sieving. *Miner. Eng.* 98, 30–39.
- Peltosaari, O.; Tanskanen, P.A.; Heikkinen, E.P.; Fabritius, T., 2015.  $\alpha$ -  $\beta$ -  $\gamma$ -phase transformation of spodumene with hybrid microwave and conventional furnaces. *Miner. Eng.* 82, 54–60. [CrossRef]
- Rosalesa, G. D.; Resenteraa, A. C. J.; Gonzalezc, J. A.; Wuilloudb, R. G.; Rodriguez, M. H., 2019. Efficient extraction of lithium from -spodumene by direct roasting with NaF and leaching; *Chemical Engineering Research and Design* 150, 320–326
- Salakjani, N.K.; Nikoloski, A.; Singh, P., 2017. Mineralogical transformations of spodumene concentrate from Greenbushes, Western Australia. Part 2: Microwave heating. *Miner. Eng.* 100, 191–199.
- Salakjani, N.K.; Nikoloski, A.; Singh, P.; Nikoloski, A. N., 2019. Production of Lithium – A Literature Review Part 1: Pretreatment of Spodumene, *Mineral Processing and Extractive Metallurgy Review*. 41:5, 335-348, DOI: 10.1080/08827508.2019.1643343



- Salakjani, N.K.; Singh, P.; Nikoloski, A., 2016. Mineralogical transformations of spodumene concentrate from Greenbushes, Western Australia. Part 1: Conventional heating. *Miner. Eng.* 98, 71–79.
- Salakjani, N.K.; Singh, P.; Nikoloski, A.N., 2020. Production of Lithium—A Literature Review Part 1: Pretreatment of Spodumene. *Miner. Process. Extr. Metall. Rev.* 2020, 41, 335–348, doi:10.1080/08827508.2019.1643343
- White, G.D.; McVay, T.N. 1958. Some Aspects of the Recovery of Lithium from Spodumene; Oak Ridge National Laboratory: Oak Ridge, TN, USA.

## **Chapter VI**

### **Flotation performance of calcined spodumene**

Muhammad Kashif Nazir, Laurence Dyer, Bogale Tadesse, Boris Albijanic, Nadia Kashif

Published in <https://doi.org/10.1016/j.appt.2022.103772>

## Abstract

Spodumene flotation in the presence of oleate is widely used in the lithium mining industry. However, there is no study investigating flotation behaviour of calcined spodumene. Thus, the main focus of this technical note is to address this matter. The results showed that the increase in the calcination temperature led to fractured spodumene surfaces as found using MLA (mineral liberation analyser), probably resulting in higher oleate adsorption on spodumene surfaces. Another reason for higher oleate adsorption on calcined samples could be due to the changes in surface properties of calcined spodumene (i.e.,  $\alpha$  to  $\beta$  transformation of spodumene). Therefore, the higher the calcination temperature, the higher the flotation recovery of calcined spodumene. This work shows that calcination before flotation can be highly beneficial pre-treatment for improving the lithium recoveries and grades.

**Keywords:** Spodumene flotation, calcination temperature, sodium oleate, adsorption

## 1. Introduction

Worlds' attention is shifting from brines to hard rock minerals for lithium extraction to meet its fast-growing demand, particularly in the battery industry. The anticipated rise in future requirements for lithium has triggered the research industry to find more effective ways to extract lithium from lithium-bearing minerals resources. Spodumene is considered to be the most important mineral for lithium production because of its high  $\text{Li}_2\text{O}$  content (Kesler et. al, 2012; Dessemond el. Al, 2019, Peltosaari, et. al, 2016). Different mineral processing techniques such as dense media separation, flotation and magnetic separation are used for spodumene beneficiation. However, flotation is one of the most effective methods for the recovery of spodumene fine particles (Tadesse et al., 2019).

The most investigated collector in spodumene flotation is sodium oleate when other aluminosilicates such as quartz and feldspar are present (Moon and Fuerstenau, 2003; Filippov et. al, 2019). However, due to the similarity in surface properties of spodumene and its gangue minerals, recovery of spodumene by flotation is challenging.

Filippov et al (2019) found that grinding of spodumene generated new surfaces with improved adsorption properties due to the breakage of longer and weaker Al-O bonds. To improve spodumene flotation performance, it may be needed to conduct calcination of spodumene before flotation. The reason is that calcination above 1000°C converts  $\alpha$  to  $\beta$ -spodumene (Abdullah et al., 2019; Lin and Wang, 1995; Nazir et al., 2022; Salakjani et al., 2016) and thus this transformation may alter the surface and physical properties of spodumene such as brittleness and thus improve flotation recovery and grade of lithium. However, there is no information about the surface properties of calcined spodumene and its impact on the flotation behaviour of spodumene.

The objective of this work is to study the flotation behaviour of calcined spodumene using sodium oleate. The flotation mechanisms will be investigated using the imaging technique (i.e., MLA (mineral liberation analyser)), adsorption tests and zeta potential measurements.

## **2. Materials and methods**

### **2.1. Ore preparations**

The spodumene ore (Bald Hill Mine Eastern Goldfields, Western Australia), used in this work, had 0.39% lithium i.e., 0.83%  $\text{Li}_2\text{O}$ ; the main gangue minerals are 71.5% feldspar and 13.9% quartz. The ore was calcined at different temperatures (540°C, 950°C or 1100°C) in a muffle furnace (Cupellation furnace, Carbolite Sheffield England) for 1 h.  $P_{80}$  of all the samples was 90  $\mu\text{m}$ . The changes in ore properties after calcination at 1100°C were characterized by MLA and shown in Figure 1. The MLA includes a FEI Quanta 600F field emission SEM (US, Oregon), two Bruker Quantax X-Flash 5010 EDX detectors (US, Massachusetts), and FEI's MLA software 3.1.3 for data acquisition and processing. As seen in Figure 1, spodumene became more fractured after calcination. The reason is due to the complete conversion of  $\alpha$  to  $\beta$  spodumene (Li and Peacor, 1968; Keat, 1954, Salakjani, et. al, 2016, Peltosaari, et. al, 2015

and 2016). Both calcined and non-calcined samples were used for flotation and zeta potential measurements.

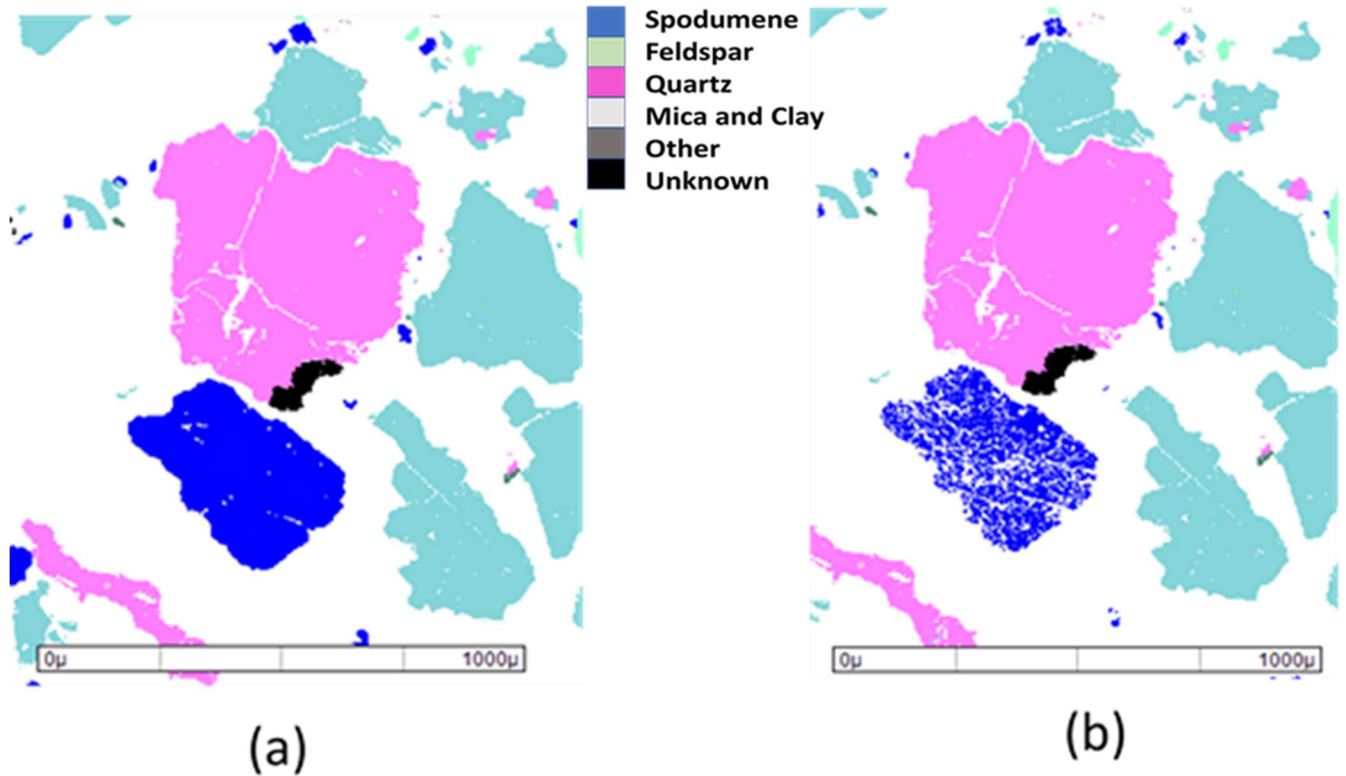


**Figure 1.** Estimation of particle properties a) before calcination and b) after calcination.

## 2.2. Flotation

The ore samples were transferred to a 2.5 L bottom-driven batch flotation cell, and the required amount of water was added to the cell (6% solid ratio); 150 g of the sample was used in all the experiments. The impeller speed was 1300 rpm. 500g/ton of the sodium oleate collector (99% purity, Sigma Aldrich), 250 g/ton of the sodium silicate depressant (99% purity, Sigma Aldrich) and 14 mg/L of the MIBC frother (Orica) were added to the flotation pulp. The flotation experiments were carried out as a function of different pH-s 5,7, 8, 10 and 12; HCl and NaOH were used to adjust the pulp pH. After 2 min of conditioning, all the experiments were performed at 15 L/min of air for 3 min. The flotation concentrates and tails were filtered

and dried. The lithium content was determined by preparing a borate glass fusion bead, digestion in 10 % citric acid, followed by the ICP-OES analysis.

### 2.3. Zeta potential

The zeta potential measurements were conducted using a Zetasizer Nano-ZS (Malvern, UK). These experiments were performed using both calcined and non-calcined samples as a function of pH (5, 7, 8 and 10) in the absence and presence of reagents (sodium oleate (1 g/L)) and sodium silicate (1 g/L)); distilled water was used in all the experiments. All the samples were ground using the laboratory pulverizer (Rocklabs, New Zealand). Before the zeta potential experiments, the suspensions (0.1% solid ratio) were kept for 5 min to allow the settling of the coarse particles. The small amount of suspension was transferred to the measurement cell. Five measurements at each pH were performed, and the average value of the measurements was used.

### 2.4. UV adsorption

The adsorption experiments were performed using the solution depletion method in which the following reagents were used: oleate solutions, copper – triethylenetetramine mixture (copper nitrate with 95% purity, Univar solutions; triethylenetetramine with 60% purity, Sigma Aldrich; ethanolamine with 98% purity, Sigma Aldrich), 20% isobutanol (99% purity, Sigma Aldrich) and 80% cyclohexane solvent (95% purity, Univar solutions) (Gregory, 1966). The solution mixture was held for 10 minutes to separate the two liquid phases. The organic phase was transferred to a test tube, and 2 drops of diethylammonium diethyldithiocarbamate dye (97% purity, Sigma Aldrich) was used to colour the organic phase. The maximum absorbance of the organic phase was determined at 435 nm wavelength with the UV-visible spectrophotometer (Lambda35, PerkinElmer, USA).

### 3. Results and discussions

Figure 2 shows the influence of calcination on flotation performance as a function of pH. As seen in Figure 2, the higher the calcination temperature, the higher the lithium recovery. It appears that the increase in calcination temperature makes spodumene more floatable. One of the reasons may be that the calcined samples have a higher degree of fracturing than the non-calcined samples (see Figure 1). As a result, the calcined samples had more adsorbed collectors than the non-calcined samples, leading to a higher floatability of calcined samples. The highest lithium flotation recovery was achieved at pH 8 considering that at this pH, the largest amount of oleate ions was present in the solution (Qiu et. al, 2013). The increase in calcination temperature improved not only lithium recovery but also lithium grade.

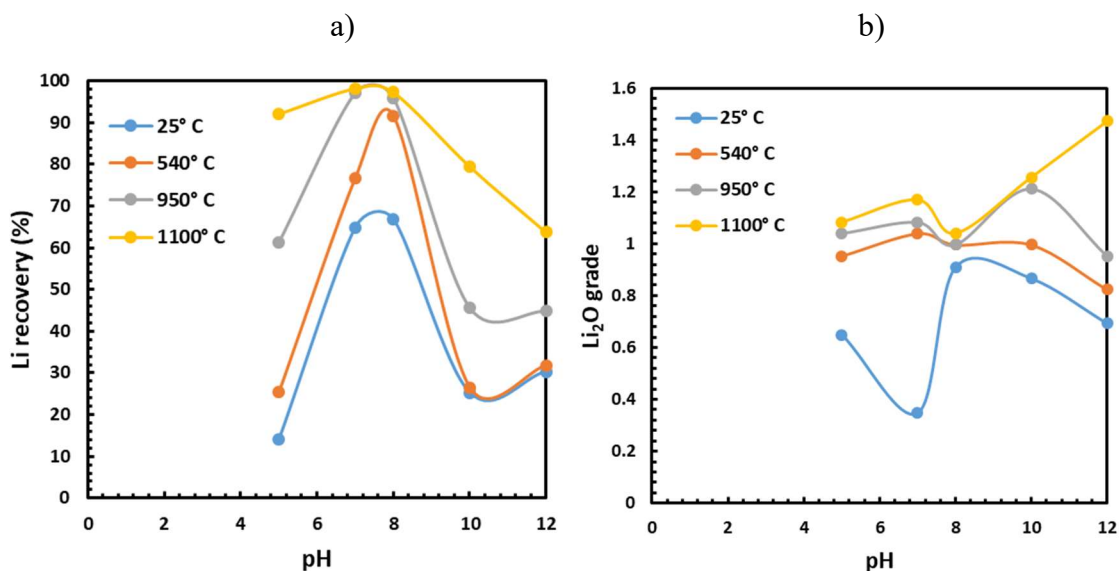


**Figure 2.** Flotation a) Li recovery and b) Li<sub>2</sub>O grade of non-calcined (25°C) and calcined samples as a function of pulp pH.

Figure 3 shows that the increase in calcination resulted in a more negative zeta potential in the distilled water (Figure 3a) and the presence of sodium oleate (Figure 3b). The reason is that calcination of spodumene leads to a higher degree of fracturing due to an increase in broken Si-O and Al-O bonds (Filippov et. al, 2019; Zhu et. al, 2019). The Al-O bonds are longer than the Si-O bonds and thus Al-O bonds are easier to break, exposing more Al ions to sodium oleate adsorption (Filippov et. al, 2019; Zhu et. al, 2019). This is very important considering

that Al sites are the most favourable sites for chemisorption of sodium oleate (Moon and Fuerstenau, 2003; Filippov et. al, 2019; Zhu et. al, 2019). It should be noted that although the four spodumene crystal surfaces (110), (010), (001) and (100) are naturally hydrophilic, the preferential sodium oleate adsorption occurred along (100) and (110) surfaces (Filippov et. al, 2019; Zhu et. al, 2019).

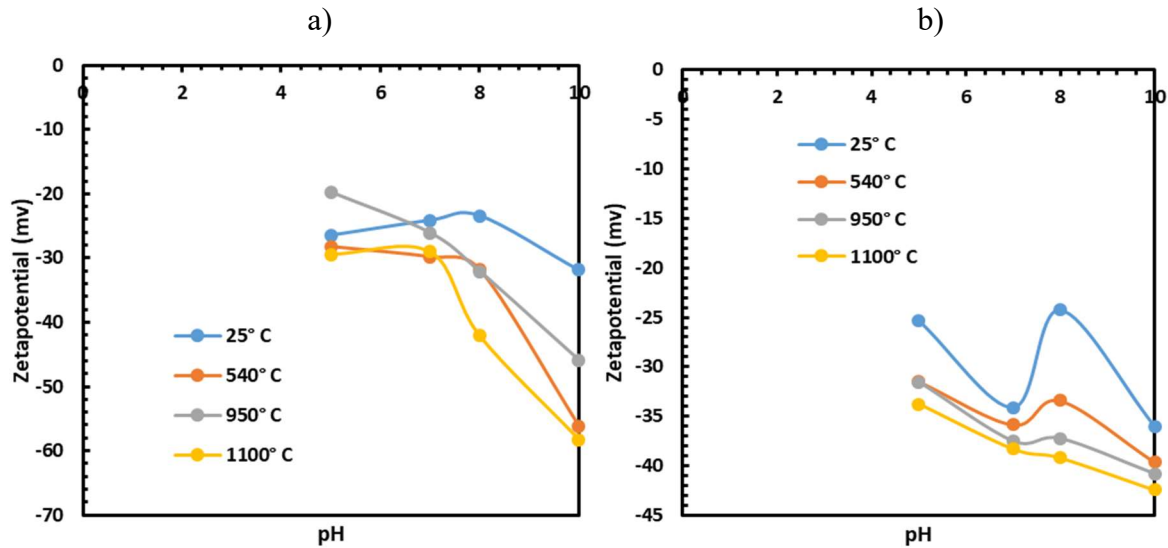


**Figure 3.** Zeta potential measurements of non-calcined and calcined samples a) in the distilled water and b) in the presence of sodium oleate.

Figure 4 shows the oleate concentration in the solutions after adsorptions of the non-calcined and calcined samples. It means that the adsorption of oleate on the investigated samples was the largest when the sample was calcined at 1100°C and the lowest for the non-calcined sample. One of the reasons is probably that calcination increased the surface area 10 times (Salakjani et al., 2016) due to the formation of more fractured surfaces (see Figure 1) and thus more adsorption of oleate occurred in the case of the calcined samples. Another reason for higher oleate adsorption on calcined samples may be due to the changes in surface properties of calcined spodumene (i.e.,  $\alpha$  to  $\beta$  transformation of spodumene). Therefore, the flotation recovery was the highest when the sample was calcined at 1100°C and the lowest for the non-calcined sample (see Figure 2).



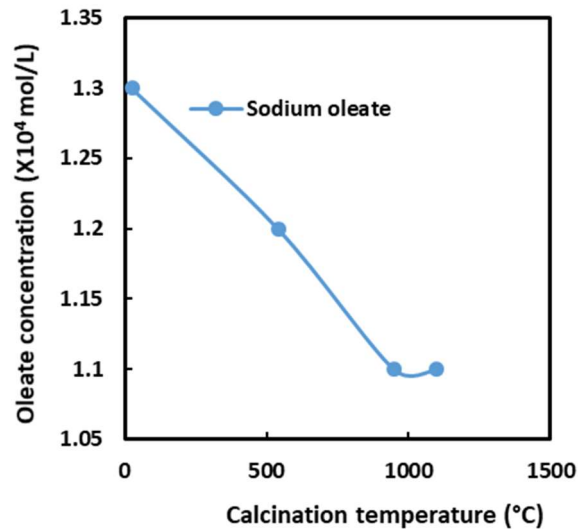


**Figure 4.** Oleate concentrations in solutions after adsorptions of the non-calcined and calcined sample at different temperatures.

#### 4. Conclusions

This technical note investigated calcined spodumene flotation in the presence of sodium oleate. It was found that the increase in the calcination temperature resulted in fractured spodumene surfaces as found using MLA as well as the transformation of spodumene from  $\alpha$  to  $\beta$  phase. As a result, the zeta potentials of the calcined samples were more negative than the zeta potentials of the non-calcined samples. The changes in surface properties of calcined samples resulted in higher adsorption of oleate as confirmed using the adsorption tests and thus a higher flotation recovery and grade. The results of this work may be useful for improving the flotation performance of spodumene ores. Further studies are required to investigate the effect of calcination on the flotation performance of different lithium ores.

#### Acknowledgements

The research was initiated as a continual of grade engineering model for hard rock lithium ore extraction, a project sponsored by CRC ORE. The financial support of the Western Australian School of Mines, Curtin University and CRC ORE for this research work is gratefully

acknowledged. Technical support of staff at Western Australian School of Mines, Curtin University is appreciated. The authors would like to thank Mr Thomas Bede Payten for providing information about the mineralogy.

## 5. References

- Abdullah, A. A., Oskierskia, H. C., Altarawneha, M. N., Senanayakea, G., Lumpkinc, G., Dlugogorskid, B. Z., 2019. Phase transformation mechanism of spodumene during its calcination. *Miner. Eng.* 140, 105883.
- Dessemond, C., Lajoie-Leroux, F., Soucy, G., Laroche, N., Magnan, J., 2019. Spodumene: The Lithium Market, Resources and Processes. *Minerals* 9(6), 334.
- Filippov, L., Farrokhpay, S., Lyo, L., Filippova, I., 2019. Spodumene flotation mechanism. *Minerals*. 9 (6), 372.
- Gregory, G.R.E.C., 1966. The determination of residual anionic surface-active reagents in mineral flotation liquors. *Analyst* 91, 251–257.
- Keat, P.P., 1954. A new crystalline silica. *Science* 120, 328–330.
- Kesler, S.E., Gruber., P.W.c, Medina., P.A., Keoleian., G.A., Everson., M.P., Wallington., T.J. Global lithium resources: Relative importance of pegmatite, brine and other deposits. *Ore Geol. Rev.* 2012, 48, 55–69.
- Li, C.T., Peacor, D.R., 1968. The crystal structure of LiAlSi<sub>2</sub>O<sub>6</sub>-II (B-spodumene). *Zeitschrift für Kristallographie* 126, 46–65.
- Lin, M.H., Wang, M.C., 1995. Crystallization behaviour of b-spodumene in the calcinations of Li<sub>2</sub>O–Al<sub>2</sub>O<sub>3</sub>–SiO<sub>2</sub>–ZrO<sub>2</sub> gels. *J. Mater. Sci.* 30 (10), 2716–2721.
- Moon, K.S., Fuerstenau, D.W., 2003. Surface crystal chemistry in selective flotation of spodumene (LiAl[SiO<sub>3</sub>]<sub>2</sub>) from other aluminosilicates. *Int. J. Miner. Process.* 72, 11–24.
- Nazir, M.K., Dyer, L., Tadesse, B., Albijanic, B., Kashif, N., 2022. Effect of calcination on coarse gangue rejection of hard rock lithium ores. *Scientific Reports* 12, 12963.
- Peltosaari, O., Tanskanen, P., Hautala, S., Heikkinen, E., Fabritius, T., 2016. Mechanical enrichment of converted spodumene by selective sieving. *Miner. Eng.* 98, 30–39.

- Peltosaari, O., Tanskanen, P.A., Heikkinen, E.P., Fabritius, T., 2015.  $\alpha$ -  $\beta$ -  $\gamma$ -phase transformation of spodumene with hybrid microwave and conventional furnaces. *Miner. Eng.* 82, 54–60.
- Qiu X.Y., He J.S., Rao Y.H., Tang Y.H., Luo C.S., Zhang J., 2013. Flotation mechanism of sodium oleate on bastnaesite. *Chin J Rare Metals* 37, 422–428.
- Salakjani, N.K., Singh, P., Nikoloski, A., 2016. Mineralogical transformations of spodumene concentrate from Greenbushes, Western Australia. Part 1: Conventional heating. *Miner. Eng.* 98, 71–79.
- Tadesse, B., Makuei, F., Albijanic, B., Dyer, L., 2019. The beneficiation of lithium minerals from hard rock ores: A review, *Min. Eng.* 131, 170-184.
- Zhu, G., Wang, X., Li, E., Wang, Y., Miller, J.D., 2019. Wetting characterisations of spodumene surfaces as influenced by collector. *Miner. Eng.* 130, 117–128.

**Chapter VII**  
**Conclusions and recommendations for future work**

## 1. Conclusions

Calcination as a first step to beneficiation of spodumene ores showed to have a positive impact on coarse gangue rejection and comminution by screening. It was found that calcination converted  $\alpha$ -spodumene to a brittle phase ( $\beta$ -spodumene) and increased lithium grade and recovery in the finest size fraction,  $-0.6$  mm. The effect of calcination on coarse gangue rejection was profound when calcination was followed by semi-autogenous grinding. However, calcination followed by crushing and autogenous grinding also improved coarse gangue rejection by screening. Energy consumed by non-calcined samples during bond ball mill work index was 42% more than that consumed by a calcined spodumene ore sample.

When calcined spodumene samples were subjected to closed circuit grinding, the maximum amount of lithium grade and recovery were obtained after first stage of grinding due to high deportment of  $\beta$ -spodumene to the finest size fraction, i.e.,  $-0.6$  mm. In the further stages of grinding, the lithium grade kept changing due to preferential grinding of calcined spodumene ore. However, the recovery was almost constant in the further stages of grinding. It was found that the open circuit grinding produced lower amounts of fines but the maximum lithium grade in the finest size fraction, i.e.,  $-0.6$ mm. The closed-circuit grinding was more energy efficient than the open circuit grinding since the closed circuit grinding produced higher amounts of fines. Particle size distribution showed that the open circuit grinding generated much finer particles than the closed circuit grinding and hence a higher lithium grade.

When the spodumene ore samples were calcined at different calcination temperatures, it was found that the samples calcined at  $540$  and  $950$  °C did not improve coarse gangue rejection significantly. This behaviour was due to the fact that  $\alpha$ -spodumene to  $\beta$ -spodumene conversion was incomplete at these temperatures as shown by the XRD analysis of the samples. At  $950$  °C, albite also became brittle and was deported to the finest size fraction and hence the lithium grade was lower in the case of the sample calcined at  $950$  °C as compared to that of the sample calcined at  $540$  °C. It should be noted that the best grade and recovery of lithium in the finest size fraction was obtained when the sample was fully calcined at  $1100$  °C since  $\alpha$ -spodumene to  $\beta$ -spodumene conversion was fully completed at this temperature.

The calcination of the spodumene ore caused fracturing of spodumene surfaces and hence made spodumene more amenable for adsorption of oleate. The samples calcined at  $1100$  °C yielded

the best lithium grade and recovery, highest adsorption of oleate and lowest zeta-potential. The samples calcined at 540 and 950 °C showed little improvement in lithium grade and recovery whereas the non-calcined samples showed the lowest lithium grade and recovery.

## **2. Future research opportunities**

- It was found that vanadium and rubidium are present in this spodumene ore and thus upgrading of these metals from this ore may be explored in the future.
- Calcination is an expensive process especially when calcining the whole feed and thus microwave heating should be investigated for ore beneficiation of hard rock lithium ores.
- Further work can be performed using energy efficient furnaces such as double pass rotary kilns with efficient burner systems eg., regenerative/ plasma/ oxy-fuel with efficient combustion.